

**ACTIVATION OF THE FELINE UMAMI RECEPTOR fT1R1-
fT1R3 BY LINEAR α -L-DIPEPTIDES: AN *IN VITRO* STUDY**

By

Carlos Juan Hernangomez de Alvaro

**Thesis submitted to the University of Nottingham
for the degree of Masters of Research**

School of Biosciences

University of Nottingham

December 2016

Table of Contents

Table of Figures.....	V
List of Tables.....	VIII
Acknowledgements.....	i
Abstract.....	iii
Abbreviations.....	iv
1 Introduction.....	1
1.1 Umami taste and cat feeding behaviour.....	1
1.2 Taste receptors - Molecular mechanisms of umami taste.....	3
1.3 Cell-based assays for the study of umami taste.....	8
1.4 Involvement of peptides with umami taste in human.....	17
1.5 Focus of this research on linear α -L-dipeptides.....	22
1.6 Possible involvement of peptides with umami taste in cat.....	24
1.7 Aims of this MRes Project.....	30
2 Materials and Methods.....	32
2.1 <i>In vitro</i> experiments.....	32
2.1.1 Cell type.....	32
2.1.2 Cell culture and induction of ft1R1-ft1R3 receptor expression.....	33
2.1.3 Fluorescence indicator loading.....	33
2.1.4 Preparation of the cells for Luminescence assay.....	34
2.1.5 Fluorescence readings.....	35
2.1.6 Luminescence readings.....	37
2.1.7 <i>In vitro</i> data analysis.....	39
2.1.7.1 Full library of 101 dipeptides screening (Fluorescence data only).....	39
2.1.7.2 Selected subset of dipeptides (33 samples) screening.....	39
2.2 <i>In silico</i> experiments.....	41
2.2.1 Molecular modelling.....	41
3 Experimental Results and Discussion.....	43

Table of Contents

3.1	Overview and sequence of the experiments conducted	43
3.2	Dipeptide library tested	45
3.3	Preliminary experiments (Fluorescence)	46
3.3.1	Primary screening of dipeptides with 2 mM IMP	51
3.3.2	Primary screening dipeptides with Tyrode's buffer only	58
3.3.3	Dose responses of potentially active compounds with the FlexStation	61
3.3.4	Summary of FlexStation 3 results	63
3.4	<i>In vitro</i> results from the FLIPR experiments (selected dipeptides).....	66
3.4.1	Fluorescence experiments	70
3.4.2	Luminescence experiments.....	80
3.4.3	Summary of the Fluorescence and Luminescence experiments	85
3.5	<i>Consolidation of in vitro experimental results</i>	90
3.5.1	Answers to the questions formulated prior to the <i>in vitro</i> experiments.....	90
3.5.2	Summary of <i>in vitro</i> experiment results	93
3.6	<i>In silico</i> experiments	96
3.6.1	Molecular modelling	96
3.6.1.1	Preliminary models with L-amino acids	96
3.6.1.2	Potential molecular mechanism for dipeptide binding	98
3.6.1.3	<i>In silico</i> modelling of the three active dipeptides.....	99
3.6.1.4	<i>In silico</i> models of inactive dipeptides	103
3.6.1.5	Possible explanations of unusual response patterns.....	104
3.6.2	Summary of the <i>in silico</i> modelling.....	105
3.7	Overall summary of the results.....	107
4	Conclusions and suggested further work.....	109
4.1	General conclusions	109
4.2	Contribution of this work to the chemoreception field.....	112
4.3	Contribution of this work to the pet food industry	<u>113</u> 113
4.4	Further work	113
	Bibliography	117

Table of Contents

Appendices.....	130
Appendix 1 - Preliminary experiments with DMSO (Fluorescence).....	130
Appendix 2 – Plate layouts.....	132
Appendix 3 - Controls used in primary screening (Fluorescence-FlexStation)	134
Appendix 4 - Primary screening results for the 101 dipeptides.....	136
Appendix 5 - Quality control checks – Chemical analysis	139

Table of Figures

Figure 1. Examples of receptor-mediated tastes in mammals (Yarmolinsky et al., 2009)	3
Figure 2. Schematic of the human umami receptor hT1R1-hT1R3 with main binding sites [adapted from Zhang et al. (2008)].....	5
Figure 3. Molecular model of the hT1R1 VFT domain (Zhang et al., 2008).....	6
Figure 4. Schematic of HEK293 transfection with human umami receptor hT1R1-hT1R3 or human sweet receptor hT1R2-hT1R3 (Ahn et al., 2016).....	10
Figure 5. Schematic of the canonical signal transduction cascade after agonist binding and intracellular release of Calcium (Kinnamon, 2016).....	11
Figure 6. Schematic illustration of drug potency and efficacy (Clarkson, 2016).....	16
Figure 7. Peptidic bond between two L-amino acids generating an alpha-L-dipeptide	23
Figure 8. Comparison of the <i>in vitro</i> response patterns of human and mouse umami receptor to 50 mM of different amino acids (Toda et al., 2013).	26
Figure 9. In silico modelling of L-serine binding to the feline umami receptor (McGrane, 2013).	29
Figure 10. FlexStation 3 (left) and FLIPR ^{TETRA} (right) microplate readers (Molecular Devices).	36
Figure 11. Dose responses of L-alanine and L-cysteine with buffer plus 0.2 mM or 2 mM IMP.	49
Figure 12. L-Alanine primary screening with 2 mM IMP and buffer and IMP baseline responses at 0.2 mM and 2 mM.	53
Figure 13. Examples of potentially active and inactive dipeptides in primary screening. ...	55
Figure 14. Unusual response pattern of dipeptides in primary screening.	56
Figure 15. Comparison of primary screening results in IMP and in buffer for His-Ala and Asn-His.	59
Figure 16. Raw data comparison of primary screening results in IMP and in buffer for Asn-His and Asn-Ala.....	60
Figure 17. Dose responses for six dipeptides in buffer + 2 mM IMP and in buffer only.....	62
Figure 18. Schematic with the conclusions from the primary screening (Fluorescence – FlexStation).....	63

Figure 19. Examples of non-specific responses found in the screening of the 101 dipeptide library.....	65
Figure 20. Example of raw fluorescence activation data of induced cells in the presence of IMP.....	71
Figure 21. Fluorescence responses summary for dipeptide samples 1-11 (F1)..	72
Figure 22. Fluorescence responses summary for dipeptide samples 12-22 (F2).	72
Figure 23. Fluorescence responses summary for dipeptide samples 23-33 (F3)..	73
Figure 24. Unusual fluorescence response pattern for some dipeptides in dose response screening. Raw FLIPR data corresponds to DP11 – Asn-Ala.	75
Figure 25. Difference in response patterns in non-specific and genuinely active compounds.	76
Figure 26. Maximum umami signal expected in fluorescence (100 mM Ala + 1 mM IMP)..	77
Figure 27. Raw fluorescence results of DP24 (Gly-Cys), DP67 (Phe-Leu) and DP94 (Tyr-Gly) using the FLIPR.	78
Figure 28. Dose responses of DP24 – Gly-Cys, DP67 – Phe-Leu and DP94 – Tyr-Gly (Fluorescence).	79
Figure 29. Example of raw luminescence activation data in the presence of IMP.	80
Figure 30. Reference umami luminescence response.....	81
Figure 31. Maximum luminescence responses summary for dipeptide samples 1-11 (L1)..	82
Figure 32. Maximum luminescence responses summary for dipeptide samples 12-22 (L2). ..	82
Figure 33. Maximum luminescence responses summary for dipeptide samples 23-33 (L3). ..	83
Figure 34. Luminescence response of DP24 – Gly-Cys (raw data).	83
Figure 35. Dose responses of DP24 – Gly-Cys, DP67 – Phe-Leu and DP94 – Tyr-Gly (Luminescence).....	84
Figure 36. Fluorescence results for the auto-fluorescent dipeptide DP76 – Ser-His..	88
Figure 37. Example of a zwitterionic amino acid (L-alanine) binding to the Venus flytrap of the ft1R1 in the cat umami receptor ft1R1-ft1R3.	97
Figure 38. Docking of Gly-Cys (DP24) in the umami active site in the VFT of ft1R1.....	100
Figure 39. Docking of Phe-Leu (DP67) in the umami active site in the VFT of ft1R1.....	102
Figure 40. Docking of Tyr-Gly (DP94) in the umami active site in the VFT of ft1R1.	103
Figure 41. Docking of Gly-Met (DP28) and Tyr-Ala (DP92) in the umami active site in the VFT of ft1R1.....	104
Figure 42. Overlap of Tyr-Gly (DP94) with GMP binding in the umami active site in the VFT of ft1R1.....	105

Figure 43. Representation of the different zwitterionic configurations in amino acids and dipeptides..... 106

Figure 44. Schematic of the response produced by an inverse agonist (Boghog, 2014). 115

Appendices:

Figure AP-1. Illustration of the effect of the solvent DMSO in the cat umami *ft1R1-ft1R3* assay..... 131

Figure AP-2A. Primary screening compound plate layout..... 132

Figure AP-2B. Example of compound layout for FLIPR..... 133

Figure AP-3A. Response to 10 μ M ATP control by induced and un-induced (mock) cells..... 134

Figure AP-3B. Response to 10 μ M isoproterenol control by induced and un-induced (mock) cells..... 135

Figure AP-3C. Response to Tyrode's buffer control by induced and un-induced (mock) cells..... 135

Figure AP-5A. LC chromatogram comparing the signals of Asn-His from the two suppliers..... 139

Figure AP-5B. MS spectra comparing the signals of Asn-His from the two suppliers..... 140

Figure AP-5C. LC chromatogram comparing the signals of Asn-Leu from the two suppliers..... 140

Figure AP-5D. MS spectra of Asn-Leu from supplier 1 (PE Biosciences)..... 141

Figure AP-5E. MS spectra of Asn-Leu from supplier 2 (AnaSpec)..... 141

List of Tables

Table 1. Summary of the possible causes of discrepancy in the reported taste descriptors of peptides.	19
Table 2. Scope of the research contained in this Thesis	24
Table 3. Comparison of key residues for acidic amino acid recognition or broadly tuning to amino acids for human and mouse [adapted from Toda et al. (2013)].	26
Table 4. Amino acid residues at positions 170 and 302 in the T1R1 active site for different species (McGrane, 2013).	28
Table 5. List of 101 dipeptides tested <i>in vitro</i>.	46
Table 6. Activity and EC₅₀S of L-amino acids tested with 0.2 mM IMP plus Tyrode’s buffer (McGrane, 2015).	47
Table 7. Comparison of EC₅₀ values of two L-amino acids tested in buffer with 0.2 mM or 2 mM.	50
Table 8. Solubility in Tyrode’s buffer of the 101 dipeptides tested.	52
Table 9. Dose response experiments performed with the FlexStation in fluorescence mode and EC₅₀ determination.	61
Table 10. Plates tested (24) in the FLIPR in Fluorescence and Luminescence mode.	68
Table 11. List of samples tested in the FLIPR in Fluorescence and Luminescence mode.	69
Table 12. Summary of the results from the 33 dipeptide samples tested in the FLIPR in fluorescence and luminescence mode.	85
Table 13. Final conclusions on the 12 possible auto-fluorescent compounds.	89
Table 14. Differences in the results between batches and between suppliers for some dipeptides.	90
Table 15. Activation profiles on the three umami-active dipeptides.	95
Table 16. Three dipeptides activating the cat umami receptor ft1R1-ft1R3 <i>in vitro</i>.	109

Appendices:

Table AP-4. Primary screening results of the 101 dipeptides (FlexStation – Fluorescence) ...	136
---	-----

Acknowledgements

I would like to thank first the WALTHAM® Centre for Pet Nutrition, the global fundamental research centre for Mars PetCare, for funding this project and giving me this opportunity. I wish to express my most sincere gratitude to my supervisors Dr. David Gray and Dr. Scott McGrane, for all their support, coaching and encouragement during this project. I would like to highlight their generosity and dedication to review my MRes. thesis. I also would like to recognise the key assistance from Prof. Andy Taylor, Prof. Stephen Harding and Prof. Jordi Rovira, without whom I would not have been able to start this amazing learning journey three years ago.

I am very indebted to my managers at WALTHAM®, Dr. Sue Skelton and Dr. Scott McGrane for their flexibility, assistance and understanding of the challenges encountered when having to balance work obligations with part-time studies, so I could complete this project. Also thanks to Dr. Denise Elliot and Dr. Darren Logan for supporting my further education journey. Special thanks to Alex Horsfall and Matt Gibbs, who taught me most of what I know about *in vitro* assays, and did not mind spending their time coaching me when I needed it. Thank you to Matt Talbot for offering his analytical chemistry expertise for quality checking my dipeptides. Thanks to all my colleagues at WALTHAM® for inspiring and supporting me.

I am obliged to our research partners for sharing their expertise and for their scientific advice, and especially to BioPredict for answering my questions, performing the *in silico* modelling and sharing my love for science.

Acknowledgements

Finally, a special mention to the loves of my life, Cat, Grace and Baby Bean. Without their love, support, encouragement, patience and understanding, I would not have been able to finish this project.

Abstract

Cats (*Felis catus*) are obligate carnivores and as such they are adapted to detect the taste of meat and its components, such as L-amino acids, which generate *umami* (or savoury) taste, analogous to the taste of MSG for humans. The umami taste receptor (T1R1-T1R3) plays an important part in the oral detection of L-amino acids by cats and other mammals. Cats can perceive all of the L-amino acids *in vivo*, however not all of them activate the feline umami receptor *in vitro*. Proteins are formed from long chains of L-amino acids bound together, which in turn can be broken down into smaller fragments or peptides through processes such as hydrolysis and fermentation. These processes are often necessary to increase the flavour, nutritional value, digestibility and hypoallergenicity of proteins used in manufacture of pet food. The aim of this research project was to determine if the dipeptides formed by the combination of the 11 umami-active L-amino acids for cats (Ala, Asn, Cys, Gly, His, Leu, Met, Phe, Ser, Trp and Tyr) were also umami-active using a cell-based cat umami taste receptor assay. The results identified that, from the library of 101 α -L-dipeptides tested, only three were active (Gly-Cys, Phe-Leu and Tyr-Gly), but had a weaker interaction with the receptor than the component L-amino acids (maximum 20-50% of activation). An unusual *in vitro* response pattern was found for several of the dipeptides, which was attributed to non-specific responses or interactions. Using an *in silico* model of the cat umami receptor, the reduction in the binding interaction of the dipeptides was proposed to be due to the increase in their zwitterionic dipole length compared to the individual L-amino acids. This made it more difficult to stabilise the closed (active) conformation in the Venus flytrap region (active binding site) of the T1R1 subunit of the cat umami receptor. This research helps to further elucidate the role of dipeptides on umami taste perception of cats.

Abbreviations

A	L-alanine (one-letter code)
AA	Amino Acid/s
ADP	Adenosine Diphosphate
α -Gust.	Alpha-Gustducin
Ala	L-alanine
AM	Acetoxymethyl (ester of the Fluorophore Fluo-4)
AMP	Adenosine Monophosphate
AnaS	AnaSpec - Cambridge Bioscience (peptide supplier)
Arg	L-arginine
Asn	L-asparagine
Asp	L-aspartic acid
ATP	Adenosine Triphosphate
Bac	BACHEM (peptide supplier)
C	L-cysteine (one-letter code)
CALHM1	Calcium Homeostasis Modulator 1
cAMP	Cyclic AMP
CaSR	Calcium Sensing Receptor (also known as Kokumi receptor)
CFF	Charmm Force Field
CHARMM	Chemistry at Harvard Macromolecular Mechanics simulations
CHO	Chinese Hamster Ovary cells
CI	Confidence Interval
Comp.	Compound
CV (%)	% Coefficient of Variation
Cys	L-cysteine
D	L-aspartic acid (one-letter code)
Da	Dalton (1Da = 1g/mol)
DAG	Diacylglycerol
$\Delta F/F$	Relative change in Fluorescence
DKP	Diketopiperazines

Abbreviations

DMEM	Dulbecco's Modified Eagle's Medium
DMSO	Dimethyl Sulfoxide (solvent)
DNA	Deoxyribonucleic Acid
DP	Dipeptide
DR	Dose Response
E	L-glutamic acid (one-letter code)
EC ₅₀	Half Maximal Effective Concentration
EF-hand	helix-loop-helix structural domain
ER	Endoplasmic Reticulum
F	L-phenylalanine (one-letter code)
F (plate)	Fluorescence (plate) at a given time
F ₀	Initial fluorescence
FBS	Foetal Bovine Serum
FEDIAF	European Pet Food Industry Federation
FLIPR	Fluorometric Imaging Plate Reader
ft1R1	Feline T1R1 taste receptor subunit
ft1R1-ft1R3	Cat (feline) umami receptor ft1R1-ft1R3 heterodimer [both subunits are feline, not a chimera (co-expression) of feline genetic material with human or mouse]
G	Glycine (one-letter code)
GABA	Gamma-Amino Butyric Acid
G α	G-protein alpha subunit
G $\beta\gamma$	G-protein beta-gamma heterodimer
GDP	Guanosine Diphosphate
Gln	L-glutamine
Glu	L-glutamic acid
Gly	Glycine
GMP	Guanosine Monophosphate
G-Protein	Enzyme protein (GTP-ase) which has its activity mediated by guanosine triphosphate (GTP) and guanosine diphosphate (GDP), so they are activated when bound to GTP and deactivated when bound to GDP
GPCR	G-Protein Coupled Receptor
GPR	G-Protein Receptor
GSH	Glutathione (reduced)

Abbreviations

GTP	Guanosine Triphosphate
H	L-histidine (one-letter code)
HB	Hydrogen Bond
HEK	Human Embryonic Kidney cells
HEPES	4-(2-hydroxyethyl)-1-piperazineethanesulfonic acid (buffer)
His	L-histidine
HPLC	High Performance Liquid Chromatography
hT1R1	Human T1R1 taste receptor subunit
HTPS	High Throughput Screening
I	L-isoleucine (one-letter code)
Ile	L-isoleucine
IMP	Inosine Monophosphate
IMP int	IMP interaction
ind.	induced cells
IP3	Inositol triphosphate
K	L-lysine (one-letter code)
Kd	Dissociation constant
KO (gene)	Knocked-out gene (made not functional)
λ	Wavelength (nm)
L	L-leucine (one-letter code)
L (plate)	Luminescence plate
L- (prefix)	Enantiomer L-; levorotatory (e.g. amino acids are L- in most biological systems)
Leu	L-leucine
Log [M]	Logarithm Molar (mol/L) concentration
Lys	L-lysine
M	L-methionine (one-letter code)
Met	L-methionine
mGluR1	Metabotropic Glutamate Receptor 1
mGluR4	Metabotropic Glutamate Receptor 4
μ M or uM	Micromolar (umol/L) concentration
mM	Milimolar (mmol/L) concentration
Mock (cells)	Un-induced cells (not expressing the taste receptor)
MRes	Masters of Research

Abbreviations

MS	Mass Spectrometry
MSG	Monosodium Glutamate
N	L-asparagine (one-letter code)
N/A	Not analysed / Not applicable / Not available
NA	Not active (inactive)
NAM	Negative Allosteric Modulator
NgAct.	Negligible Activity
NS	Non-specific (response)
NTD	N-Terminal Domain
Out	Outlier / error in pipetting
P	L-proline (one-letter code)
PAI	Peak After Injection
PAM	Positive Allosteric Modulator
Part. Sol.	Partially Soluble
PDB	Protein Data Bank
PE Bio	PE Biosciences (peptide supplier)
Phe	L-phenylalanine
PIP	Phosphatidylinositol-4,5-bisphosphate
PLC	Phospholipase C
PLS	Partial Least Squares (regression)
Pro	L-proline
PS	Primary Screening
Pure	In buffer only
P2X2 (or 3)	Neuronal Purinoreceptor 2 (or 3) (ATP sensor)
Q	L-glutamine (one-letter code)
QSAR	Quantitative Structure-Activity Relationship
R	L-arginine (one-letter code)
RFU	Relative Fluorescence Units
RGS	Regulator of G protein Signalling
RLU	Relative Luminescence Units
S	L-serine (one-letter code)
SAR	Structure-Activity Relationship
SB	Salt Bridge
SD	Standard Deviation

Abbreviations

SEM	Standard Error of the Mean
Ser	L-serine
STD	Standard
T	L-threonine (one-letter code)
Thr	L-threonine
TMD	Trans-Membrane Domain
TR	Taste Receptor
TRC	Taste Receptor Cells
Trp	L-tryptophan
TRPM	Transient Receptor Potential ion channels
Unk	Unknown
UV	Ultra-Violet (light)
V	L-valine (one-letter code)
Val	L-valine
VFT	Venus Fly Trap
VGNC	Voltage-Gated sodium (Na) ion Channel
W	L-tryptophan (one-letter code)
WALTHAM	Waltham Centre for Pet Nutrition (part of Mars Inc.)
Y	L-tyrosine (one-letter code)

1 Introduction

This project is related to the area of chemosensory perception, with a focus on cats. This multi-disciplinary area involves biology, chemistry, food science, bioinformatics, neuroscience, psychology, genetics and sensory science, amongst other disciplines, so the research in this area can be addressed from very different angles. In this MRes project the objective is to develop the knowledge in this field from the angle of molecular biology, especially *in vitro* screening, but also *in silico* modelling.

According to data from the European Pet Food Industry Federation (FEDIAF), there are 7.5 million cats kept as pets in the UK and around 70 million pet cats in the European Union. The pet food industry and related pet services represent a combined annual turnover of over € 30 billion, being pet food sales € 15 billion, and pet services (veterinary care, pet accessories and other services) the other €15 billion (FEDIAF, 2014). Cat food manufacturing requires protein-derived ingredients to deliver the required nutrition for the growth, development and wellbeing of the animal. Many of these proteinaceous ingredients contain free peptides, indeed, peptides could be produced intentionally due to nutritional, hypoallergenic, organoleptic or process-related reasons, thus the interest for the cat food industry in the taste of peptides.

1.1 Umami taste and cat feeding behaviour

Umami taste, first described by Kikunae Ikeda in 1909 from *Kombu* algae extract (in *dashi*) and meaning “delicious” in Japanese, is one of the five generally recognised tastes (Ikeda, 1909, Ikeda, 2002). It is the typical taste attribute of monosodium glutamate (MSG) and 5'-

ribonucleotides, which act synergistically (Yamaguchi, 1967), and it is described as “meaty” or “savoury” to humans.

Cats (*Felis catus*) are obligate carnivores and as such are adapted to detect the taste of meat and its components such as L-amino acids (Bradshaw, 1991, Bradshaw et al., 1996, Bradshaw, 2006). Early neurophysiological studies on cat nerve fibres struggled to separate umami responses to salt responses, using MSG and disodium 5'-ribonucleotides as agonists (Adachi et al., 1967), although later physiological and behavioural studies showed nerve activation and flavour preferences of L-amino acids, nucleotides and protein hydrolysates with cats (White and Boudreau, 1975, Boudreau, 1987, Beauchamp et al., 1977). Umami synergism at the nerve fibre level was also found in other species such as rats (Yoshii et al., 1986) and dogs (Kumazawa et al., 1991). In terms of other taste modalities, cats reject bitter and sour foods (Bradshaw et al., 1996, MacDonald et al., 1985), but their taste perception is different to many other mammals, as they cannot perceive simple sugars and artificial sweeteners due to the lack of a functional sweet taste receptor gene *fTasr2-fTasr3* (Li et al., 2005, Li et al., 2006, Jiang et al., 2012). Cats have been reported to have low sensitivity to salt (Boudreau et al., 1985, Bradshaw, 1991, Bradshaw et al., 1996) and respond to sodium chloride taste only at relatively high concentrations (Carpenter, 1956, Kruger and Boudreau, 1972).

Due to their feeding behaviour, it is reasonable to expect cats are biologically specialised in detecting umami taste, but no specific research on the cat taste receptor area was publicly available until relatively recently, after the cat genome was sequenced (Pontius et al., 2007, Sandau and Rawson, 2014, McGrane, 2013, McGrane and Taylor, 2014). Umami compounds in food are hypothesised to be the principal appetitive stimuli for cats (Bradshaw et al., 1996, McGrane, 2013, McGrane and Taylor, 2014).

1.2 Taste receptors - Molecular mechanisms of umami taste

The discovery of the taste receptors, expressed in the membrane of the taste-cells located in the taste buds, which mediate all taste modalities at a molecular level (see Figure 1), was a paradigm shift in chemosensory research in vertebrates and invertebrates (Yarmolinsky et al., 2009). This new approach, in particular for the umami taste modality, in human and other mammalian species, opened a new avenue for research on the taste of proteinaceous food (Lindemann, 2001).

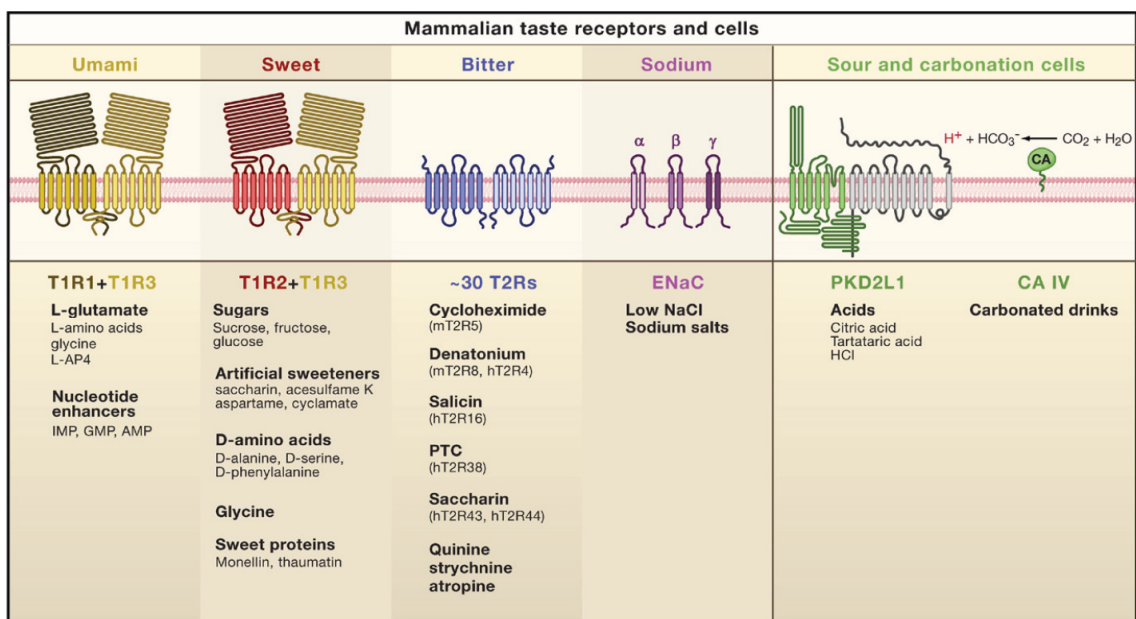


Figure 1. Examples of receptor-mediated tastes in mammals (Yarmolinsky et al., 2009)

Chemical and physical signals from the cell environment can induce a variety of responses in cells (and therefore in tissues), which are able to react to light, ions, neurotransmitters, hormones, nutrients, pheromones, odours and tastes (Pin et al., 2004). Chemical signals (ligands) may bind to receptors (membrane proteins) embedded in the cell membrane (a phospholipid bilayer), producing a change in conformation of the receptor protein, from “inactive” to “active”. Membrane receptors span from the outside to the inside of the cell, thus having extracellular, transmembrane and intracellular regions or “domains”. These *cell*

membrane receptors can be *ionotropic* (produce a fast response mediated by an ion channel pore in the cell membrane when activated after ligand binding) or *metabotropic* (produce a slow response by initiating enzymatic reactions releasing intracellular chemicals after ligand binding).

G-protein Coupled Receptors (GPCRs) are the largest family of membrane receptors and are metabotropic receptors “coupled” to a trimer of proteins inside the cell (*alpha, beta* and *gamma*) needed for the transmission of the “signal”. Alpha G-proteins are specialised in binding guanosine diphosphate (GDP) or guanosine triphosphate (GTP) (thus the “G”-protein name). The receptor activates the G-proteins after ligand binding through a conformational change. G-proteins are inactive when bound to GDP and active when bound to GTP. When active, the G-proteins start the enzymatic reactions which propagate the signal inside the cell. All GPCRs have seven transmembrane domains (alpha-helices). The amino acid L-glutamate is one of the major neurotransmitters in the mammalian central nervous system, therefore, it binds to numerous GPCRs found in mammalian cells (Kew and Kemp, 2005).

In terms of the biology of mammalian taste, the cells involved in perception are *Taste Receptor Cells (TRC)* located in the taste buds contained in the oral cavity (Chaudhari and Roper, 2010).

In relation to the umami taste modality, the first umami-sensing receptor discovered in these cells was a variation of a metabotropic glutamate receptor, the taste-mGluR4 (Chaudhari et al., 2000). However, the umami taste receptor T1R1-T1R3, discovered later (Li et al., 2002, Nelson et al., 2002, Zhao et al., 2003), was and it is still considered the main receptor for umami taste perception in mammalian species. Further research discovered additional receptors able to respond to umami-taste molecules (e.g. L-amino acids) also expressed in the oral cavity, for example, the metabotropic glutamate receptor mGluR1, GPRC6A, the calcium-sensing receptor (CaSR) and the peptone receptor GPR92 amongst others (Chaudhari et al., 2009, Wellendorph and Brauner-Osborne, 2009, San Gabriel et al., 2009, Conigrave et al., 2007, Haid

et al., 2013, Pal Choudhuri et al., 2015). The multiple receptor hypothesis for umami taste, has also been supported by work in mice, where genetically-modified T1R3-KO mice could still respond to MSG (Damak et al., 2003).

The umami receptor T1R1-T1R3 belongs to “class C” of the G-protein Coupled Receptors (GPCRs), characterized by possessing a large extracellular domain (called “Venus Fly-Trap”; VFT). It can be described as a heterodimer containing two different proteins (subunits), each of them possessing a large extracellular N-terminal domain for ligand recognition and binding, seven transmembrane domains, and an intracellular C-terminal domain for signal transduction (Zhang et al., 2008).

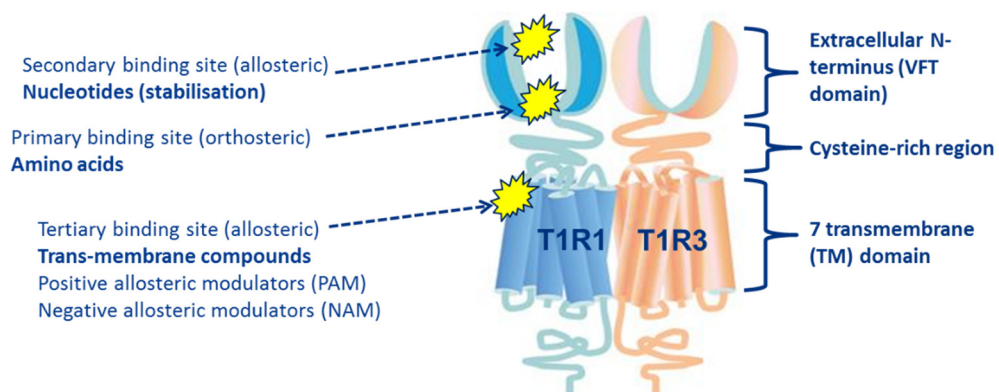


Figure 2. Schematic of the human umami receptor hT1R1-hT1R3 with main binding sites [adapted from Zhang et al. (2008)]. Orthosteric site is the place where the natural molecules would bind to the receptor, the primary site, or the site where the receptor main function occurs. Allosteric sites are any other sites where molecules could bind to the receptor, thus performing different roles (mainly modulation of the response of the receptor).

The human umami taste receptor (hT1R1-hT1R3), has three main binding sites (Figure 2): one primary (“active” or *orthosteric* site) for the umami L-amino acids (e.g. MSG) in the hinge region of the T1R1-VFT, one secondary (*allosteric* or “in another place”) for 5'-ribonucleotides (e.g. IMP) in the outer cleft “pincer” region of the T1R1-VFT, and a third one for *allosteric*

modulators (e.g. carboxamide S807) in the trans-membrane domain (TMD) of T1R1, which enhance or inhibit the *affinity* of the ligands for the receptor or the *efficacy* of the activation of the receptor protein and the propagation of its signal into the cell (Zhang et al., 2008, Mouritsen and Khandelia, 2012, Suess et al., 2015).

The two-step molecular mechanism explaining why the umami taste perception of glutamate and aspartate is synergistically enhanced by the presence of 5'-ribonucleotides has been elucidated for humans (Figure 3):

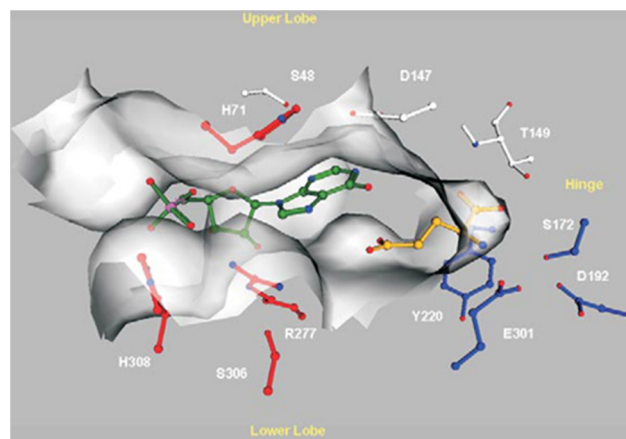


Figure 3. Molecular model of the hT1R1 VFT domain (Zhang et al., 2008). The key residues for glutamate and for IMP binding are represented in blue and red, respectively. The upper lobe is represented on the top and the lower lobe on the bottom. The VFT hinge region is on the right, and the VFT opening is on the left. The L-glutamate (in gold) is located deep inside the VFT domain near the hinge region, whilst IMP (in green) is located close to the opening of the VFT domain.

First the alpha-carboxylate group of the amino acid (glutamate; agonist) binds via hydrogen bonds with a group of residues close to the hinge of the VFT, and the amino group in the amino acid coordinates with residues in the upper and lower lobe.

Then, the nucleotide stabilises the active (closed) conformation of the umami receptor due to electrostatic interactions between its phosphate groups and the positive charges in the pincer

residues near the cleft opening in the VFT, which strengthens the bond between the upper and lower lobes, enhancing the intensity of the signal (Zhang et al., 2008).

The stereochemistry of the molecule binding to the receptor is very important and only the L-form of amino acids has the right conformation to strongly interact with the orthosteric site. Furthermore, this stereospecificity is also seen with nucleotide molecules in the pincer region: From a 5'-ribonucleotide derivatives library of 16 compounds evaluated by Festring and Hofmann (2011) in the presence of MSG, the (S)-configured isomers showed higher taste impact (up to seven times the umami taste enhancement of IMP), whereas the (R)-isomers showed only marginal umami enhancement in comparison with IMP.

Even when the synergy between L-amino acids and nucleotides has been observed in other species and many of the residues in the VFT domain of the umami receptor are conserved, the perception of L-amino acids has been shown to be different in different mammalian species (Nelson et al., 2002, Roura et al., 2011, Toda et al., 2013). There seems to be a specific response pattern for humans, which can only perceive L-glutamate and L-aspartate as umami (Li et al., 2002), whilst other mammals, like mouse, can perceive many other L-amino acids as umami, at least at the receptor level, making T1R1-T1R3 a more broadly-tuned receptor for L-amino acids (Nelson et al., 2002, Zhao et al., 2003, Toda et al., 2013). The molecular mechanism of this different umami perception of L-amino acids in human and mouse is known (Toda et al., 2013) and some researchers have highlighted the species differences not only on the binding site but also in other areas of the VFT that could influence binding (Roura et al., 2011, McGrane, 2013).

As mentioned before, in addition to being perceived by the umami receptor T1R1-T1R3, L-amino acids (and also peptides) can also be perceived by other receptors, like the extracellular calcium sensing receptor (CaSR) and act as taste enhancers for umami or other taste modalities (Conigrave et al., 2007, Maruyama et al., 2012). *Kokumi*, which means “rich taste” or “mouthfulness” in Japanese, is one of the last additions to the taste perception repertoire. In the oral taste perception context, CaSR is referred as the Kokumi receptor (Ohsu et al., 2010). The complexity of the taste perception of L-amino acids and peptides is evident from the volume of past research. In this research project, only taste perception via the cat umami receptor fT1R1-fT1R3 will be investigated.

1.3 Cell-based assays for the study of umami taste

Taste and odourant receptor research has been developed using the same approach used in pharmaceutical research, where large libraries of possible therapeutic candidates are screened *in silico* (performed by computer simulations using a model mimicking the biological reality), *in vitro* (using living cells from the organism of interest or another organism and expressing the gene in a very controlled environment) and *in vivo* (using a whole living organism).

The research conducted *in silico*, has the advantage of being relatively rapid, inexpensive and safe as no actual chemicals, laboratory resources or animals are used, and it is normally conducted at the beginning of the discovery pipeline to support *in vitro* and *in vivo* studies. Pharmacophore modelling is extensively used to find new drugs (Ferreira et al., 2015). Quantitative structure-activity relationship (QSAR) computer models are also used extensively, especially in drug development, to predict toxicity (Valerio, 2010), but also in taste and smell (Morini et al., 2011, Di Pizio and Niv, 2014), and to generate hypothesis in the quest for active compounds *in vitro* (Kristiansen, 2004, Zhang et al., 2008, Zhang et al., 2010).

Introduction

The *in vitro* research requires investment in laboratory facilities and chemicals, but is inexpensive in comparison to clinical trials, and has the flexibility of being able to study any genetic target and not having to consider the safety of the experimental subjects as these are cell models and not animals or humans.

In vivo tests are necessary to finally prove the efficacy, metabolism and safety of the active compounds identified, but are the most expensive, ethically challenging and difficult due to safety reasons, which is why *in silico* and *in vitro* can help reducing the risk and maximising the efficacy of the *in vivo* experiments dramatically (Andersen and Krewski, 2009).

In vitro cell models can be used to study taste receptor function. The main receptor mediating the umami taste (T1R1-T1R3), and other GPCRs mediating umami, sweet and bitter taste, can be studied in cell-based assays. One of the most widely used cell type for *in vitro* research in mammalian taste is the human embryonic kidney cell (HEK293) (Chandrashekar et al., 2000, Li et al., 2002, Bassoli et al., 2014), although Chinese hamster ovary cells (CHO) are also used (Chaudhari et al., 2000).

Transfection is a procedure that introduces foreign nucleic acids into cells to produce genetically modified cells (Kim and Eberwine, 2010). The gene of interest (e.g. human, murine or feline) is cloned into a suitable expression vector such as a plasmid. This can be incorporated into the cell by a process known as *transfection*. Transfected cells will then express the encoded protein (e.g. a taste receptor) which can be translocated to the cell surface after a chemical induction process (Li and Servant, 2008, Servant et al., 2010). The cells expressing the gene of interest can be selected with the help of antibiotics. An illustration of the expression of the human umami receptor (T1R1-T1R3) or human sweet receptor (T1R2-T1R3) dimer in a HEK293 cell is shown in Figure 4. Cells can be first stably transfected with human T1R3 and then transiently transfected with either human T1R1 or T1R2 (Ahn et al., 2016). All transfection

methods deliver the DNA materials to the nucleus of the cell. However, *stable* transfection provides cells with the gene of interest integrated in their chromosomes so it can be passed on generation after generation, whilst cells *transiently* transfected will only contain the gene of interest for a reduced time (a few days) in the nucleus and will not be able to pass on this information to the next generation after cell division, as it is not incorporated in their chromosomes. However, the high amounts of transiently transfected genetic material leads to high levels of expressed protein (taste receptor) within the period that it exists in the cell (Chalberg et al., 2001).

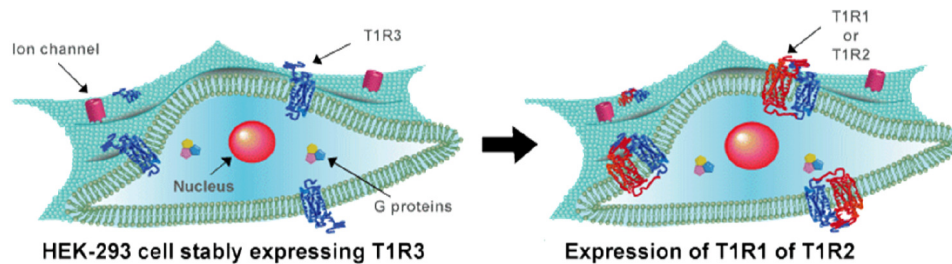


Figure 4. Schematic of HEK293 transfection with human umami receptor hT1R1-hT1R3 or human sweet receptor hT1R2-hT1R3 (Ahn et al., 2016).

The functionality of the taste receptor thus expressed is confirmed by its response to known umami ligands such as L-glutamic acid (in human) or L-alanine (in cat) and the cell functionality is confirmed by response to Adenosine Triphosphate (ATP). The activation of the receptor can be detected by calcium imaging techniques due to an intracellular release of calcium after the ligand binds to the receptor.

The taste signal transduction cascade starts when the chemical agonists bind to the taste receptor (e.g. bitter, sweet or umami GPCRs) producing a change in its conformation (from inactive/open to active/closed).

As mentioned before, Class C GPCRs have a large N-terminal domain involved in ligand binding and a C-terminal domain associated with a heterotrimeric G-protein, which consist of an alpha subunit ($G\alpha$) and a beta-gamma heterodimer ($G\beta\gamma$). The $G\alpha$ subunit contains a nucleotide-binding domain, which in the inactive state is bound to guanosine diphosphate (GDP). After ligand binding, the bound GDP is replaced by guanosine triphosphate (GTP) from the cytosol and the $G\alpha$ and $G\beta\gamma$ subunits dissociate from the receptor and from each other, performing different roles (targeting different effector enzymes, such as adenylyl cyclase, phospholipase C, or phosphodiesterases). In the case of taste receptors, after $G\beta\gamma$ dissociates from the receptor, it targets and activates the membrane enzyme phospholipase C β 2 (PLC β 2), which hydrolyses the membrane lipid phosphatidylinositol-4,5-bisphosphate (PIP2), producing diacylglycerol (DAG), which remains in the membrane, and inositol triphosphate (IP3), which is a cytosolic messenger and binds to the type III IP3 receptor located in the membrane of the endoplasmic reticulum (ER, see Figure 5).

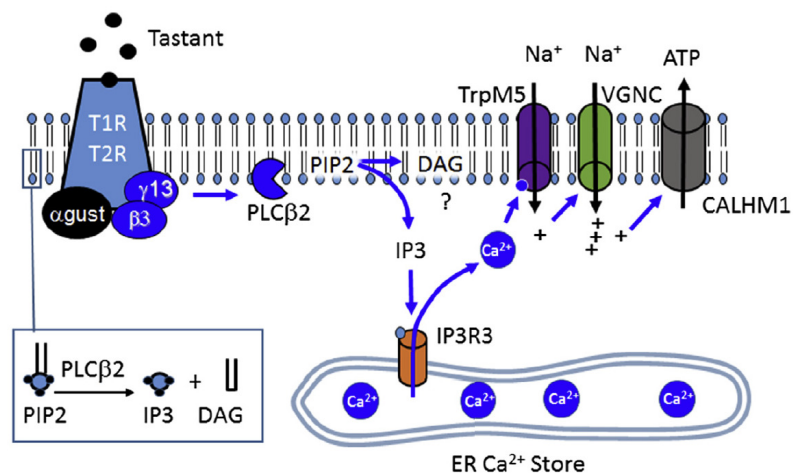


Figure 5. Schematic of the canonical signal transduction cascade after agonist binding and intracellular release of Calcium (Kinnamon, 2016).

After binding to this receptor in the ER, Ca²⁺ is released into the cytoplasm from the internal calcium stores in the ER. The elevated cytoplasmic Ca²⁺ level depolarizes the membrane via

sodium (Na^+) influx by a cation channel, TRPM5. The increase in Na^+ activates voltage-gated Na^+ channels (VGNC), which further depolarise the membrane by generating action potentials (Kinnamon, 2016). The combined action of elevated Ca^{2+} and membrane depolarization opens the large pores of gap junction hemi channels, likely composed of CALHM1, resulting in neurotransmitter adenosine triphosphate (ATP) release onto the gustatory afferent fibres of the facial (chorda tympani branch) and glossopharyngeal nerves, which transmit the signal from the taste buds in the oral cavity to the brain (Finger et al., 2005, Kinnamon, 2009, Chaudhari and Roper, 2010, Behrens et al., 2011). The taste receptor activation cycle is completed by the hydrolysis of the GTP bound to the $G\alpha$ subunit to GDP due to cytosolic phosphorylases, resulting in the re-association of the $G\alpha$ and $G\beta\gamma$ subunits and their binding to the receptor, which deactivates the receptor and terminates the signal (Svoboda et al., 2004). The length of the signal is controlled by the duration of the binding of GTP to the $G\alpha$ subunit, which can be regulated by RGS (regulator of G protein signalling) proteins which also bind to the $G\alpha$ subunit or by covalent modifications like phosphorylation (Hollinger and Hepler, 2002, Chen and Manning, 2001).

However, the proposed canonical mechanism for umami taste transduction is still controversial, for example, it has been stated that TRPM5 KO mice (which cannot use this ion channel to depolarise the cell and release ATP as neurotransmitter) can still respond to bitter, sweet and umami compounds (Damak et al., 2006) which suggest additional TRPM5-independent signal transduction mechanisms. Nevertheless, the participation of the voltage-gated ATP release channel CALHM1, which releases ATP to activate ATP (purinergic) receptors P2X2 and P2X3 on afferent nerve fibres (Finger et al., 2005), is now widely accepted (Taruno et al., 2013, Hellekant et al., 2015, Kinnamon, 2016).

Therefore, the enhanced intracellular Ca^{2+} level produced by the tastants binding to the receptor can be used to evaluate their activity, and this intracellular release of calcium can be detected by *fluorescence* or *luminescence* reporting systems. The production of light (photons), the reporting signal or wavelength that is detected and measured, is realized through chemiluminescence and fluorescence, as a consequence of energy transitions from excited-state molecular orbitals to lower energy orbitals. However, in chemiluminescence, the excited states are produced by exothermic chemical reactions, whereas in fluorescence the excited states are created by light absorption. The intensity of the light is proportional to the concentration of free calcium in the cell.

There are generally two classes of fluorescent Ca^{2+} indicators: (a) genetically encoded fluorescent proteins and (b) chemically engineered *fluorophores* (Paredes et al., 2008). In terms of fluorescent dyes, they chelate calcium selectively, generating a fluorescent chemical structure called a *fluorophore* (Bootman et al., 2013a). Fluorescent Ca^{2+} indicators bind and interact only with freely diffusible Ca^{2+} ions. Cytosolic Ca^{2+} is buffered 100 to 1, meaning that for every 100 Ca^{2+} ions in the cytosol, only 1 ion is free to diffuse. These systems have been widely used in taste receptor research (Bufe et al., 2002, Bassoli et al., 2014).

There is a wide variety of fluorescent Ca^{2+} indicators available, with excitation and emission spectra ranging from ultraviolet (UV) to the far red, in addition to differences in Ca^{2+} affinity, basal fluorescence, and cell permeability. Ca^{2+} -sensitive fluorescent indicators can be broadly divided into (a) *ratiometric* (dual-wavelength) or (b) *single-wavelength* indicators based on their response to an increase on Ca^{2+} concentration. Ratiometric indicators (like Fura-2) are the most useful for quantitative measurements of Ca^{2+} concentration, whereas single-wavelength indicators (like Fluo-4) are more commonly used for qualitative data, indicating relative changes in Ca^{2+} (Bootman et al., 2013a, Bootman et al., 2013b).

Introduction

An important parameter in the selection of a suitable indicator is its affinity for Ca^{2+} , which is measured by the *dissociation constant* (K_d), and should be chosen in function of the range of Ca^{2+} concentrations to be measured during the experiment. Around the K_d the relationship between indicator fluorescence and Ca^{2+} concentration is linear, but outside this range, large changes in Ca^{2+} concentration can be represented by only small changes in fluorescence. Low-affinity indicators (e.g. Mag-Fura-2, Mag-Fura-Red) are suitable for large Ca^{2+} signals, but may barely resolve small Ca^{2+} changes. On the other hand, high-affinity fluorescent Ca^{2+} indicators (e.g. Fura-2, Fluo-3 and Fluo-4) are suitable for relatively small changes in Ca^{2+} concentration, but may become saturated (and therefore not report accurately) by substantial Ca^{2+} changes (Bootman et al., 2013a).

Ca^{2+} indicator dyes are commercially available in three chemical forms: salts, dextran conjugates or acetoxymethyl (AM) esters. This third type of Ca^{2+} indicator dyes are the most modern and were engineered with AM esters to offer a more convenient method for loading hydrophilic dyes into cells. AM dyes are sufficiently hydrophobic in that they are membrane permeable and can be passively loaded into cells simply by adding them to the extracellular medium. Intracellular esterases then cleave the AM group and trap the dye inside cells (Paredes et al., 2008).

Another method to measure the release of intracellular calcium is by using a *luminescent* protein that reacts with the calcium (Toda et al., 2011). Bioluminescent proteins from invertebrate marine animals like jellyfish and other *coelenterates* (e.g. anemones, corals) have been used for measurement of intracellular release of calcium since the 1960s, especially *aequorin*, but also *obelins*, *clytins* and *mitrocomins* (Vysotski and Lee, 2004).

All Ca^{2+} -regulated photoproteins show high sequence homology and contain three “EF-hand” calcium-binding consensus motifs. The EF hand arrangement is a helix-loop-helix structural

domain or *motif* found in many calcium-binding (photo-)proteins in which the Ca^{2+} ions are coordinated by residues within the loop forming a Ca^{2+} binding pocket with a pentagonal bipyramidal geometry (Zhou et al., 2009).

Photoprotein apoproteins (e.g. apoclytin) can be artificially expressed by *Escherichia coli* and then converted into active photoproteins (e.g. clytin) by incubating them with synthetic *coelenterazine* (a light-emitting molecule) under calcium-free conditions in the presence of O_2 and reducing reagents (Shimomura and Johnson, 1975, Inouye and Sahara, 2007). The energy-yielding reaction in photoprotein bioluminescence is an oxidative decarboxylation of the coelenterazine (2-peroxide) moiety of the photoprotein, after the addition of Ca^{2+} , with the release of CO_2 , coelenteramide, apoprotein and the emission of a photon (wavelength corresponding to blue or green for most photoproteins). The oxidized end-product is called *coelenteramide* which is separated from the apoprotein. The oxygen required for the reaction is derived from the peroxy-substitution on the coelenterazine itself and so explains why the reaction kinetics is not influenced directly by the availability of free molecular oxygen (Vysotski and Lee, 2004, Inouye and Sahara, 2007). The main benefit of using luminescence reporting systems versus fluorescence is the reliable measurement of signals from compounds that are fluorescent themselves (autofluorescent), in addition to a reduction of the influence of the testing environment and the artifacts caused by the ligand itself (Toda et al., 2011).

This intracellular Ca^{2+} measurement methodology enables High Throughput Screening (HTPS) of the response of the cells containing the taste receptor to libraries of different ligands (tastants) using automated plate reading systems (Zhang et al., 2008, Meyerhof et al., 2010). Generally, if the ligand activity is confirmed, a dose response experiment is subsequently performed to determine the potency or affinity of the tastant (Behrens et al., 2004). The dose response curve is then fitted by a variation of a 4-parameter logistic model (symmetric

sigmoidal curve around its inflection point), including minimum response, maximum response, half-way between minimum and maximum and the steepness of the curve, or with its simplification, which is a 3-parameter logistic model (Hill's equation), which assumes zero as the minimum response. This equation models receptor data better than any other model. With the sigmoidal curve thus generated it is possible to measure the maximum response, half maximal effective concentration (EC_{50}) and the activation threshold, all of which will help determining the affinity of the tastant with the receptor. The most *potent* agonist (tastant) will be the one with the lowest EC_{50} , and the most *efficacious* agonist (tastant) will be the one with the highest maximum response (Figure 6). *Potency* relates to the amount of drug/tastant needed to produce an effect of given intensity, or the tenacity with which a drug/tastant binds to its receptor (also the affinity, the statistical probability that a drug/tastant will bind to an available receptor at a given time). *Efficiency* relates to the ability of a drug/tastant to produce a maximum response (or signal), or the biological effect produced once the drug/tastant is bound to the receptor (Clarkson, 2016).

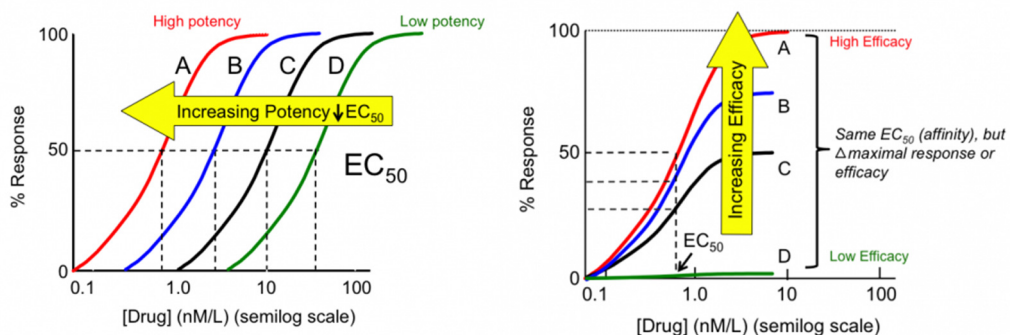


Figure 6. Schematic illustration of drug potency and efficacy (Clarkson, 2016). (LEFT) Dose-response curves for a series of agonists (A, B, C and D) that have the same efficacy, but differ in terms of their potency. The most potent drug (Drug A) has the lowest EC_{50} value. (RIGHT) Dose-response relationships for four agonists that vary in efficacy. Each drug has essentially the same EC_{50} value (equipotent), but differ in terms of the maximum response they can produce at high concentrations that saturate all available receptor sites. Drug A has a relative efficacy that is twice that of Drug C.

After a toxicology risk assessment, the tastants eliciting the strongest response *in vitro* can then be selected for confirmation of the response *in vivo*. If the structure of the receptor of interest (exact model) or a similar receptor (homology model) is known, compounds can also be screened using computer models *in silico* (Morini et al., 2011).

1.4 Involvement of peptides with umami taste in human

Even when peptides are known to contribute to the taste and flavour of food, the potential umami taste of peptides in particular is a controversial subject even in humans (Monastyrskaia et al., 1999, Beksan et al., 2003, Temussi, 2012, Methven, 2012). There is a lot of research literature spanning decades. The early literature, before the year 2000 (mainly from Japanese researchers), is based on human sensory and chemical analysis, with no receptor data.

Peptides are widely found in foods that undergo flavour-generating changes such as hydrolysis or fermentation, for example cheese, soy sauce, protein hydrolysates (casein, soy, wheat, meat, fish, vegetable), miso, sake, fish sauce, maturation of meat and many others (Maehashi et al., 1999). Peptides found in food can have a wide range of bioactive activities, for example, antimicrobial, antioxidant, antihypertensive, opioid agonist and antagonist, mineral-binding, etc. (Van Lancker et al., 2011, Park and Nam, 2015). Peptides can also be precursors of aroma in cooked foods, as their amine residues can take part in the Maillard reaction (Horvat and Jakas, 2004, Van Lancker et al., 2011, Van Lancker et al., 2012).

In relation to taste, it is widely accepted that after hydrolysis, the peptidic fractions with molecular weight lower than 1000 Da (including free amino acids and peptides up to octapeptide size), are generally the taste active ones (Fujimaki et al., 1973), although in

fermented products (e.g. cheese) this size cut off point can be as high as 3000 Da (Lee and Warthesen, 1996, Engel et al., 2001).

Some of the taste-active peptides have been synthesised or isolated and identified in raw materials and then tested using human sensory panels (Kirimura et al., 1969, Tamura et al., 1989). There are natural or synthetic peptides linked to all taste modalities (i.e. bitter, sour, salty, sweet and umami), however, bitter is the taste modality better described for small peptides, where links between hydrophobicity and size of the amino acids in the sequence, spatial conformation, sequence order and length have been related to bitterness (Ney, 1971, Ishibashi et al., 1988, Kim and Li-Chan, 2006).

Whilst there is evidence that acidic fractions from protein hydrolysates have a savoury/umami taste for humans which has been attributed to peptides (Arai et al., 1972, Fujimaki et al., 1973, Noguchi et al., 1975), most of the peptides reported in this early work normally contained L-glutamic acid (Glu; E) or L-aspartic acid (Asp; D) in their sequence, and were hydrophilic, acidic and polar in nature (Arai et al., 1973, Ohyama et al., 1988, Kuramitsu et al., 1996). Nevertheless, some peptides containing other amino acid residues were also reported as umami, but in many cases this was not the only taste modality identified (Ishibashi et al., 1988, Tamura et al., 1989).

An important discovery from this period, based only on human sensory panel data (before the umami taste receptor was discovered), was the “beefy-meaty” or “delicious” octapeptide from a beef extract obtained with papain, which was reported to have umami taste and later synthesised (Yamasaki and Maekawa, 1978, Yamasaki and Maekawa, 1980). This peptide, which contains L-glutamic and L-aspartic acid in its sequence (Lys-Gly-Asp-Glu-Glu-Ser-Leu-Ala; KGDEESLA), was also described by many other researchers as umami (Tamura et al., 1989, Nakata et al., 1995, Spanier et al., 1995, Wang et al., 1996). However, the umami taste of this peptide was later challenged (van Wassenaar et al., 1995, Hau et al., 1997). This is not unusual

in flavour and sensory science, and there is a lack of consensus in the scientific literature on the identification of umami tasting peptides for human (van den Oord and van Wassenaar, 1997, Temussi, 2012, Methven, 2012).

Some of the causes for these taste descriptor discrepancies are summarised in Table 1. The complexity of the peptide tastes cannot in many cases be described by panellists as coming only from one taste modality (Solms, 1969, Kirimura et al., 1969). The vehicle used for tasting the sample (e.g. in water or broths), the purity, pH and the concentration of the sample (van Wassenaar et al., 1995), the sensory methodology and the characteristics of the panellists (Bartoshuk and Beauchamp, 1994, Satoh-Kuriwada et al., 2014, Running, 2015) can also contribute to the variety of descriptors given.

Table 1. Summary of the possible causes of discrepancy in the reported taste descriptors of peptides.

A - Compound-related	<ul style="list-style-type: none">• Concentration used in relation to threshold• pKa of the compound (acid-base properties)• Optical activity (D/L, R/S, Z/E)• Mixture of isomers (racemic, cycles)• Purity (plus pure vs in salt form) and solubility• Dissolved or crystalline• Stability (oxidation, hydration, decomposition)• Taste of possible degradation products• Complexity of taste (multimodal)
-----------------------------	---

(Continues in next page)

Table 1 (cont.). Summary of the possible causes of discrepancy in the reported taste descriptors of peptides.

B - Matrix-related	<ul style="list-style-type: none"> • pH of the matrix • Presence of taste enhancers • Use of salty water as background • Use of tastant mixtures as background (interactions) • Use of broths (meat, fish or vegetable) • Use of oil or emulsions to deliver the taste • Texture of the sample
C - Sensory methodology-related	<ul style="list-style-type: none"> • Panel methodology • Level of bias towards Type I or Type II errors • Training of panellists • Sensory room environment • Standards used (references) and scales • Single or multiple descriptor allowed • Separation of aroma and taste (nose clips) • Peer pressure and researcher aim bias
D - Panellist-related	<ul style="list-style-type: none"> • Age and Gender • Health and nutritional status • Background diet and previous exposure • Cultural influences • Genetics [<i>ageusia</i>/lack of all taste perception or taste-specific <i>ageusia</i> (e.g. lack of bitter taste only) driven by gene polymorphisms]

More recently, and after the discovery of taste receptors for umami molecules, many peptides from raw materials and extracts, fermented products and hydrolysates have been reported as umami, with different levels of scientific evidence:

(a) In some cases, the raw material has been fractionated with physicochemical techniques, the umami fractions have been sensory-tested and then further analysed with the attribution of taste to the peptide pool present in the fraction, without chemically identifying or characterizing any particular peptide (Apriyantono et al., 2004, Bagnasco et al., 2013).

(b) In some other cases, the identification of some of the peptides has been only tentative without comparison with reference standards (Yamamoto et al., 2014).

(c) Other researchers reported purified or synthetic peptides as umami-enhancing, but they had not been sensory-tested on their own, but in a flavoured mixture, like chicken or beef broth, MSG or salty solutions, which caused the peptides to be kokumi-active instead of umami active, especially if they did not have taste on their own (Ueda et al., 1997, Park et al., 2002, Dunkel et al., 2007, Dunkel and Hofmann, 2009, Toelstede et al., 2009, Liu et al., 2015).

(d) There has been also some research done on assigning taste attributes to peptides by statistically correlating their levels in food (e.g. in soy sauce) with the sensory attributes of the food (e.g. umami), using multivariate analysis techniques such as orthogonal PLS regression (Yamamoto et al., 2014).

Therefore, it is very difficult to differentiate between:

- (i) Peptides having really an umami taste.
- (ii) Umami-enhancing peptides (often referred as kokumi peptides).
- (iii) Peptides that have no taste at all (as what was being tasted was the background).

- (iv) Peptides that are at high levels in umami foods or umami-tasting fractions (*correlation*) but are not necessarily umami themselves (*causation*).

For example, the small molecular weight (< 500Da) fraction of soy sauce contains numerous peptides, including glutamyl-peptides, and its taste is strongly umami, however the *cause* of the umami taste is the free L-glutamic and L-aspartic acid, not the presence of glutamyl-peptides (*correlation*), as described by Lioe et al. (2006).

In spite of these challenges, there are many umami raw materials which have been relatively recently claimed to contain umami peptides, such as soy sauce (Zhuang et al., 2016), cheese (Gómez-Ruiz et al., 2007), dry-cured ham (Dang et al., 2015), fish and fish sauce (Park et al., 2002, Hou et al., 2011, Zhang et al., 2012), rice by-products (Hamada et al., 1998, Bagnasco et al., 2013), wheat gluten hydrolysate (Schlichtherle-Cerny and Amado, 2002) and peanut hydrolysate (Su et al., 2012), amongst others. Some of these have also been challenged, and the umami taste has been re-assigned to other compounds different to the peptides, such as free L-glutamic acid and free L-aspartic acid in the presence of salt in cheese (Salles et al., 1995, Salles et al., 2000, Andersen et al., 2008, Zhao et al., 2016), dry-cured ham (Sentandreu et al., 2003) and in soy sauce (Lioe et al., 2004, Lioe et al., 2006, Lioe et al., 2010).

1.5 Focus of this research on linear α -L-dipeptides

In the previous section, the controversial aspect of umami peptides in human sensory has been described (especially Glu- and Asp-related), and the conclusion is that it is not clear if peptides have umami taste on their own for human, and if this is the case it is probably weak, and dependant on other components in the matrix, such as free amino acids, salts, nucleotides and organic acids (Gómez-Ruiz et al., 2007, Lioe et al., 2010). Even when umami taste

characteristics are still being reported for peptides today, the most widely agreed role of peptides in taste seems to be *enhancers* of umami and other tastes, or subtle contributors to the *body* or flavour completeness of the food (Kirimura et al., 1969), especially in the case of the kokumi-active gamma-glutamyl peptides (Toelstede and Hofmann, 2009, Hillmann et al., 2016).

The diversity of peptide structures and the complexity of the physical, chemical and biological properties of peptides has been explored in the previous review, and, as a result, it was required to narrow down the scope of this project to only a smaller family of peptides: linear α -L-dipeptides, and leave out taste-active variations that do not help to test the hypothesis that dipeptides formed from at least one umami taste-active L-amino acid are taste-active for cats. Linear α -L-dipeptides are the simplest peptides of all (Figure 7), and they are the next step from the free L-amino acids in order to hypothesise structure-activity relationships (SAR) (Belitz and Wieser, 1985, Grigorov et al., 2003).

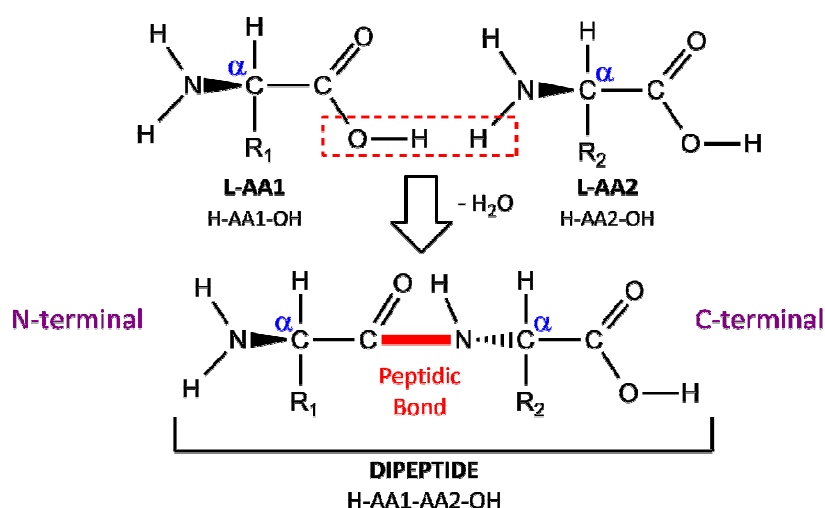


Figure 7. Peptidic bond between two L-amino acids generating an alpha-L-dipeptide

Table 2 lists what is in scope and out of scope for this project. As there are 20 *proteogenic* amino acids (capable of producing proteins), there are 400 different possible α -L-dipeptides (as a different order of the amino acids in the peptide produces different dipeptides). From these, there are 319 containing at least one umami taste-active L-amino acid and 121 containing two umami-taste active amino acids (best case scenario; reduced/focused list). This list of 121 was also further reduced due to some dipeptides derived from umami-active amino acids not being commercially available, as it is explained in the next section.

Table 2. Scope of the research contained in this Thesis

In scope for this Thesis	Out of scope for this Thesis
✓ Dipeptides only (two residues)	☒ Peptides with > 2 residues
✓ α -amino acids and peptide bond	☒ D-amino acids
✓ L-amino acids in the dipeptide only	☒ Beta-amino acids
✓ Proteogenic amino acids	☒ Cyclic dipeptides (Diketopiperazines, DKPs)
✓ Chemically un-modified	☒ Chemically modified (esters, phosphates)
✓ From amino acids active <i>in vitro</i> with the feline umami receptor	☒ Pyro-glutamyl dipeptides
	☒ γ -glutamyl or β -aspartyl dipeptides

1.6 Possible involvement of peptides with umami taste in cat

Humans can perceive only L-glutamic and L-aspartic salts as umami (Kawai et al., 2012), and perceive most of the other L-amino acids as sweet, bitter or sour. The perception of L-amino acids as umami by humans is different to other mammals (e.g. mice, pig, dog and cat) due to specific changes in their umami taste receptor (hT1R1-hT1R3), both in the orthosteric site and

in other parts of the receptor, which make it narrowly-tuned (Toda et al., 2013, McGrane, 2013).

In the mouse, as the five main residues for L-glutamate binding according to (Zhang et al., 2008) are conserved versus human, then additional residues critical for amino acid recognition must be responsible for these differences. Moreover, the mouse umami receptor is widely tuned.

The mouse umami receptor responds to 11 amino acids *in vitro* when tested alone: Glycine, L-alanine, L-serine, L-glutamine, L-histidine, L-methionine, L-cysteine, L-threonine, L-valine, L-arginine and L-asparagine, but when tested with IMP, seven additional ones become active: L-aspartic acid, L-glutamic acid, L-lysine, L-proline, L-leucine, L-phenylalanine and L-Isoleucine, accounting for a total of 18 L-amino acids. Additionally, there is a synergistic enhancement of the response of the previous 11 amino acids in the presence of IMP due to synergy (Nelson et al., 2002). From the research just mentioned, it is also important to highlight that the response to the acidic amino acids in mice was found to be much weaker compared with the other amino acids, opposite to human.

According to Toda et al. (2013), the combination of two distinct determinants, amino acid selectivity at the orthosteric site and receptor activity modulation at the non-orthosteric sites, may mediate the ligand specificity of T1R1/T1R3. Toda et al. (2013) compared the umami responses to L-amino acids *in vitro* with the human and mouse receptors (Figure 8), and found, using human-mouse receptor chimeras, site directed mutagenesis and *in silico* modelling that the extracellular Venus fly trap domain (VFT) in the T1R1 was the critical domain for both human-type and mouse-type amino acid recognition.

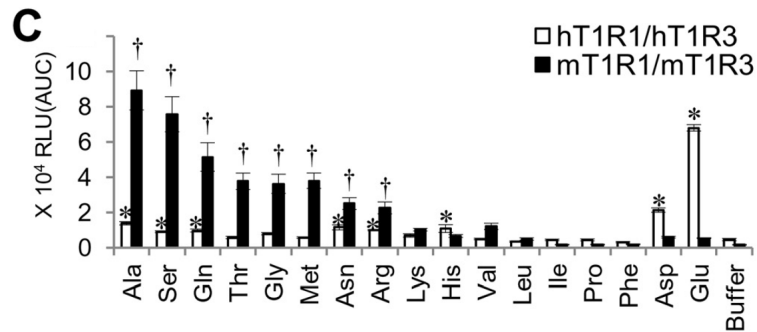


Figure 8. Comparison of the *in vitro* response patterns of human and mouse umami receptor to 50 mM of different amino acids (Toda et al., 2013).

According to Toda et al. (2013), there are six key amino acid residues for acidic amino acid ligand recognition in human and mice, although Ala-170 and Ala-302 in hT1R1 (Glu-171 and Asp-303 in mT1R1) are the most critical as they are paired at the edges of the upper and lower lobes of the L-glutamate binding site, respectively. Five of the residues are located in the hinge region, but Asp-435, is located outside. There are also six residues that are critical for the broadly tuned response to amino acids (Table 3), but these lie in regions that are distinct from the orthosteric binding site, four of them close to the predicted IMP binding region near the cleft of the VFT and the other two (Met-320 and Lys-328) in other sites in the VFT.

Table 3. Comparison of key residues for acidic amino acid recognition or broadly tuning to amino acids for human and mouse [adapted from Toda et al. (2013)].

Key residues for acidic amino acid recognition						
Human	S148	R151	A170	E174	A302	D435
Mouse	N149	H152	E171	V175	D303	K436
Key residues for broadly tuning to amino acids						
Human	R307	M320	K328	K377	K379	K460
Mouse	T308	T321	Q329	E378	G380	E461

Introduction

These researchers found that the residues that are critical for broadly tuned responses modulate the receptor activity in a manner that is distinct from that of IMP (Toda et al., 2013).

Furthermore, acidic amino acid recognition is primarily attributable to the properties of the orthosteric ligand binding site, and the differences between human T1R1 and mouse T1R1 affect the electrostatic profile of this region. Moreover, the mutation of A170 (human) to E-171 (mouse) is expected to affect acidic amino acid binding due to the electrostatic repulsion between the negative charges of the carboxylic acid moieties (Toda et al., 2013).

On the other hand, the six residues that are responsible for the mouse-type broadly tuned response modulate the activities of not only the ligands of mT1R1/mT1R3 but also acidic amino acids, which are assumed to bind at the orthosteric binding site. This modulation could affect the conformational change that affects the association and/or dissociation rate of ligands at the orthosteric site (affinity), and/or affect the signalling capacity after the binding of the amino acid to the orthosteric binding site (efficacy). Other researchers proposed that Arg-307 in human T1R1 (Table 3) was critical for preventing a broad amino acid recognition and suggested that the presence of a neutral polar residue such as Thr in mouse T1R1 at this position rather than Arg (which is a charged polar residue) allows a wider range of L-amino acids to enter and interact with the orthosteric ligand binding site (Roura et al., 2011).

In cats, distinct from human and mice umami receptors, 11 out of the 20 proteogenic amino acids can bind to the cat umami receptor fT1R1-fT1R3 heterodimer *in vitro* in the presence of IMP: Glycine, L-alanine, L-serine, L-leucine, L-histidine, L-methionine, L-cysteine, L-phenylalanine, L-tryptophan, L-tyrosine and L-asparagine (McGrane, 2015). In terms of the orthosteric site for L-glutamate, and in particular the two most critical residues indicated by Toda et al. (2013) (Table 4), the residues are the same as in the mouse (and also the same as in pig, dog and rat), so it is consistent with the cat umami receptor being broadly tuned as well.

Table 4. Amino acid residues at positions 170 and 302 in the T1R1 active site for different species (McGrane, 2013)

Species	Amino Acid position	
	170	302
Human	Ala (A)	Ala (A)
Pig	Asp (D)	Asp (D)
Cat	Glu (E)	Asp (D)
Dog	Glu (E)	Asp (D)
Mouse	Glu (E)	Asp (D)
Rat	Glu (E)	Asp (D)

An example of binding of the amino acid L-serine to the feline umami receptor in the orthosteric site can be seen in Figure 9. These 11 amino acids activating the feline umami receptor *in vitro* have very different chemical properties in terms of hydrophobicity, charge and acidity due to the variety of side chains, which makes it difficult to hypothesise any structure-activity relationships (SAR).

Given the taste receptor differences between species, it is reasonable to hypothesise that the fact that no umami-tasting α -L-dipeptides have been confirmed un-challenged in human [with only two umami-active amino acids, Glu (E) and Asp (D)], does not mean there are no umami dipeptides for other mammalian species such as cats, having a more broadly-tuned umami receptor (with 11 umami-active amino acids). There are several differences between the amino acid residues in the VFT for the different species, which suggests that the human umami mechanism is not representative of all species. Furthermore, the prediction of ligand specificity requires modelling the whole VFT region, not only the orthosteric (active) site, and ideally support from additional *in vivo* and *in vitro* experiments (Toda et al., 2013; McGrane, 2013).

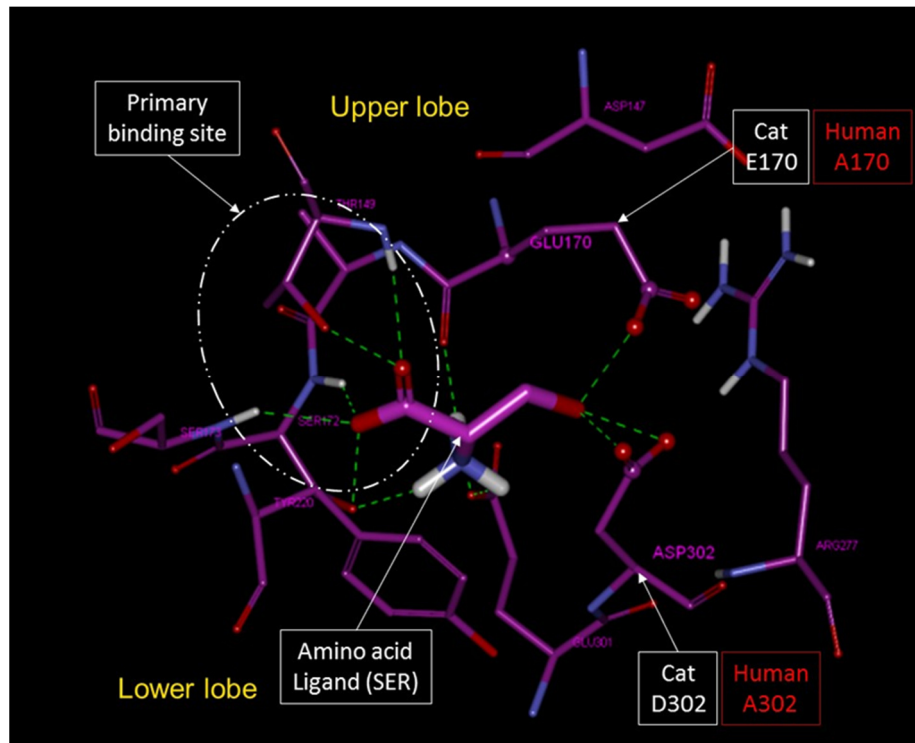


Figure 9. *In silico* modelling of L-serine binding to the feline umami receptor (McGrane, 2013).

This is the key novel aspect of this research project, which will investigate the response *in vitro* of the feline umami receptor ft1R1-ft1R3 to a selection of α -L-dipeptides constituted by pair combinations of the 11 L-amino acids known to activate the feline umami receptor *in vitro*. As the scope is only linear dipeptides constituted entirely by the 11 umami-active amino acids, there are 121 different α -L-dipeptides to study within this project (i.e. 11 x 11). Only commercially available dipeptides will be tested (there will not be synthesised as part of this project). If active umami dipeptides are discovered, it would expand the understanding of umami taste perception in cats and its differences with human.

1.7 Aims of this MRes Project

Fermented raw material extracts and protein hydrolysates (rich in small peptides) can deliver taste and are often included in animal feeds. We are interested in more fully understanding the profile of peptides that may be found in such extracts and hydrolysates that stimulate the umami receptors in cats. This information will drive raw material selection for cat feed formulations. Based on the literature review, it was found that the umami perception of linear dipeptides by cats has yet to be studied. Given the large number of possible dipeptide combinations, and in order to focus the experimental work whilst maximising the chance of success of the project, only dipeptides containing entirely amino acids active *in vitro* when screened with the cat umami receptor fT1R3-fT1R3 heterodimer will be studied. For the sake of being concise throughout the thesis the cat umami receptor fT1R1-fT1R3 heterodimer will be referred as fT1R1-fT1R3. Although the cat may have other taste receptors that are activated by umami compounds (e.g. mGluRs) these alternative umami receptors are out of scope for this thesis.

- Aim: Determine if linear α -L-dipeptides containing active amino acids are active *in vitro* when screened with the feline umami receptor fT1R1-fT1R3 heterodimer, using a range of different experimental conditions.
- Project hypothesis: There will be some linear α -L-dipeptides active *in vitro*. Dipeptides containing L-amino acids, known to be umami taste active in cats, will stimulate the fT1R1-fT1R3 receptor.
- Objectives:
 - Source candidate dipeptides.
 - Select a suitable *in vitro* model to test feline umami perception.
 - Validate the selected *in vitro* method.

Introduction

- Test a library of dipeptides using fluorescence and luminescence assays in different conditions.
- Summarise the conclusions.
- Interpret the results using *in silico* modelling inputs.
- Make recommendations on next steps

2 Materials and Methods

The *in vitro* experiments were performed at the Mars Inc. Laboratories at WALTHAM® (Melton Mowbray, Leicestershire, UK) and at the laboratory of a Mars Inc. external research partner (confidential). The *in silico* experiments were performed at BioPredict Inc. (Oradell, NJ, USA).

2.1 *In vitro* experiments

2.1.1 Cell type

The cells used were human embryonic kidney cells (HEK293T) sourced from a Mars inc. external research partner expressing stably a chimeric G-protein α -subunit. The full description of the cells used is: *HEK293T-pEAKrapid / mG15i1 / pSwitch / fTas1r1 (inducible) / fTas1r3 / NatClytin cells*.

The HEK cell type was a commercially available version chosen for its versatility. The G-protein for receptor coupling was a G15 mouse chimera i1 enabling Ca^{2+} release in the signal transduction (which was the method used to measure receptor activation). The cells included an inducible expression system with Mifepristone enabling expression of the feline T1R1 and dimerization with the feline T1R3 already expressed in the stable cell line. Additionally, the cells contained a chimeric version of the photoprotein Clytin-1 with a tag from another natural *Clytin* to facilitate the expression in the mitochondrial membrane (the expression of this photoprotein allowed the same cell line to be used not only in fluorescence but also in luminescence experiments).

2.1.2 Cell culture and induction of fT1R1-fT1R3 receptor expression

Reagents and media were obtained from commercial sources. The HEK293T cells had been previously stably transfected with *fTas1r1 (inducible)* / *fTas1r3* umami taste receptor gene and stored frozen at -80°C with 10% DMSO until use.

The 2 ml vials containing the cells were thawed and mixed in a Corning™ Falcon™ 50 ml conical centrifuge tube with 10 mL of media made with DMEM GlutaMAX™ (Life Technologies, Thermo Fisher Scientific; Waltham, MA, USA) containing 1% antibiotics (Penicillin-Streptomycin) from Invitrogen and 10% of heat-treated dialysed FBS (foetal bovine serum) from Invitrogen (referred to as “plating media” in this document). The tube was then centrifuged at 125-g for 5 minutes at room temperature to separate the cells from the DMSO-containing media.

The cells were then re-suspended in 25 mL of plating media and plated in poly-D-lysine 384-well plates from Corning (Corning, NY, USA) at a density of 17500 cells/well (700 cells/μl). After 24 hours in culture at 37°C with 10% CO₂, fT1R1 receptor expression was induced in half of the cell wells with 1 μM Mifepristone from Invitrogen (Carlsbad, CA, USA) diluted in ethanol (induced cells expressing the receptor). The other half of the cell wells were treated with an equivalent innocuous volume of ethanol (mock, un-induced or control cells).

The cells were then incubated for a further 24 hours at 37°C with 10% CO₂.

2.1.3 Fluorescence indicator loading

The physiological buffer for the fluorescence (and luminescence) cell assays was a Tyrode's buffer consisting of 130 mM NaCl, 5 mM KCl, 2 mM CaCl₂, 5 mM NaHCO₃, 1 mM MgCl₂ and 20 mM HEPES, and adjusted to pH 7.4 with 10 mM NaOH solution. All the buffer components as

well as the NaOH solution used to adjust its pH were cell culture grade (or molecular biology grade) and purchased from Sigma-Aldrich (St. Louis, MO, USA).

The calcium dye used was Fluo-4AM packed for HTPS (Molecular Probes, Eugene, OR, USA) dissolved in DMSO, and it was prepared in Tyrode's buffer with the addition of water-soluble Probenecid (Molecular Probes, Eugene, OR, USA), which is an anion transport inhibitor used to slow the process of dye extrusion from the cells. Final concentrations in the fluorescent dye preparation were 2.5 mM Probenecid and 2 μ M Fluo-4AM.

The 384-well plates containing the HEK cells at this point expressing the feline T1R1-T1R3 receptor were taken out of the incubator, checked for normal growth and adhesion to the plate (about 90-100% confluency) and the media removed. Then 100 μ l of the fluorescent dye preparation were added to each well, and the cells were incubated for 30 min at 37°C with 10% CO₂ in the incubator. Then the cells were incubated for a further 30 min in the dark at room temperature (standard aerobic conditions). These two incubations had the aim of optimally loading the cells with the fluorophore.

The excess fluorescent dye was then washed using a 16-channel Biochrom Asys Atlantis microplate washer (Biochrom, Cambridge, UK) when the readings were performed at WALTHAM or with a 384-channel Biotek automated plate washer (Winooski, VT, USA) when the readings were performed at the external research partner laboratories.

2.1.4 Preparation of the cells for Luminescence assay

The protocol for cell culture and induction of fT1R1-T1R3 receptor expression was the same as in the fluorescence assay, only that a Ca-fluorescence dye was not loaded into the cells and a plate washer was not necessary. Instead, the cells were incubated for 3 hours in the dark with

coelenterazine and oxygen in the presence of Glutathione (GSH) (final concentrations 10 μ M coelenterazine and 30 μ M GSH). After this period the cells were ready for the experiment.

The photoprotein formed (Clytin) containing coelenterazine 2-peroxide reacted later in the microplate reader with the intracellular calcium Ca^{2+} released in the signal transduction cascade, with formation of coelenteramide, CO_2 , apoclytin and the emission of light (λ max \sim 470 nm) which constituted the luminescence signal.

2.1.5 Fluorescence readings

Straight after washing, the 384-well plates were sent to the microplate reader. This was a desktop FlexStation 3 (Molecular Devices Co., Sunnyvale, CA) when working at WALTHAM or a Fluorometric Imaging Plate Reader, FLIPR^{TETRA} station (Molecular Devices) when at the external research partner laboratories (see Figure 10), which is a high throughput screening (HPTS) instrument.

The HEK cells expressing the feline T1R1-T1R3 receptor were then challenged with different agonists (alpha-dipeptides, 101 in total) which were tested at 1, 10 and 100 mM (primary screening) or at a wider range of concentrations with eight different concentration levels (dose response experiments).

The dipeptides used, were purchased from Bachem (Bubendorf, Switzerland) (84 out of 101) and from PE Biosciences (Shanghai, China) (17 out of 101) and were all of a purity \geq 90%. The umami activation reference controls, L-alanine and inosine monophosphate (IMP) and all L-amino acids were used in the assay and were purchased from Sigma-Aldrich. The concentrations used as umami reference signal to calculate the % activation were 100 mM L-alanine with 1 mM IMP, due to L-alanine having a strong and robust response at this concentration in the *in vitro* assay in the presence of IMP (at 100 mM the maximum response

of L-alanine is normally reached). Furthermore, in the water panel (*in vivo*) the cats give a very clear response with this combination of tastants. The selected concentrations are therefore physiologically relevant to the cat from a taste point of view. These concentrations are also relevant by the natural levels found in the diet of cats. The additional cell health and functionality controls, ATP and Isoproterenol, were also purchased from Sigma-Aldrich.



Figure 10. FlexStation 3 (left) and FLIPR^{TETRA} (right) microplate readers (Molecular Devices).

The FLIPR is a high-throughput screening (HTPS) instrument: It takes around 1 min reading per plate vs. around 50 min per plate in the FlexStation.

Clear compound plates (384-well type from Corning) were loaded with 100 μ l of agonist, either dissolved in just Tyrode's buffer, or in buffer with IMP and/or L-alanine. All the agonist concentrations were double (x2) to the intended final concentration to compensate for the residual cell media. The plate readers followed a single injection protocol.

In the FlexStation 3, changes in fluorescence intensity (excitation at 485 nm, emission at 525 nm, and cut-off at 515 nm) were monitored at 2s intervals, with 3 readings per well. The scanning continued for 90s (reaching 45 reads in total). A parallel protocol was followed for the FLIPR^{TETRA}.

The response was expressed as the Δ RFU (delta relative fluorescence units) calculated as the difference between the maximum and the minimum fluorescence values. The responses were averaged from at least three wells receiving the same stimulus.

The signal/background ratios and EC_{50} values for the ligand-receptor interactions were determined from the concentration-response curves generated using SoftMax[®] Pro[™] v5.4.1 software (Molecular Devices). The signal / background ratio was determined as the maximum signal / minimum signal. The obtained calcium signals were corrected for the response of mock transfected cells and normalized to the fluorescence of cells prior to the application of the stimulus using $\Delta F/F = (F-F_0)/F_0$.

2.1.6 Luminescence readings

After 3 hours incubation with coelenterazine and GSH, the cells were sent to the high throughput screening microplate reader. This was a Fluorometric Imaging Plate Reader, FLIPR^{TETRA} (Molecular Devices) when working at the external research partner laboratories.

No Luminescence work was done at WALTHAM, although it would have been possible following the same protocol using the FlexStation 3 instrument.

The HEK cells expressing the feline T1R1-T1R3 receptor and also expressing the photoprotein which was then activated were then challenged with the same agonists and controls as before in the fluorescence experiments (the only difference was the type of calcium release measurement).

Compound plates were loaded with 100 μ l of ligand solution in each well, prepared exactly in the same way as for the fluorescence assay. The plate readers followed again a single injection protocol. In this case, luminescence measurements were made (maximum emission around

470 nm) and were monitored at 1s intervals, with 3 readings per well. The scanning continued for around 60s (reaching around 60 reads in total).

The response was expressed as relative luminescence units (RLU) being the minimum luminescence value being always zero, or % normalised response (using the reference umami response as comparison). The responses were averaged from at least four wells receiving the same stimulus. The signal/background ratios and EC₅₀ values for the ligand-receptor interactions were determined using ScreenWorks® Peak Pro™ software (Molecular Devices). The signal / background ratio was determined as the maximum signal / minimum signal.

2.1.7 *In vitro* data analysis

2.1.7.1 *Full library of 101 dipeptides screening (Fluorescence data only)*

SoftMax® Pro was used to run the FlexStation 3 microplate reader but also to visualise and analyse the initial primary screening fluorescence data and the initial dose response experiments data. The primary screening results were calculated as the average of the maximum response of six wells for each concentration tested, with the error expressed as %CV.

For the dose response curves, the compounds were measured at least in triplicate at different concentrations (eight, including blank, up to 100 mM) in order to determine the umami activity of the compound tested. Each data point was calculated as the average of the maximum response of at least three wells for each concentration tested, with the error expressed as %CV. The EC₅₀ values and maximum response for the receptor activation by the ligand were estimated from the concentration dose response curves generated using SoftMax® Pro, with some basic statistical parameters (e.g. standard error of the mean) which were not easy to visualise. Thus, some of the dose response data were re-plotted using Prism 7 for windows v7.01 (GraphPad software, La Jolla, CA, USA) in order to determine additional statistical error parameters for the EC₅₀ and maximum response.

2.1.7.2 *Selected subset of dipeptides (33 samples) screening*

ScreenWorks® Peak Pro™ was used to run the FLIPR^{TETRA} microplate reader but also to visualise and analyse the data at the external research partner laboratories. Further data analysis and visualisation using non-linear regression techniques were done with JMP v12 (SAS Software, Cary, NC, USA), and Prism 7® for windows.

The **fluorescence readings** for each data point in the protocol were recorded for 120 s. The raw data were analysed using ScreenWorks® and then plotted using Prism 7®. All the wells were visualised first in ScreenWorks® and the compounds responding at the maximum concentration were examined more in detail, to see if the response was dependent on the concentration. The averages of each measurement were taken from four replicates.

In order to avoid considering the anomalous spike in fluorescence after injection as real data (when is probably an optical phenomenon), or the decrease in fluorescence after injection, and in order to identify local peaks of activation, only the data recordings from 20s to 60s (first cut) and 15s to 50s (second cut) were exported to Prism 7® response analysis. For the data from 20s to 60s, the minimum response was subtracted from the maximum response to correct for a decrease of fluorescence below baseline. The analysis of only certain time ranges was done because the big peak of perception in the “standard umami” control (100 mM Ala + 1 mM IMP) usually happens at around 30s in the fluorescence assay.

The readings were plotted both as maximum RFU (over/under baseline) and standardised as $\Delta F/F$ (where a “1” would mean a 100% or double activation than baseline). EC_{50} values were calculated for each of the active dipeptides.

The **luminescence readings** for each data point in the protocol were recorded for 60 s. As with the fluorescence experiment, the raw data were analysed using ScreenWorks® and then plotted using Prism 7®. All the wells were visualised first in ScreenWorks® and the compounds responding at the maximum concentration were examined more in detail, to see if the response was dependent on the concentration. No time cut-offs were done as luminescence as it was expected to have less interference than in fluorescence and a clear sharp luminescence signal at around 20s.

The readings were plotted both as maximum RLU and standardised (as a %) using the maximum luminescence response of the umami mixture 100 mM Ala + 1 mM IMP as the 100% benchmark. EC₅₀ values were calculated for each of the active dipeptides.

2.2 *In silico* experiments

2.2.1 Molecular modelling

All *in silico* work was performed by BioPredict (Oradell, NJ, USA). Three-dimensional homology models of the feline T1R1 flytrap domain (active site) were produced based on known crystal structures from Metabotropic Glutamate Receptors (e.g. mGluR1) from the Protein Data Bank (PDB), using computer modelling programs such as Biovia Discovery Studio Visualizer and modeller (Accelrys - Dassault Systèmes Software, Vélizy-Villacoublay, France).

The active compounds detected were docked and the model optimised using Chemistry at Harvard Macromolecular Mechanics simulations (Charmm) and Charmm Force Field (CFF), which are molecular dynamics simulation programs (in the specialist program for ligand-protein interactions, the force fields are calculated using atomic partial charges derived from complex quantum mechanics calculations of the interactions between model compounds and water as solvent with the protein).

Hydrogen bonds, hydrophobic interactions, salt bridges, Van der Waals parameters, cation-pi, aromatic pi-pi, and other interactions were measured for each docking scenario.

Energetic optimization was performed at each stage by adjusting translation, rotation, ligand bond rotation, and side-chain rotations for selected protein side chains. Constraints were imposed using the Method of Lagrange Multipliers. Relative free energies of binding to the fT1R1-fT1R3 receptor were evaluated by comparing energies of optimised unbound ligands and unbound protein (receptor) to ligand-protein complexes.

As the focus of this project was an *in vitro* study, the screening of the dipeptides was conducted using the cat umami fT1R1-fT1R3 heterodimer *in vitro* assay. The *in silico* modelling was used *a posteriori* to identify key binding interactions resulting in the activation of the T1R1T1R3 receptor by the dipeptides and not *a priori* as a screening tool. Hence, the *in silico* modelling was conducted by the modellers with a knowledge of the results from the *in vitro* screening.

3 Experimental Results and Discussion

Two types of experiments were run as part of this research project: *in vitro* and *in silico*. The results from the *in vitro* experiments were divided in different sections: First, an initial whole peptide library screening (only using Fluorescence in a FlexStation instrument) and second, a focused screening of a selected group of dipeptides (using both Fluorescence and Luminescence in a FLIPR instrument). The initial FlexStation experiments were performed at the Mars Inc. laboratories at WALTHAM® (Melton Mowbray, Leicestershire, UK) and the focused FLIPR experiments were performed at the laboratory of a Mars Inc. external research partner (confidential). The final active dipeptides identified from the *in vitro* experiments were subsequently tested *in silico*, at BioPredict Inc. (Oradell, NJ, USA).

The objective was to generate data in order to be able to answer the following questions after finishing all the *in vitro* and *in silico* experiments:

1. Which of the dipeptides are active?
2. Can the non-specific responses observed be assigned to a particular cause such as the experimental conditions or the compounds?
3. Is it possible to differentiate between auto-fluorescence and non-specific responses?
4. Do dipeptides with different batches from the same supplier or from a different supplier perform equally?
5. Do the experiments suggest a different activation mechanism for the dipeptides?

3.1 Overview and sequence of the experiments conducted

This research project on the umami activity of dipeptides with the ft1R1-ft1R3 receptor was conducted in the following sequence:

- I. Selection and acquisition of the final 101 dipeptide library samples.
- II. Preliminary experiments to determine the optimum conditions for the assay.
- III. Screening of all the 101 dipeptides using a fluorescence assay (on the FlexStation), in two conditions: **(a)** dipeptide dissolved in IMP plus Tyrode's buffer and **(b)** dipeptide dissolved in just Tyrode's buffer. This screening was run as a simplified "primary" screening, in which only three concentrations were tested (1, 10 and 100 mM) in order to rapidly select the potentially active dipeptides.
- IV. A subset of potentially active dipeptides from the primary screening (six) were then tested in dose response mode (fluorescence assay in the FlexStation) in two conditions: **(a)** IMP and buffer and **(b)** just buffer in order to determine their activity and estimate dipeptide potency (half-maximal response, EC₅₀) and efficacy (maximum response).
- V. A selected subset of dipeptides (30, plus three replicates) were then screened using both a fluorescence and a luminescence assay [in a higher throughput plate reader (FLIPR)], in three conditions: **(a)** dipeptides dissolved in IMP plus Tyrode's buffer, **(b)** dipeptides dissolved in L-alanine plus Tyrode's buffer and **(c)** dipeptides dissolved in just Tyrode's buffer. This was run as a full "dose response" screening, in which eight concentrations following a logarithmic dilution series were tested. The control (un-induced cells) was only tested in one condition (IMP plus buffer).
- VI. Computer models of the active dipeptides were developed using a homologous model of the FT1R1-FT1R3 receptor (*in silico* experiments) in order to ascertain possible molecular mechanisms of interaction with the receptor.

3.2 Dipeptide library tested

As mentioned in the previous Chapters, only linear α -L-dipeptides generated by combining the 11 L-amino acids activating the feline umami receptor fT1R1-fT1R3 (Gly, Ala, Leu, Ser, Met, Cys, Asn, His, Phe, Trp and Tyr) were used.

From a possible library of 121 dipeptides (11 x 11), 21 of them contained Cys in either the N-terminal (first-) or C-terminal (-second) position in the dipeptide. However, only two Cys-containing dipeptides (Gly-Cys and Cys-Gly) were tested, as the others could not be purchased from a catalogue or custom-synthesised as they were unstable in monomer form due to oxidation of their –SH group. In addition, the synthesis of one dipeptide (Ser-Trp) also failed (custom synthesis from a commercial source, PE Biosciences) so it could not be tested. In the end, the final library contained 101 dipeptides from two different suppliers: Bachem (84 dipeptides) and PE Biosciences (17 dipeptides).

At a later stage and for quality control purposes, two additional replicate samples of dipeptides in the list of 101 (Asn-His and Asn-Leu) were purchased from a third supplier (AnaSpec, Cambridge Bioscience, UK).

In terms of purity, 84 dipeptides tested had a purity of at least 95%, and the remaining 17 had a purity of at least 90% (Phe-His, Phe-Asn, His-Asn, Asn-Ala, Asn-Phe, Asn-Gly, Asn-His, Asn-Leu, Asn-Met, Asn-Asn, Asn-Ser, Asn-Trp, Asn-Tyr, Trp-His, Tyr-Met, Tyr-Asn and Tyr-Ser).

Dipeptides were given a code (DP1 to DP101) to facilitate sample management and prevent researcher bias (Table 5).

If the dipeptide had been tested using replicates from different batches of the same supplier or from different suppliers, letters were added at the end of the code to differentiate between samples (this will be shown later in this document in the FLIPR experiments section).

Table 5. List of 101 dipeptides tested *in vitro*.

Code	Dipeptide	Code	Dipeptide	Code	Dipeptide	Code	Dipeptide	Code	Dipeptide
DP1	Ala-Ala (AA)	DP21	Cys-Gly (CG)	DP41	His-Trp (HW)	DP61	Met-Trp (MW)	DP81	Ser-Tyr (SY)
DP2	Ala-Asn (AN)	DP22	Gly-Ala (GA)	DP42	His-Tyr (HY)	DP62	Met-Tyr (MY)	DP82	Trp-Ala (WA)
DP3	Ala-Gly (AG)	DP23	Gly-Asn (GN)	DP43	Leu-Ala (LA)	DP63	Phe-Ala (FA)	DP83	Trp-Asn (WN)
DP4	Ala-His (AH)	DP24	Gly-Cys (GC)	DP44	Leu-Asn (LN)	DP64	Phe-Asn (FN)	DP84	Trp-Gly (WG)
DP5	Ala-Leu (AL)	DP25	Gly-Gly (GG)	DP45	Leu-Gly (LG)	DP65	Phe-Gly (FG)	DP85	Trp-His (WH)
DP6	Ala-Met (AM)	DP26	Gly-His (GH)	DP46	Leu-His (LH)	DP66	Phe-His (FH)	DP86	Trp-Leu (WL)
DP7	Ala-Phe (AF)	DP27	Gly-Leu (GL)	DP47	Leu-Leu (LL)	DP67	Phe-Leu (FL)	DP87	Trp-Met (WM)
DP8	Ala-Ser (AS)	DP28	Gly-Met (GM)	DP48	Leu-Met (LM)	DP68	Phe-Met (FM)	DP88	Trp-Phe (WF)
DP9	Ala-Trp (AW)	DP29	Gly-Phe (GF)	DP49	Leu-Phe (LF)	DP69	Phe-Phe (FF)	DP89	Trp-Ser (WS)
DP10	Ala-Tyr (AY)	DP30	Gly-Ser (GS)	DP50	Leu-Ser (LS)	DP70	Phe-Ser (FS)	DP90	Trp-Trp (WW)
DP11	Asn-Ala (NA)	DP31	Gly-Trp (GW)	DP51	Leu-Trp (LW)	DP71	Phe-Trp (FW)	DP91	Trp-Tyr (WY)
DP12	Asn-Asn (NN)	DP32	Gly-Tyr (GY)	DP52	Leu-Tyr (LY)	DP72	Phe-Tyr (FY)	DP92	Tyr-Ala (YA)
DP13	Asn-Gly (NG)	DP33	His-Ala (HA)	DP53	Met-Ala (MA)	DP73	Ser-Ala (SA)	DP93	Tyr-Asn (YN)
DP14	Asn-His (NH)	DP34	His-Asn (HN)	DP54	Met-Asn (MN)	DP74	Ser-Asn (SN)	DP94	Tyr-Gly (YG)
DP15	Asn-Leu (NL)	DP35	His-Gly (HG)	DP55	Met-Gly (MG)	DP75	Ser-Gly (SG)	DP95	Tyr-His (YH)
DP16	Asn-Met (NM)	DP36	His-His (HH)	DP56	Met-His (MH)	DP76	Ser-His (SH)	DP96	Tyr-Leu (YL)
DP17	Asn-Phe (NF)	DP37	His-Leu (HL)	DP57	Met-Leu (ML)	DP77	Ser-Leu (SL)	DP97	Tyr-Met (YM)
DP18	Asn-Ser (NS)	DP38	His-Met (HM)	DP58	Met-Met (MM)	DP78	Ser-Met (SM)	DP98	Tyr-Phe (YF)
DP19	Asn-Trp (NW)	DP39	His-Phe (HF)	DP59	Met-Phe (MF)	DP79	Ser-Phe (SF)	DP99	Tyr-Ser (YS)
DP20	Asn-Tyr (NY)	DP40	His-Ser (HS)	DP60	Met-Ser (MS)	DP80	Ser-Ser (SS)	DP100	Tyr-Trp (YW)
								DP101	Tyr-Tyr (YY)

3.3 Preliminary experiments (Fluorescence)

These experiments enabled the selection of optimal experimental conditions for the main study. It was necessary to find the conditions needed to obtain a detectable response from the ft1R1-ft1R3 receptor assay with the dipeptides.

In order to determine these, the experimental conditions used in the screening of L-amino acids were used as a reference [from previous work by McGrane (2015)]. The EC₅₀ calculated from the dose response experiments of the 11 active L-amino acids (shown in Table 6) were examined. In the dose response experiments, it was observed that some of the L-amino acids had a clear concentration dependency and followed a standard sigmoidal curve as expected (Ala, Ser, Asn, Trp, Gly, Phe, Tyr), whilst others did not follow a standard sigmoidal curve (His, Cys, Leu, Met). In some cases, the plateau of the dose response curve was not achieved (receptor binding site not saturated) so the EC₅₀ could only be estimated.

Table 6. Activity and EC₅₀s of L-amino acids tested with 0.2 mM IMP plus Tyrode’s buffer (McGrane, 2015). In some cases it was not possible to determine an EC₅₀ (curve plateau not reached). In these cases, even when an EC₅₀ could be estimated (as higher than a certain concentration), the error in its determination was too high to be added, so this was not determined (N/D). Maximal effective concentration (EC₅₀) was the concentration of amino acid which induced a response halfway between the baseline and the maximum.

Code	Name	Active	Conc. (mM)		$\Delta F/F$ (max.)	Conf. Int.
			EC50	Conf. Int.		
Ala	L-Alanine	Yes	15.5	1.7	1.131	0.025
Asn	L-Asparagine	Yes	> 30	N/D	0.694	0.049
Cys	L-Cysteine	Yes	12.6	0.7	1.106	0.09
Gly	Glycine	Yes	11.9	0.7	1.158	0.041
His	L-Histidine	Yes	9.9	0.9	0.380	0.011
Leu	L-Leucine	Yes	> 30	N/D	0.355	0.004
Met	L-Methionine	Yes	17.0	3.0	0.349	0.044
Phe	L-Phenylalanine	Yes	8.3	0.9	1.142	0.028
Ser	L-Serine	Yes	16.1	1.0	1.069	0.044
Trp	L-Tryptophan	Yes	7.3	0.9	1.036	0.054
Tyr	L-Tyrosine	Yes	15.7	3.9	0.988	0.036

It was known from previous work (McGrane, 2015) that the *in vitro* cat umami receptor assay needed a minimum concentration of nucleotide in the buffer (e.g. IMP) to enhance the response of L-amino acids in order to be detected, and a minimum concentration of L-amino acid (e.g. Ala) to enhance the response of nucleotides in order to be detected. If the hypothesis that the dipeptides containing active L-amino acids in their sequence were active was true (see Introduction Chapter), the dipeptides would follow a similar activation pattern to the L-amino acids, and these would not activate the fT1R1-fT1R3 receptor in the *in vitro* assay unless they were tested in buffer in the presence of a nucleotide (IMP) to enhance their response.

In order to identify the concentration of IMP to use in the buffer to maximise the possibility of detecting a response from the dipeptides, dose responses of a subset of L-amino acids known to be active (L-alanine and L-cysteine) were performed with 0.2 mM and 2 mM IMP (Figure 11).

The results for the amino acids were similar to the original dose response data used as reference (Table 6). The EC₅₀ results for L-alanine with either the higher or the lower IMP concentrations were very similar (Table 7), which suggested that bias was not being introduced by increasing the concentration of IMP. The maximum responses were also higher with 2 mM IMP than with 0.2 mM IMP with buffer for both L-amino acids, without affecting the dependency of the activity with the concentration.

After analysing these preliminary results and after comparing their maximum responses and EC₅₀ values, and in order to maximise the enhancement response, it was decided to use the higher concentration of IMP in buffer (2 mM) in subsequent dipeptide experiments.

Using the new assay condition (Tyrode's buffer with 2 mM IMP), the amino acids showed clear activity, and the L-cysteine dose response was now visible as a full sigmoidal curve (Figure 11). The effect on the calculated EC₅₀ value of the amino acids was negligible, whereas the increase of the maximum response (as RFU and $\Delta F/F$) was very significant (Table 7). As several of the dipeptides to be screened contained one of these two amino acids (Ala or Cys) in their sequence, and in order to be able to detect even very low umami activities, it was decided to select 2 mM IMP in buffer as the best experimental condition to perform the umami screening of the 101 dipeptides.

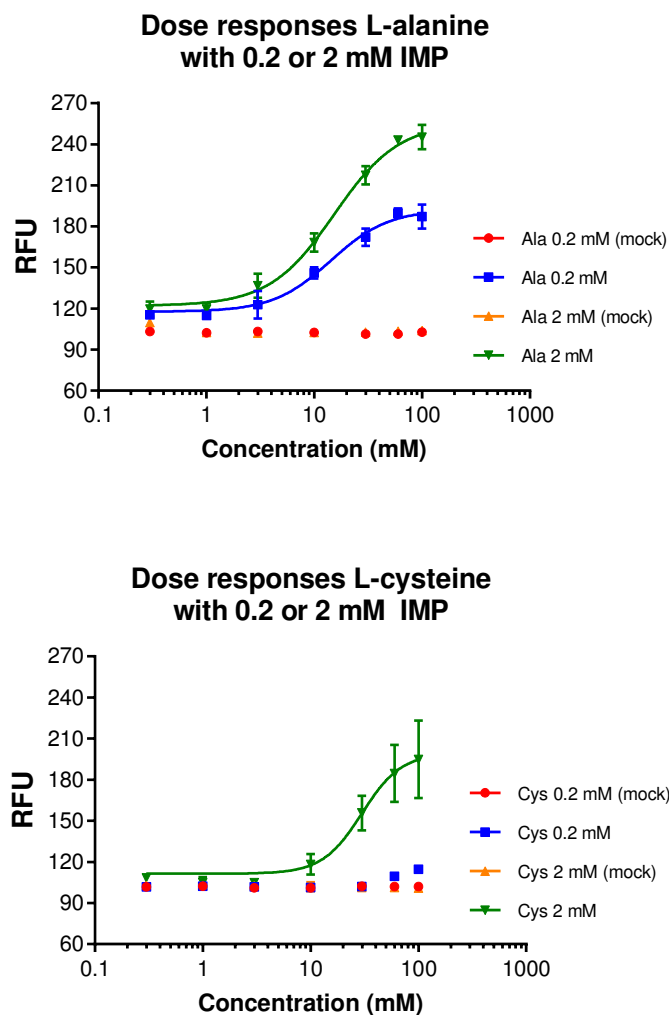


Figure 11. Dose responses of L-alanine and L-cysteine with buffer plus 0.2 mM or 2 mM IMP. (Left) Ala with 0.2 and 2 mM IMP. (Right) Cys with 0.2 mM and 2 mM IMP. Induced cells responses are represented in blue (0.2 mM) or green (2 mM) and un-induced (mock) cells responses are represented in red (0.2 mM) or orange (2 mM). Error bars indicate 95% confidence intervals. Relative Fluorescence Units (RFU) is the measure of the total fluorescent light emitted by a substance after excitation, registered by the instrument, corrected for different sensitivity at different wavelengths, and calculated as a function of the extinction coefficient, concentration, quantum yield (ratio of photons absorbed/emitted), excitation intensity, length of path and emission collection efficiency. RFUs allow comparison of fluorescence measurements from different instruments.

Table 7. Comparison of EC₅₀ values of two L-amino acids tested in buffer with 0.2 mM or 2 mM. $\Delta F/F$ means relative change of fluorescence signal. It is normally calculated by subtracting the initial/baseline or the minimum fluorescence from the maximum fluorescence or the fluorescence at a certain time, divided by the initial/baseline or the minimum fluorescence. A value of 1 (or 100%) indicates double the fluorescence of the baseline or reference.

Code	Name	Active	with 0.2 mM IMP			with 2 mM IMP			
			EC50	Std. err.	$\Delta F/F$	Active	EC50	Std. err.	$\Delta F/F$
Ala	L-Alanine	Yes	14.3	1.57	0.64	Yes	15.4	1.21	1.10
Cys	L-Cysteine	Yes	> 40	N/D	0.17	Yes	29.9	4.40	0.79

Finally, and in order to plan for the unlikely case that the dipeptides did not follow an amino acid but a nucleotide activation pattern with the ft1R1-ft1R3 receptor, a dose response of IMP in the presence of L-alanine in buffer (at 20 mM) was also performed, to confirm that this experimental condition provided enough resolution so it could be used at a later stage if necessary. The results confirmed 20 mM Ala plus buffer to test nucleotides in the assay.

Given that several of the amino acids which form the dipeptides in the library were hydrophobic, solubility was identified *a priori* as one of the potential challenges to address. It was believed that some of the dipeptides would need to be solubilised first in DMSO (Dimethyl sulfoxide, a water-miscible solvent that has wide applications in solubilising active molecules in cell biology). However, in the end, DMSO was not used to dissolve the peptides, as the majority of them dissolved in just buffer (also to avoid promoting oxidation of the dipeptide side-chains, especially when containing Cys or Met). Nevertheless, a small number of experiments to determine the effect of DMSO in the ft1R1-ft1R3 assay were conducted as a contingency (see Appendix 1). Additionally, temperature-controlled water baths and sonication were used to maximise the concentration in solution of the dipeptides with lower solubility.

3.3.1 Primary screening of dipeptides with 2 mM IMP

The experimental plan was to perform a primary (initial) screening of all the dipeptides and then conduct dose response experiments only on the active dipeptides. The 101 dipeptides were first tested with 2 mM IMP in Tyrode's buffer, as the hypothesis was that they would behave similarly to L-amino acids, and these needed IMP present in the solution to be detected. As mentioned previously, the dipeptides were more soluble than expected given the hydrophobicity of their constituent amino acids (i.e. 68 out of 101 were completely soluble in Tyrode's buffer, see Table 8), so no DMSO was used for this screening. The dipeptides with lower solubility were mixed using a vortex and/or a sonicator (and/or a water bath at 40°C) for at least 2 min, in order to obtain a solution saturated with dipeptide. This did not allow determination of the actual concentration tested, but provided a qualitative answer on the activity of the dipeptide, and allowed a study of its concentration dependency. In the case of dipeptides with lower solubility, the supernatant liquid was pipetted for the *in vitro* screening when possible in order to prevent interference from undissolved particles with the assay.

The primary screening included three concentrations for all dipeptides: 1 mM, 10 mM and 100 mM (versus eight concentrations in a dose response curve). Each concentration in the primary screening had six replicates for the induced cells and another six for the un-induced cells for comparison (see Appendix 2A). L-Alanine was tested in dose response mode as a control in every experiment. The other controls were ATP (to check for cells and signal transduction cascade working), isoproterenol (to check for heterologous expression of the receptor having taken place in the induced cells) and Tyrode's buffer (to check for cells not responding in the absence of a stimulus; see Appendix 3). All experiments were done in 384-well plates, so the maximum number of dipeptides tested in any condition in primary screening in the same plate

was eight. As there were 101 dipeptides to test, 13 plates were necessary (another 13 plates were later used to repeat the primary screening in Tyrode's buffer only).

Table 8. Solubility in Tyrode's buffer of the 101 dipeptides tested.

Dipeptide	Solubility								
Ala-Ala	Soluble	Cys-Gly	Soluble	His-Trp	Soluble	Met-Trp	Part. sol.	Ser-Tyr	Soluble
Ala-Asn	Soluble	Gly-Ala	Soluble	His-Tyr	Soluble	Met-Tyr	Part. sol.	Trp-Ala	Soluble
Ala-Gly	Soluble	Gly-Asn	Soluble	Leu-Ala	Soluble	Phe-Ala	Soluble	Trp-Asn	Soluble
Ala-His	Soluble	Gly-Cys	Soluble	Leu-Asn	Soluble	Phe-Asn	Soluble	Trp-Gly	Soluble
Ala-Leu	Soluble	Gly-Gly	Soluble	Leu-Gly	Soluble	Phe-Gly	Soluble	Trp-His	Soluble
Ala-Met	Soluble	Gly-His	Soluble	Leu-His	Part. sol.	Phe-His	Soluble	Trp-Leu	Part. sol.
Ala-Phe	Soluble	Gly-Leu	Soluble	Leu-Leu	Part. sol.	Phe-Leu	Part. sol.	Trp-Met	Part. sol.
Ala-Ser	Soluble	Gly-Met	Soluble	Leu-Met	Soluble	Phe-Met	Part. sol.	Trp-Phe	Part. sol.
Ala-Trp	Soluble	Gly-Phe	Soluble	Leu-Phe	Part. sol.	Phe-Phe	Part. sol.	Trp-Ser	Part. sol.
Ala-Tyr	Part. sol.	Gly-Ser	Soluble	Leu-Ser	Soluble	Phe-Ser	Soluble	Trp-Trp	Part. sol.
Asn-Ala	Part. sol.	Gly-Trp	Part. sol.	Leu-Trp	Part. sol.	Phe-Trp	Part. sol.	Trp-Tyr	Soluble
Asn-Asn	Soluble	Gly-Tyr	Soluble	Leu-Tyr	Part. sol.	Phe-Tyr	Part. sol.	Tyr-Ala	Soluble
Asn-Gly	Soluble	His-Ala	Soluble	Met-Ala	Soluble	Ser-Ala	Part. sol.	Tyr-Asn	Soluble
Asn-His	Soluble	His-Asn	Soluble	Met-Asn	Soluble	Ser-Asn	Soluble	Tyr-Gly	Part. sol.
Asn-Leu	Soluble	His-Gly	Soluble	Met-Gly	Soluble	Ser-Gly	Soluble	Tyr-His	Soluble
Asn-Met	Soluble	His-His	Soluble	Met-His	Soluble	Ser-His	Soluble	Tyr-Leu	Part. sol.
Asn-Phe	Soluble	His-Leu	Part. sol.	Met-Leu	Soluble	Ser-Leu	Part. sol.	Tyr-Met	Soluble
Asn-Ser	Soluble	His-Met	Soluble	Met-Met	Part. sol.	Ser-Met	Soluble	Tyr-Phe	Part. sol.
Asn-Trp	Soluble	His-Phe	Part. sol.	Met-Phe	Part. sol.	Ser-Phe	Part. sol.	Tyr-Ser	Soluble
Asn-Tyr	Soluble	His-Ser	Soluble	Met-Ser	Soluble	Ser-Ser	Part. sol.	Tyr-Trp	Part. sol.
								Tyr-Tyr	Part. sol.

The results of the control (L-alanine + 2 mM IMP) in primary screening mode, showed a clear activation of the receptor, as there was an increase of 50 RFUs from 1 mM to 10 mM Ala, and another increase of 50 RFUs from 10 mM to 100 mM Ala (Figure 12A). This meant that, if the dipeptides had an amino acid-like activation in primary screening similar to L-alanine, for example, the activation would be expected to be in the region of 100 RFU in size. However, the dipeptide results were not so clear, and most experiments only showed activations around 40 RFU (from 1 mM to 100 mM dipeptide). Furthermore, it was found that the 2 mM IMP alone provided a residual response or "baseline activity" of around 30-40 RFU (very similar to the one found with the dipeptide plus IMP). This was observed in the induced cells (expressing the

receptor) but not in the un-induced (mock) cells, so it was a true effect. A smaller but noticeable baseline activation (10-20 RFU) was also found for 0.2 mM IMP (see Figure 12B). This experimental condition (0.2 mM IMP) was also tested for comparison. The IMP baseline found was therefore concentration-dependant, and always present. This baseline IMP activation was considered normal, but it had to be taken into account when assessing the possible activity of the dipeptides in the primary screening when tested with IMP.

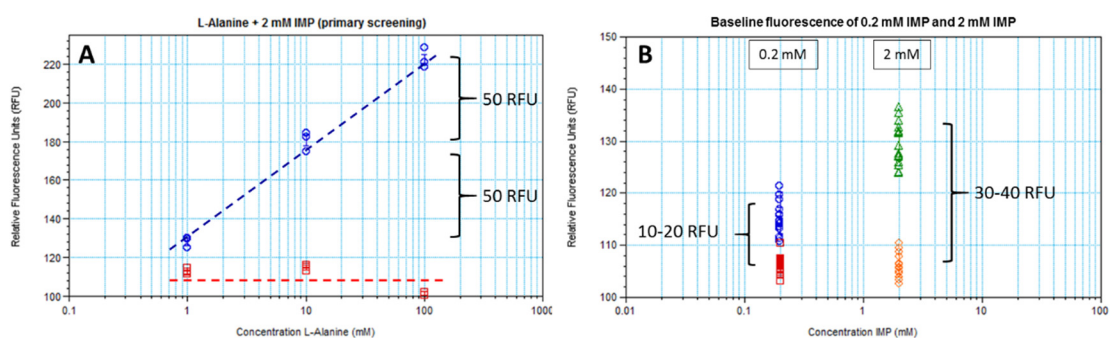


Figure 12. L-Alanine primary screening with 2 mM IMP and buffer and IMP baseline responses at 0.2 mM and 2 mM. (A) L-Alanine + 2 mM IMP responses. Induced cells in blue and un-induced (mock) cells in red. (B) Baseline activation with 0.2 mM IMP is shown on the left (induced cells in blue and mock cells in red). Baseline activation with 2 mM IMP is shown on the right (induced cells in green and mock cells in orange).

The primary screening of the dipeptides tested with 2 mM IMP provided a wide range of response patterns (see Figure 13 for some examples). For some dipeptides, when tested with the 2 mM IMP, the baseline activity of the IMP decreased from 40 RFU to 10 RFU or even zero, as the concentration of dipeptide increased (from 1 mM to 10 mM and to 100 mM). It was hypothesised that this was due to the dipeptide interacting with the IMP, hindering its baseline activity, and that dipeptides with this response pattern were potentially not active (Figure 13A). This interference with the concentration was not seen in the cells not expressing the receptors (mock cells or control).

On the other hand, and as a consequence of the previous hypothesis of the dipeptides interfering with the IMP baseline activity, the dipeptides maintaining or increasing their baseline activity as the concentration increased were selected as potentially active (Figures 13B and 13C).

The dipeptides that *maintained* their baseline activity were also considered potentially active as, if the dipeptide was still binding to the receptor and displacing the IMP, there was the possibility that the decrease in fluorescent response due to IMP displacement by the dipeptide could be compensated by the increase in fluorescence due to the activity of the dipeptide (bearing in mind that another possibility would be that the dipeptide was inactive and did not interfere with the IMP at all). Therefore, the criteria to identify potential active dipeptides at this stage was lenient, as the main purpose in the primary screening was to detect any potential activity, with the objective of proving or disproving this later using dose-response experiments.

Finally, if the mock cells were also activated, this was considered as a non-specific response, not an effect of binding to the fT1R1-fT1R3 receptor [non-specific responses (NS) are those not a consequence of the compound/ligand (e.g. dipeptide) binding to the taste receptor, but to other receptors in the cell surface or inside the cells, with the same consequence of a genuine response, which is the intracellular release of calcium]. (Figure 13D).

Experimental Results and Discussion

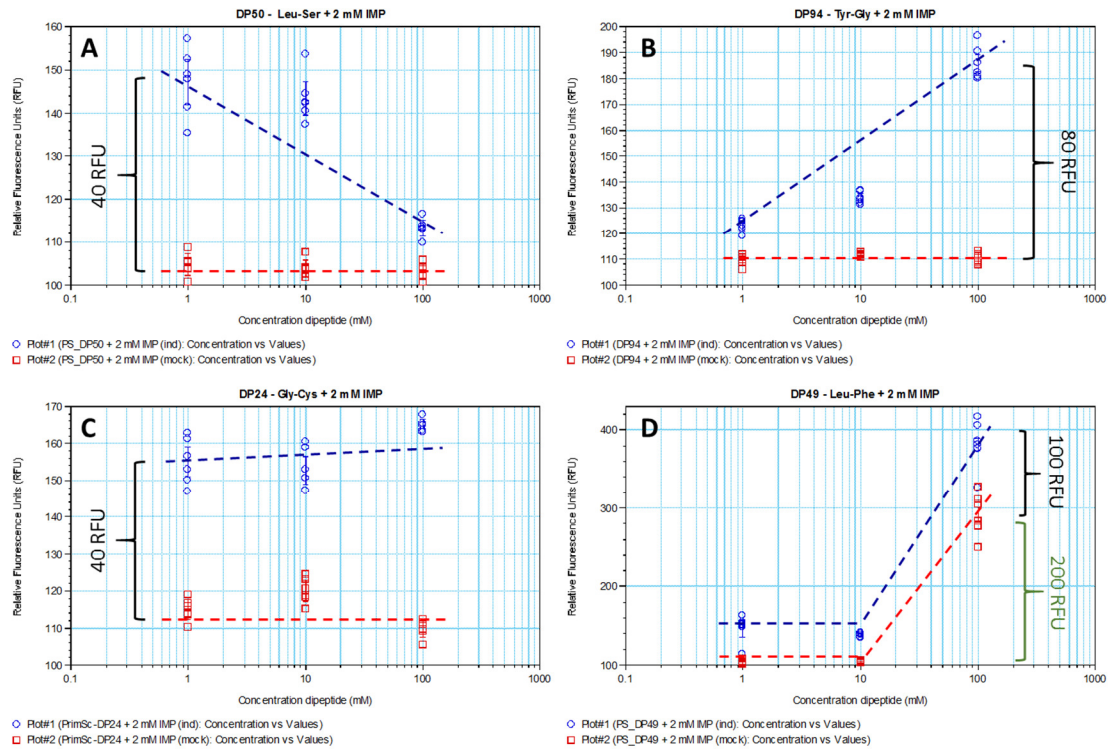


Figure 13. Examples of potentially active and inactive dipeptides in primary screening. (A - Inactive) DP50 – Leu-Ser + 2 mM IMP. (B - Active) DP93 – Tyr-Asn + 2 mM IMP. (C – Potentially Active) DP24 – Gly-Cys + 2 mM IMP. (D – Potentially Inactive) DP49 – Leu-Phe + 2 mM IMP. Induced cells are represented in blue and mock cells in red.

In order to examine the response of the dipeptides from the primary screening in more detail, the raw data (full record of fluorescence readings of the FlexStation every 2 seconds during at least 90 seconds) was also examined. The shape of the raw data of 2 mM IMP on its own was compared to the raw data pattern of the dipeptides plus the 2 mM IMP, in order to elucidate if there was any activation on top of the baseline activation due to the IMP. The standard activation of L-alanine with 2 mM IMP was also included in the comparisons.

When the activation patterns of (a) the dipeptide tested with 2 mM IMP in buffer, (b) L-alanine tested with 2 mM IMP in buffer (standard expected response) and (c) the IMP on its own (in buffer) were compared (Figure 14A), it was evident that the dipeptides were interacting with

the IMP or the cells in a different way than the L-amino acid, as the activation pattern was very distinct.

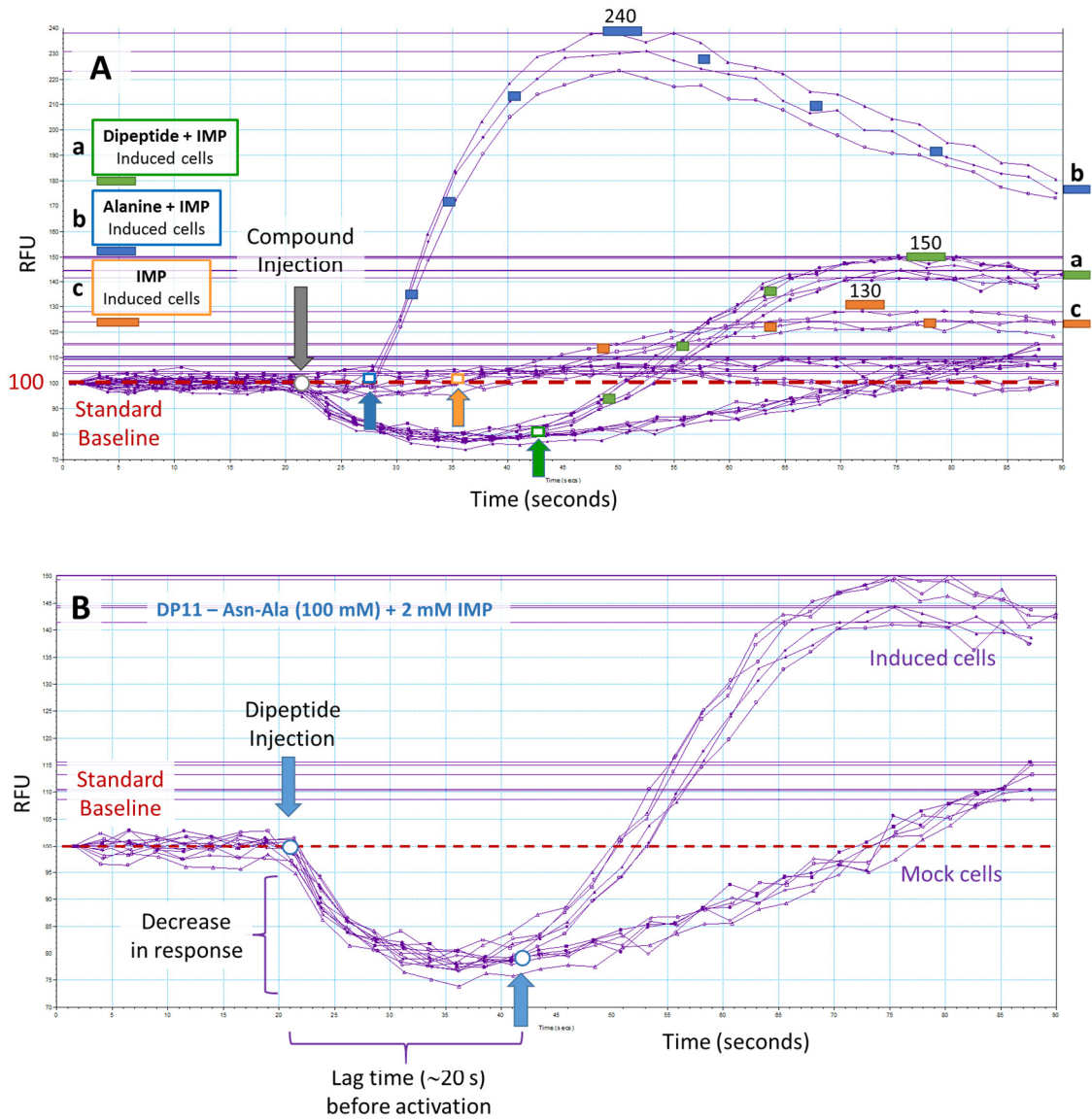


Figure 14. Unusual response pattern of dipeptides in primary screening. (A) (Top): Comparison of the unusual response pattern of a dipeptide with the response of L-alanine and the response of IMP on its own. All three with 2 mM IMP in buffer. Lag times: (a) dipeptide DP11 (~21s; green), (b) Ala (~6s; blue) and (c) IMP (~13s; orange). Maximum fluorescence: (a) dipeptide (150 RFU/green), (b) Ala (240 RFU/blue) and (c) IMP (130 RFU/orange). Baseline fluorescence = 100 RFU. (B) (Bottom): Unusual response pattern of one of the dipeptides possibly active in primary screening. “Lag time and belly” response pattern. Raw FlexStation fluorescence data corresponds to DP11 – Asn-Ala (100 mM) tested with 2 mM IMP.

The activation was delayed for the dipeptide (a), but it started shortly after injection for L-alanine (b). Also the steepness of the curve was much higher in the case of the amino acid, which followed a more usual activation pattern. Also the maximum fluorescence for L-alanine (around 140 RFU) was much higher than the maximum for the dipeptide (around 50 RFU), which was similar to the one of IMP on its own (around 30-40 RFU). It appeared that the maximum response for the dipeptide with IMP (a) could be similar but slightly higher than the maximum response of the IMP on its own (c).

Furthermore, the raw data highlighted an unusual response pattern for the dipeptides, when they were examined at an “active” concentration. The activation had a delay in the response (lag time) in comparison with what would be expected from the L-amino acids plus IMP, or from the IMP on its own. Next, the activation (RFU) dipped below the original baseline for some seconds, before reaching a minimum and increasing again (forming a kind of a “belly” in the curve). Finally, the increase in fluorescence continued to the end of the recording, many times not reaching a plateau or going down again, as it would be expected (Figure 14B). This pattern appeared for both the induced and the un-induced cells, so it was concluded that a non-specific response induced by the dipeptide was occurring, or maybe a combination of activation plus a non-specific response.

As mentioned before, the *in vitro* fT1R1-fT1R3 assay being used needed IMP to enhance the response signal of L-amino acids up to a detectable level, and 2 mM had been selected as optimal concentration to maximise the response of the dipeptides, after preliminary experiments with some L-amino acids (Ala and Cys). The preliminary work was not done directly with dipeptides because it was not known which ones were active. However, IMP seemed to be complicating the primary screening assessment of the potential activity of the

dipeptides, and a potential interaction (maybe steric hindrance or competition reaching the binding site of the receptor) between the dipeptides and the IMP was discovered.

It was clear at this point that more experiments in different conditions were necessary in order to examine the extent of the interference of the IMP (necessary to get any amino acid activation) and clarify some of the possible non-specific responses and unusual response patterns. Therefore, in the next stage of the project, the 101 dipeptides were tested in just Tyrode's buffer, with the objective of detecting interactions between the dipeptides and the cells (without IMP involved) which could explain some of the possible non-specific responses. This would simplify the experiment in order to disentangle the possible phenomena happening simultaneously. At this point, it was also vital to investigate if the unusual response pattern of the "lag time and belly" persisted in the absence of IMP.

3.3.2 Primary screening dipeptides with Tyrode's buffer only

All 101 dipeptides were tested in Tyrode's buffer only (in the absence of IMP) in order to (a) eliminate the baseline response of IMP and (b) determine if the unusual response pattern found persisted in the absence of IMP. It was known that these conditions would prevent amino acid-like responses to be detected, so it would help with investigating the main hypothesis of dipeptides containing active amino acids in their sequence being active through a similar mechanism. A variety of responses were obtained again with just buffer, which complemented the information given by the experiments with 2 mM IMP in buffer.

Most of the compounds believed to be inactive in the primary screening with IMP had no activation with just buffer, which supported the hypothesis of these dipeptides not being active and interfering with the response that IMP would provide on its own in some form (see

Figures 15A and 15B). These dipeptides were marked as “not active” (or “inactive”) and were not investigated further.

In other cases, the dipeptides that had a flat response pattern with the IMP (Figure 13C) or small activation at intermediate concentrations (Figure 15C), had no response at the lower concentrations but some activation at the higher concentrations (Figure 13B) even in only buffer (Figure 15D). This was initially thought to be a proof of either non-specific response or activity through a different mechanism (or binding site in the receptor), so they were marked as “possible actives” for further investigation, bearing in mind that if the dipeptides behaved in the fT1R1-fT1R3 receptor assay in a similar way as the amino acids, there should not be a response without any IMP present in the media. Again, at this point they were taken forward as possible actives, even if they could be active due to a different mechanism, or exhibit another type of non-specific response.

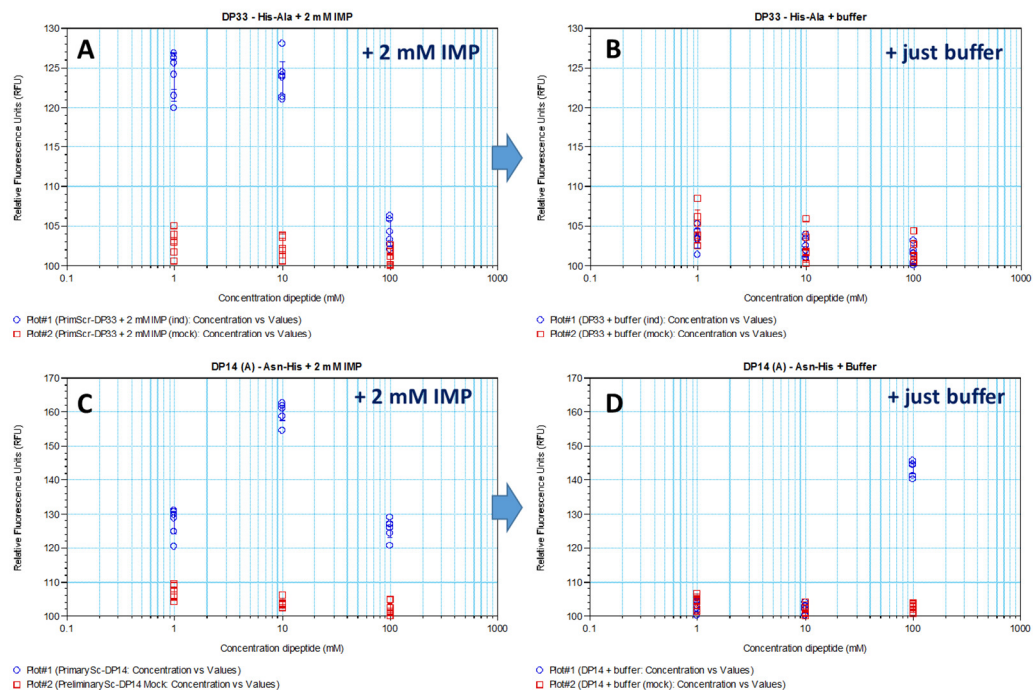


Figure 15. Comparison of primary screening results in IMP and in buffer for His-Ala and Asn-His. (A/B) DP33 - His-Ala, (A) with 2 mM IMP and (B) with buffer only. (C/D) DP14A - Asn-His, (C) with 2 mM IMP and (D) with buffer only. Induced cells are represented in blue and mock cells in red.

In this experiment, more information was also gathered on the dipeptides suspected to be auto-fluorescent, as the fluorescent response in this case should be similar for the experiments conducted with Tyrode's buffer plus IMP and with Tyrode's buffer only, due to auto-fluorescence being dependent on the compound tested, not the assay conditions.

In terms of the unusual response pattern ("lag time and belly") found for many of the dipeptides in the experiments in buffer with 2 mM IMP, it was discovered that this effect was probably not driven by the IMP, as a similar activation pattern was also found in the dipeptides showing activity in buffer only. This supported the hypothesis of the dipeptides being the cause of this behaviour, however, the unusual activation pattern was different in the induced and the un-induced (mock) cells, and also different for different dipeptides (Figure 16).

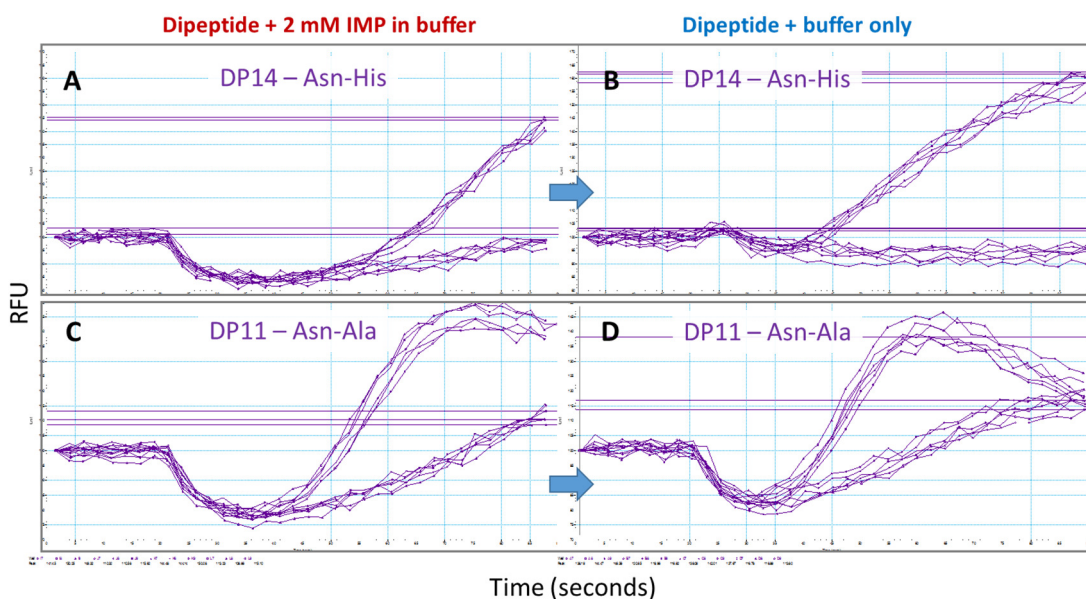


Figure 16. Raw data comparison of primary screening results in IMP and in buffer for Asn-His and Asn-Ala. DP14A - Asn-His (A: 10 mM + 2 mM IMP). DP14A - Asn-His (B: 100 mM + buffer). DP11 - Asn-Ala (C: 100 mM + 2 mM IMP). DP11 - Asn-Ala (D: 100 mM + buffer). The unusual decrease in fluorescent response after injection changes more for Asn-His (top) than for Asn-Ala (bottom) when in buffer, but is still visible.

3.3.3 Dose responses of potentially active compounds with the FlexStation

A subset of six of the dipeptides identified in the primary screening as being potentially active were subsequently screened in a full dose response experiment including eight concentrations, in order to determine the EC₅₀ value of the dipeptide. The dose responses were conducted with both buffer plus IMP and buffer only. This determination was completed with the aim of helping to estimate the potency of the dipeptides in comparison with the EC₅₀ values of the individual L-amino acids.

Another objective of these dose response experiments was to determine if the activation of the receptor by the dipeptide was non-specific (an artefact) or genuine; as a real activation pattern should be concentration-dependent. The results are shown in Table 9. In all cases, the activation increased with increased concentration and then decreased (DP14, DP16, DP85 and DP93), or continued to increase without reaching a plateau (DP94), or the difference between the baseline and the maximum activation was very small (DP24) as shown in Figure 17. Also in the case of DP94, an approximate EC₅₀ was calculated by the software (> 100 mM), given that it was a partially soluble compound and the actual dipeptide concentration in solution was not known. As these results were also unusual and not conclusive, further experiments were conducted.

Table 9. Dose response experiments performed with the FlexStation in fluorescence mode and EC₅₀ determination. “NS” means non-specific response.

Code	Dipeptide	Solubility	In 2 mM IMP		In Tyrode's buffer	
			EC ₅₀	Comments	EC ₅₀	Comments
DP14A	Asn-His	Soluble	Unknown	Potential NS	Unknown	Potential NS
DP16	Asn-Met	Soluble	Unknown	Potential NS	Unknown	NS
DP24	Gly-Cys	Soluble	Unknown	Potential NS	N/A	Inactive
DP85	Trp-His	Soluble	Unknown	Potential NS	Unknown	Potential NS
DP93	Tyr-Asn	Soluble	Unknown	NS	Unknown	NS
DP94	Tyr-Gly	Part. Sol.	> 100 mM	Active	N/A	Inactive

Experimental Results and Discussion

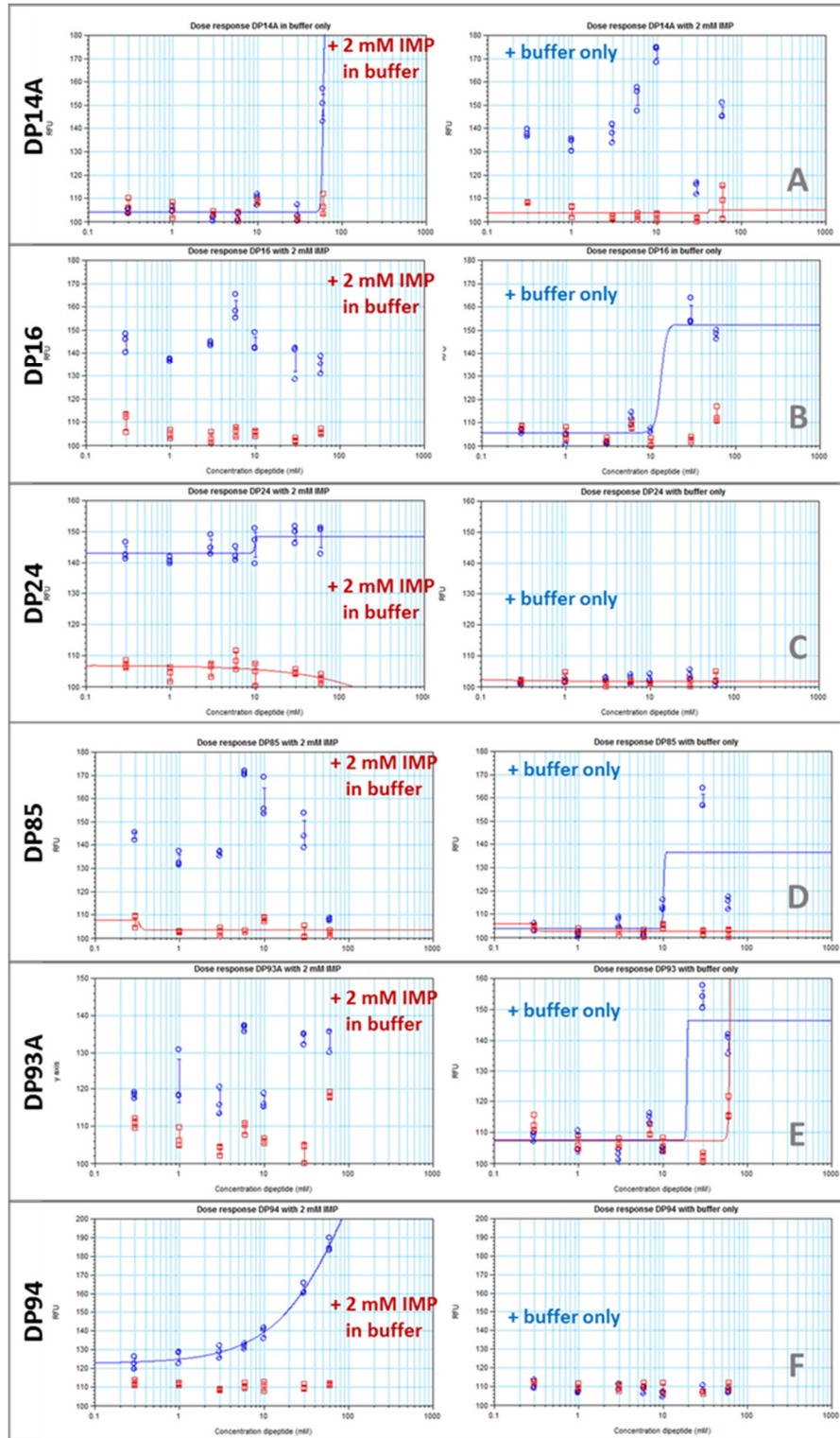


Figure 17. Dose responses for six dipeptides in buffer + 2 mM IMP and in buffer only. (A) DP14A - Asn-His. (B) DP16 - Asn-Met. (C) DP24 – Gly-Cys. (D) DP85 - Trp-His. (E) DP93A – Tyr-Asn. (F) DP94 – Tyr-Gly. (Left) dipeptide plus IMP in buffer; (Right) dipeptide in just buffer.

3.3.4 Summary of FlexStation 3 results

From the previous experiments with the FlexStation using the fluorescence assay and the two experimental conditions, it was discovered that:

1. Thirty-six out of the 101 dipeptides tested with IMP in buffer could be active (or exhibit a non-specific response) and 65 were probably inactive (at least 14 out of these 65 dipeptides had strong activity in the un-induced cells, so they were causing non-specific responses or artefacts).
2. Eighteen out of the 101 dipeptides tested with just Tyrode's buffer displayed some activity (maybe due to a non-specific response) and needed to be further investigated, whilst 83 were not active.
3. There was some overlap (17 dipeptides) between the compounds showing activity in primary screening with buffer plus IMP and with buffer only (see Figure 18).



Figure 18. Schematic with the conclusions from the primary screening (Fluorescence – FlexStation). 101 total. Red box (19) – Potentially active compounds in buffer + 2 mM IMP. Blue box (1) – Compounds showing activation in the buffer only. Purple box (17) – overlap (potentially active in both conditions of buffer + IMP and buffer only). Grey box (64) – Inactive compounds in both experimental conditions. Underlined and bold (12) – Potential auto-fluorescent compounds.

4. The visualisation of the raw data for the activation pattern of the compounds suggested that possibly 12 out of the 101 dipeptides could be auto-fluorescent (see Figure 19C).
5. None of the dose response experiments for the six dipeptides identified as being potentially active provided clear results.

The detailed results from the screening of the 101 dipeptides using a fluorescence assay in two experimental conditions (with 2 mM IMP or with Tyrode's buffer) can be seen in Appendix 4. These results were analysed and compared qualitatively in order to identify possible active dipeptides.

It was found that 19 out of 101 dipeptides were active with IMP and buffer but not with buffer only, which could mean they had actual umami activity. Also, 17 out of 101 dipeptides were classified as possibly active in both assay conditions, which meant they could be potentially non-specific responses. One of the 101 dipeptides was active with buffer only but not with IMP and buffer, which would support a non-specific response. And finally, 64 out of 101 dipeptides had no activity in any of the assays, which confirmed them as not active.

At this point, a qualitative review of the raw FlexStation data was conducted, and some of the responses, especially the differences between an actual non-specific response and other abnormal responses like auto-fluorescence could be explained (see Figure 19). The visualisation of the raw data in the IMP and buffer experiments and buffer only experiments also provided examples of possible particles interfering with the assay for the less soluble compounds, which were previously designated as non-specific responses.

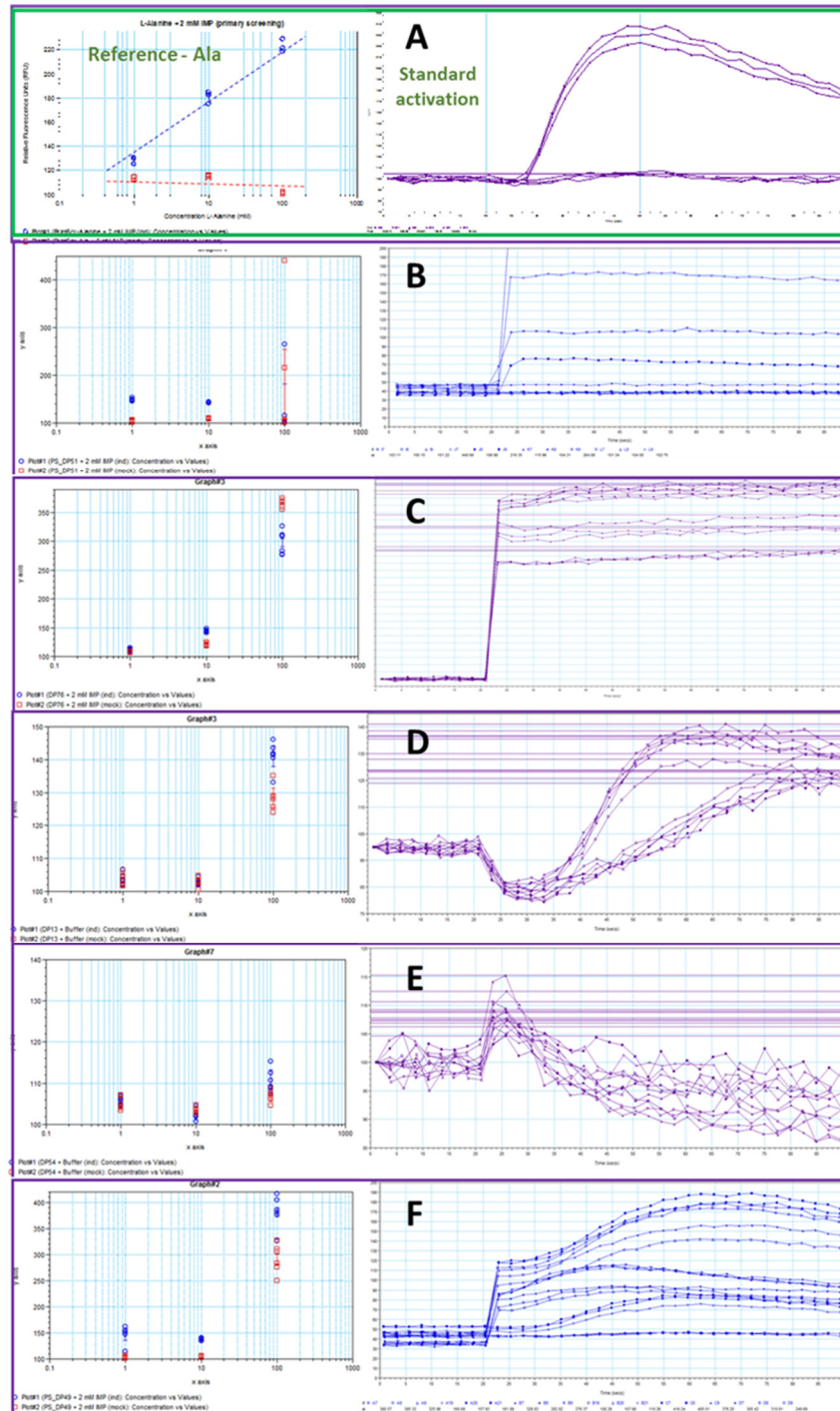


Figure 19. Examples of non-specific responses found in the screening of the 101 dipeptide library. All raw data corresponded to the 100 mM concentration of dipeptide. L-Alanine activation pattern is shown as a reference. **(A)** L-Alanine with IMP – Standard activation curve. **(B)** Leu-Trp with IMP – Solids (partially soluble). **(C)** Ser-His with IMP – Auto-Fluorescent. **(D)** Asn-Gly in buffer – Non-specific response (“lag time and belly”). **(E)** Met-Asn in buffer – Non-specific response after injection (refraction). **(F)** Leu-Phe with IMP – Solids or auto-fluorescence response plus non-specific response.

In any case, the majority of the experiments run either in primary screening or in dose response mode up to this point were far from having the same umami activation pattern as the L-amino acids (e.g. Ala in Figure 19A), and even when it was clear when the dipeptides had no activity, it was still difficult to differentiate when a dipeptide had a genuine umami activity or when it was exhibiting a non-specific response.

It was decided to conduct additional experiments using a luminescence reporting system at this point, as auto-fluorescent compounds do not interfere with luminescence, and in order to clarify further the possible non-specific responses.

3.4 *In vitro* results from the FLIPR experiments (selected dipeptides)

A subset of dipeptides identified as potentially active, plus others suspected to cause non-specific responses and/or auto-fluorescence were selected to be studied further using an expanded experimental design and additional experimental conditions (using Fluorescence and Luminescence).

As the FLIPR instrument is highly automated and has a much higher throughput than the FlexStation, it was decided to use it to screen the subset of dipeptides in dose response mode (eight concentrations each) using both fluorescence and luminescence detection to enable direct comparison of the results. Also the experiment was expanded to include three instead of two experimental conditions:

1. Tyrode's buffer only.
2. Tyrode's buffer plus 1 mM IMP.
3. Tyrode's buffer plus 20 mM Ala.

The three experiments above were run with induced cells only. The control with un-induced (mock) cells was conducted in only one experimental condition, with buffer plus 1 mM IMP:

4. Tyrode's buffer plus 1 mM IMP.

For these experiments, the concentration of IMP was reduced to 1 mM IMP in order to reduce the possible interference of IMP in the response of the dipeptides. Also, previous work on the cat umami receptor *FT1R1-FT1R3* had shown this concentration was optimal for amino acid testing with this instrument (FLIPR). L-alanine was added to the conditions in the experimental design to test for a potential nucleotide-like mechanism of activation (as mentioned before, amino acids needed the nucleotide enhancement in order to be detected, while nucleotides needed amino acid enhancement to be detected). The reason to only run one experimental condition with the mock cells was due to the amount of compound left that required prioritisation of the experiments, and the experimental conditions more able to test the hypothesis (activation by an amino acid-like mechanism) were with IMP.

In relation to the experimental data, 33 samples were tested using 24 plates (384-well plates), as a result of the combination of the following factors ($4 \times 3 \times 2 = 24$):

- Four experimental conditions (3 for the induced cells and 1 for the mock cells).
- Three different sample sets (with 11 samples each).
- Two different detection systems (Fluorescence and Luminescence).

A summary of the test plates tested can be seen in Table 10). An additional control plate for luminescence was also tested prior to the screening for correct cell performance checks.

Table 10. Plates tested (24) in the FLIPR in Fluorescence and Luminescence mode. Plate names contain three pieces of information. For example, in “F1-ind-IMP”, the “F1” meant “F” fluorescence and “1” first compound setup (samples 1-11); “ind” meant tested with induced cells; “IMP” meant tested with IMP in buffer as experimental conditions.

Compounds tested		12 Fluorescence plates								12 Luminescence plates							
		Induced cells				Mock				Induced cells				Mock			
		with 20 mM Ala	with 1 mM IMP	with just buffer	with 1 mM IMP	with 20 mM Ala	with 1 mM IMP	with just buffer	with 1 mM IMP	with 20 mM Ala	with 1 mM IMP	with just buffer	with 1 mM IMP				
Comp. setup 1	Samples 1-11	1	F1-ind-Ala	4	F1-ind-IMP	7	F1-ind-Buffer	10	F1-mock-IMP	13	L1-ind-Ala	16	L1-ind-IMP	19	L1-ind-Buffer	22	L1-mock-IMP
Comp. setup 2	Samples 12-22	2	F2-ind-Ala	5	F2-ind-IMP	8	F2-ind-Buffer	11	F2-mock-IMP	14	L2-ind-Ala	17	L2-ind-IMP	20	L2-ind-Buffer	23	L2-mock-IMP
Comp. setup 3	Samples 23-33	3	F3-ind-Ala	6	F3-ind-IMP	9	F3-ind-Buffer	12	F3-mock-IMP	15	L3-ind-Ala	18	L3-ind-IMP	21	L3-ind-Buffer	24	L3-mock-IMP

It must be mentioned at this point that two quality control experiments were also planned at this stage: (a) a batch-to-batch check and (b) a supplier check. The same dipeptide was tested from two different batches from the same supplier, and also from another supplier. This test was to confirm the quality of the dipeptides purchased for the experiment, not to estimate the variability introduced by batch or supplier in the experiment.

Overall, the questions to answer with the experiments conducted in the selected subset of dipeptides in expanded experimental conditions using the FLIPR were:

1. Were the peptides selected as possibly active in the experiments using the FlexStation, really active?
2. Were the non-specific responses observed (e.g. “lag time and belly” unusual activation pattern) due to the researcher, the experimental conditions or the compounds?
3. Which compounds were auto-fluorescent and which had non-specific responses?
4. Do compounds with different batches from the same supplier or from a different supplier perform equally?

- Do the extra experimental conditions (e.g. test with Ala) suggest a different activation mechanism for the dipeptides?

The selected 33 sample set consisted of 29 dipeptides potentially active from the primary screening in the FlexStation fluorescence experiments plus three quality controls. Also in order to confirm and understand better the previous data, one inactive compound (DP66) was also added to the list. Given that there were more compounds that were possibly active to investigate than spaces in the experimental set-up (33), groups of compounds that gave a nearly identical activation pattern were represented by one or two compounds instead of all of them being re-tested (this allowed the list to be reduced to 33 samples). In summary, 30 dipeptides (but 33 samples) were tested in the experiments using the FLIPR. The final list of dipeptide samples tested with the FLIPR are shown in Table 11. Replicates are indicated by adding letters (A, B or C) to the dipeptide codes.

Table 11. List of samples tested in the FLIPR in Fluorescence and Luminescence mode. 33 samples in total were tested. Peptides with a letter “A” in the code meant first batch, “B” meant second batch of same supplier and “C” meant a batch from a different supplier. The table contains the information from the previous FlexStation fluorescence experiment (Figure 18). “AF” means auto-fluorescence, compounds selected as “Yes” were highlighted as possible AF from the primary screening.

Samples 1-11					Samples 12-22					Samples 23-33				
Code	Dipeptide	Suppl.	Active	AF	Code	Dipeptide	Suppl.	Active	AF	Code	Dipeptide	Suppl.	Active	AF
DP11	Asn-Ala	PEBio	Yes	No	DP21	Cys-Gly	Bac	Yes	Yes	DP20	Asn-Tyr	PEBio	Yes	Yes
DP12	Asn-Asn	PEBio	Yes	Yes	DP34	His-Asn	PEBio	Yes	No	DP24	Gly-Cys	Bac	Yes	No
DP13	Asn-Gly	PEBio	Yes	No	DP42	His-Tyr	Bac	Yes	Yes	DP36	His-His	Bac	Yes	Yes
DP14A	Asn-His	PEBio	Yes	No	DP49	Leu-Phe	Bac	Yes	Yes	DP41	His-Trp	Bac	Yes	Yes
DP14B	Asn-His	PEBio	Yes	No	DP64	Phe-Asn	PEBio	Yes	No	DP60	Met-Ser	Bac	Yes	No
DP14C	Asn-His	AnaSp	Yes	No	DP66	Phe-His	PEBio	No	No	DP76	Ser-His	Bac	Yes	Yes
DP15	Asn-Leu	PEBio	Yes	No	DP67	Phe-Leu	Bac	Yes	No	DP93A	Tyr-Asn	PEBio	Yes	No
DP16	Asn-Met	PEBio	Yes	No	DP85	Trp-His	PEBio	Yes	No	DP94	Tyr-Gly	Bac	Yes	No
DP17	Asn-Phe	PEBio	Yes	No	DP91	Trp-Tyr	Bac	Yes	No	DP97	Tyr-Met	PEBio	Yes	No
DP18	Asn-Ser	PEBio	Yes	No	DP93C	Tyr-Asn	AnaSp	Yes	No	DP98	Tyr-Phe	Bac	Yes	No
DP19B	Asn-Trp	PEBio	Yes	Yes	DP95	Tyr-His	Bac	Yes	No	DP99	Tyr-Ser	PEBio	Yes	No

Due to the number of experiments that needed to be conducted and the amount of compound remaining, for some compounds it was sometimes possible to test up to 60 mM in the dose response, but for other compounds only maximum concentrations of 30, 20 or 10 mM could be reached with the amount of material available. The final number of replicates for each data point in the dose responses was four. For an example of dose-response dilutions in a plate layout see Appendix 2B.

3.4.1 Fluorescence experiments

The raw fluorescence data was first analysed and visualised using ScreenWorks®, which was the software used on the FLIPR. From the whole plate readings, it was evident that all wells had some activity, which increased with the concentration, but the activation patterns found were often non-standard at the higher concentrations, with a “lag time and belly” shape, which suggested non-specific responses. This and other non-specific responses can be seen in Figure 20 (the example represents fluorescence plate F1 with induced cells in the presence of 1 mM IMP plus buffer; a variety of responses can be found in the region inside the box).

As the dipeptides were tested in three different conditions with induced cells (Ala, IMP and Buffer) and in one condition with mock cells (IMP), this helped to differentiate between genuine and non-specific responses. Many of the responses detected were below the baseline, which agreed with the “lag time and belly” responses found with the FlexStation (which proved repeatability). As mentioned in the Methodology section, the response data was cut at certain times (15-50s and 20-60s) in order to avoid non-specific responses at the beginning (e.g.

disturbance straight after injection) and at the end of the recording (e.g. potentially dye leaching out of the cells). It was known from the controls that a standard umami response peak (100 mM Ala + 1 mM IMP) should occur at around 30s. Only the maximum signal was measured in the 15-50s data extract, and local response as maximum minus minimum signal was measured in the 20-60s data extract. The responses were very low in general. An illustration of the maximum fluorescence results for the different plates, using the time cut-off which provides the most clear results, can be seen in Figures 21 (samples 1-11), 22 (samples 12-22) and 23 (samples 23-33).

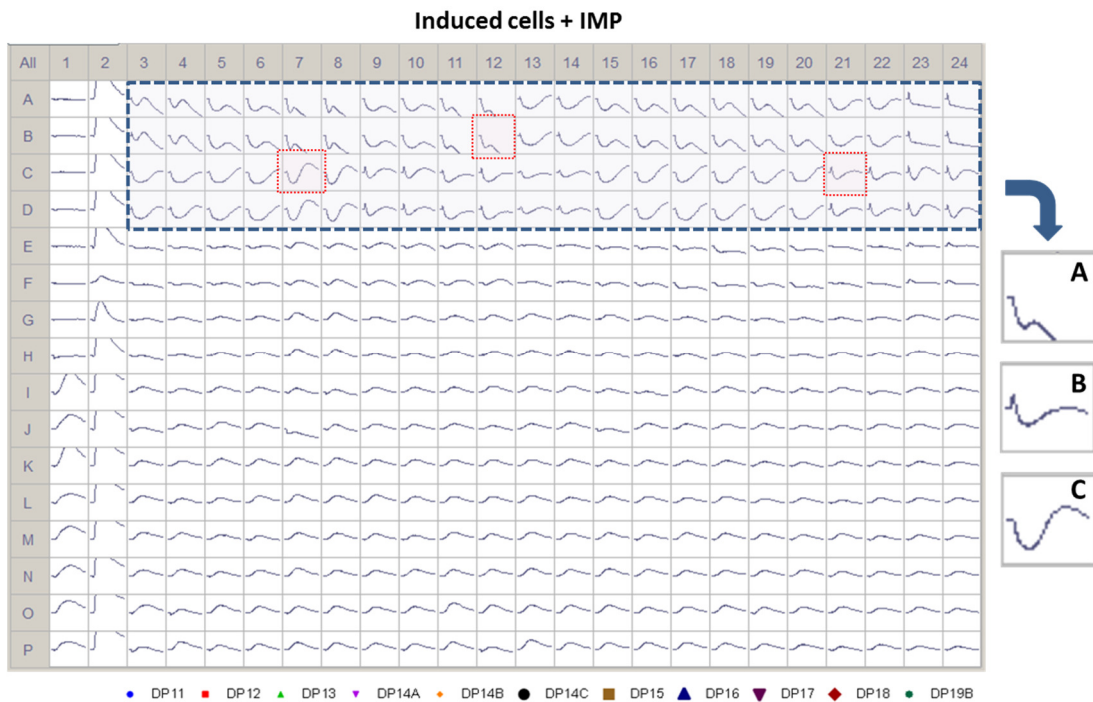


Figure 20. Example of raw fluorescence activation data of induced cells in the presence of IMP. Unusual response patterns (A, B and C) are seen at the higher concentrations (highlighted in top box), many of which could be non-specific activation. **A** – Drop in activity well below baseline. **B** – Peak after injection plus “lag time and belly” curve shape. **C** – Unusual response pattern “lag time and belly” shape.

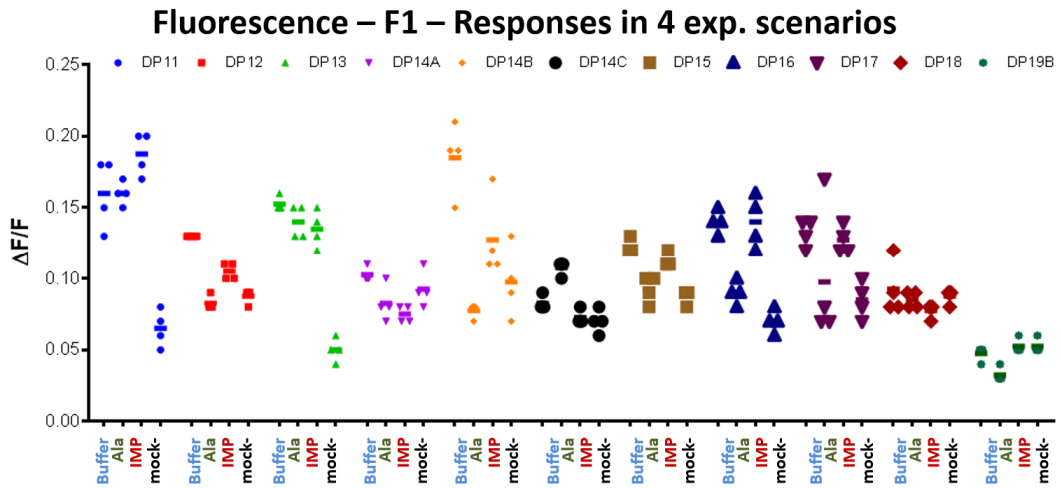


Figure 21. Fluorescence responses summary for dipeptide samples 1-11 (F1). The values are provided for the three experimental conditions with the induced cells (buffer, Ala, IMP) and the mock cells with IMP.

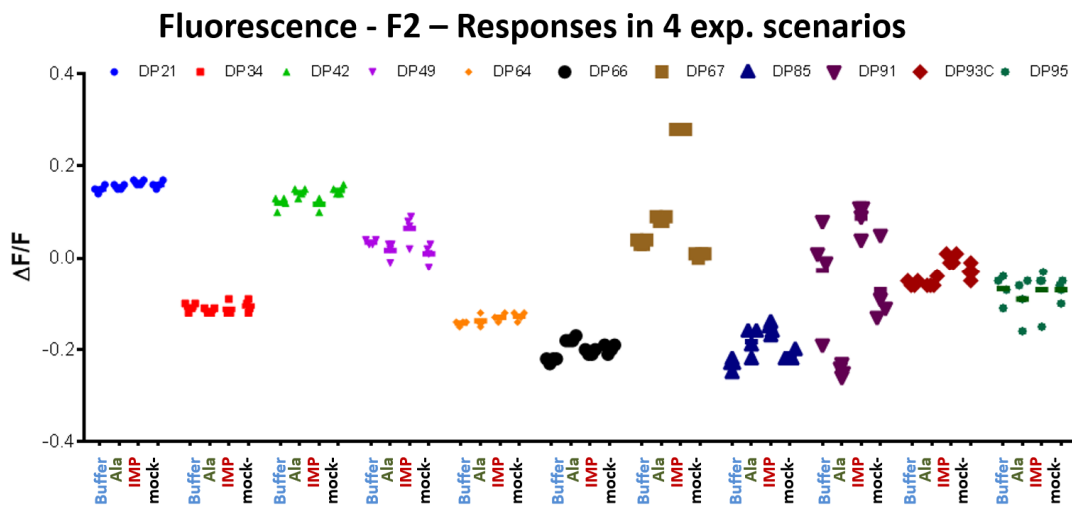


Figure 22. Fluorescence responses summary for dipeptide samples 12-22 (F2). The values are provided for the three experimental conditions with the induced cells (buffer, Ala, IMP) and the mock cells with IMP.

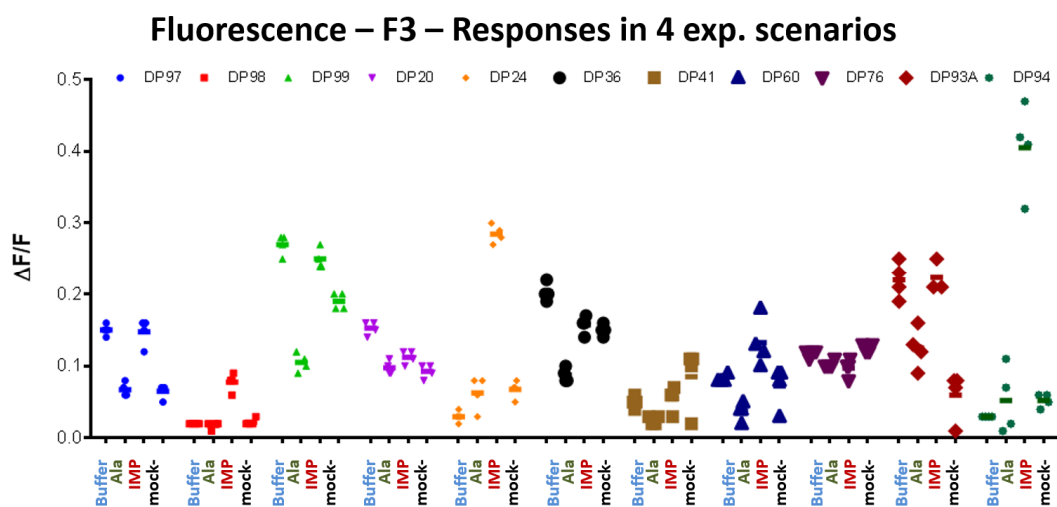


Figure 23. Fluorescence responses summary for dipeptide samples 23-33 (F3). The values are provided for the three experimental conditions with the induced cells (buffer, Ala, IMP) and the mock cells with IMP.

The results were given in $\Delta F/F$ (corrected by the baseline activity) instead of RFU. From the previous results shown it is clear none of the dipeptides were very active, as they should be around 1 in $\Delta F/F$ (at least double than baseline) to have a response similar to L-alanine. For a response to be specific, the result must be repeatable, the mock cells should not respond or have minimal response to the dipeptide, and also it should be concentration-dependent.

In Figure 21 (samples 1-11; F1), showing maximum fluorescence results (plus the raw data examination), it was possible that DP11 and DP13 had some response, as the mock cells did not activate as much as the induced, but there were no differences between buffer, L-alanine and IMP, which could mean the dipeptide interacted differently with the receptor than expected.

Also, in Figure 22 (samples 12-22; F2), DP67 seemed to have a considerable activity with IMP whereas responses for the other dipeptides like DP66 were considered artefacts (as the mock cells equally responded).

Finally, in Figure 23 (samples 23-33; F3) and from the examination of the raw data it appeared that DP24 and DP94 were found only to be active with IMP, whilst DP76 was auto-fluorescent, which was supported by the fact that all its maximum responses (in the four assays) were similar.

The analysis of the results so far confirmed the previous fluorescence experiments, but it was not definitive in terms of differentiating between genuine and non-specific responses.

It was obvious at this stage that the only way to finally confirm the activity was to represent the raw data as dose response curves, in order to detect the correct relationship between activity and concentration.

One of the findings from the fluorescence experiment with the FLIPR was that the unusual response pattern found for some dipeptides with the FlexStation (“lag time and belly”) was also seen, especially at the higher concentrations, in all the experimental conditions and with both the induced and the un-induced (mock) cells (Figure 24). This meant the response was due to the compound, and not to the instrument, the experimental conditions or the batch of cells, which suggested there was an interaction with other parts of the cell and not with the cat umami receptor fT1R1-fT1R3.

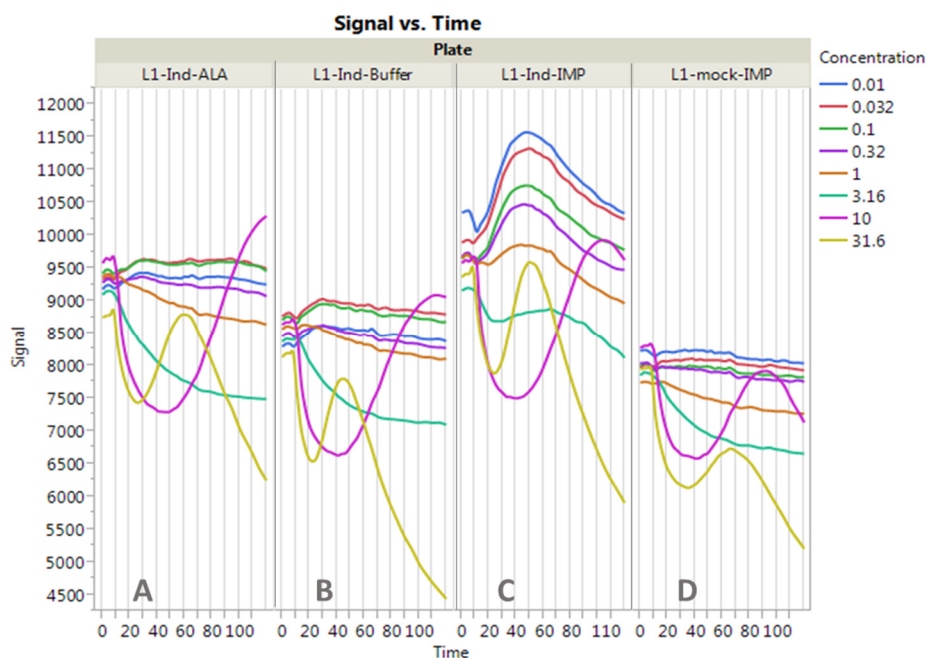


Figure 24. Unusual fluorescence response pattern for some dipeptides in dose response screening. Raw FLIPR data corresponds to DP11 – Asn-Ala. The first panel (A) starting on the left corresponds to the experiments using the induced cells with L-alanine, the second (B) with just buffer, the third (C) with IMP and the fourth (D) shows the mock cells (with IMP). All the panels show the unusual “lag time and belly” response pattern at 10 mM.

Another finding from these experiments, enabled by the raw data visualisation of different concentrations of the same dipeptide in different colours, was a possible way of differentiating dipeptide responses from IMP-driven responses for the less clear cases:

If the dipeptide was just interfering with the activation produced by the IMP, the fluorescence signal increased as the concentration of dipeptide decreased (Figure 25 left), due to the IMP being either less displaced from its binding site (if the dipeptide binding site overlapped with it) or the IMP molecules being more able to reach the binding site due to having less interference from the dipeptide molecules in solution.

On the other hand, if a dipeptide was really active, the fluorescence signal increased as the concentration of dipeptide increased (Figure 25 right). When this criteria was applied to the

compounds for which it was not possible to differentiate between a genuine and a non-specific response, it enabled the identification of the dipeptides with real umami activity.

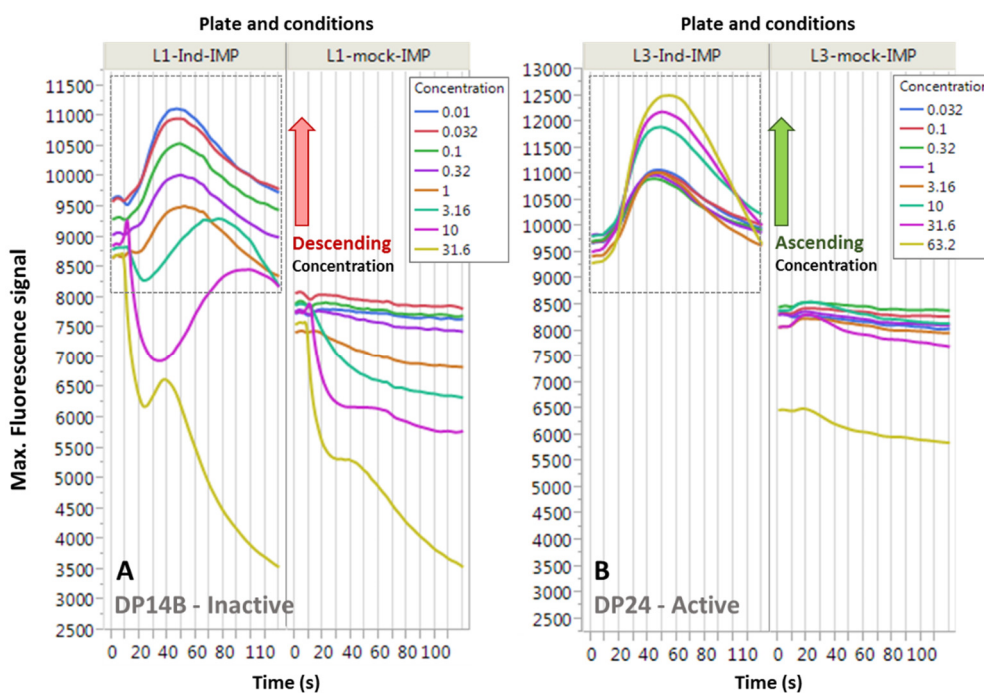


Figure 25. Difference in response patterns in non-specific and genuinely active compounds.

Raw FLIPR data corresponds to (A - Left) – Inactive / non-specific DP14B – Asn-His (first pane with induced cells and second pane with mock cells, both with IMP) and (B - Right) – Active DP24 – Gly-Cys (two panes as well). The fluorescence signal increases as the concentration of dipeptide decreases (left) or the fluorescence increases as the concentration of dipeptide increases (right). This allowed to differentiate between when the dipeptide is inactive but interferes with the activation coming from the IMP (A - left) and when the activation comes from the dipeptide (B - right). Mock cells should not show a response in genuine activation.

The controls used in the FLIPR fluorescence experiment were also very useful: The responses of the maximum umami signal expected (corresponding to 100 mM Ala + 1 mM IMP) were found to be between 17000 and 19000 RFU for the induced cells, and the baseline for the mock cells with the same stimuli was around 8500 RFU (Figure 26). These values helped putting into perspective the magnitude of the activation observed.

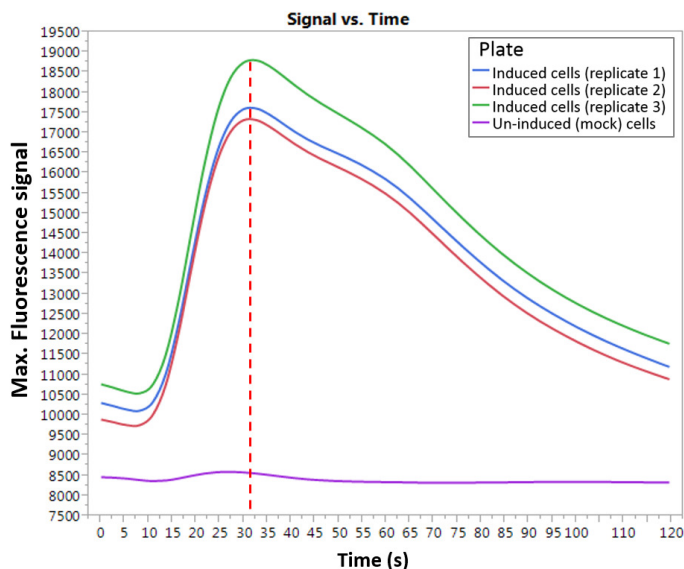


Figure 26. Maximum umami signal expected in fluorescence (100 mM Ala + 1 mM IMP). Maximum value was found to be 19000 RFU (9000 when correcting for initial fluorescence - $\Delta F/F = 0.9$). Expected activation time for the maximum was 31-32 s. Mock cells did not respond.

After the dipeptide screening in fluorescence mode, only three dipeptides had a significant activation (DP24 – Gly-Cys, DP67 – Phe-Leu and DP94 – Tyr-Gly) (see raw signal vs. time data in Figure 27). It was attempted then to obtain dose response and determine EC_{50} values for these dipeptides. The dose responses for DP24 – Gly-Cys, DP67 – Phe-Leu and DP94 – Tyr-Gly can be seen in Figure 28. The majority of the other responses in fluorescence (the other 30 samples) were found to be either non-specific (a response could be seen in the mock cells too, especially at high concentrations) or corresponding to the baseline response of IMP (which was more or less hindered by the dipeptides depending on their concentration).

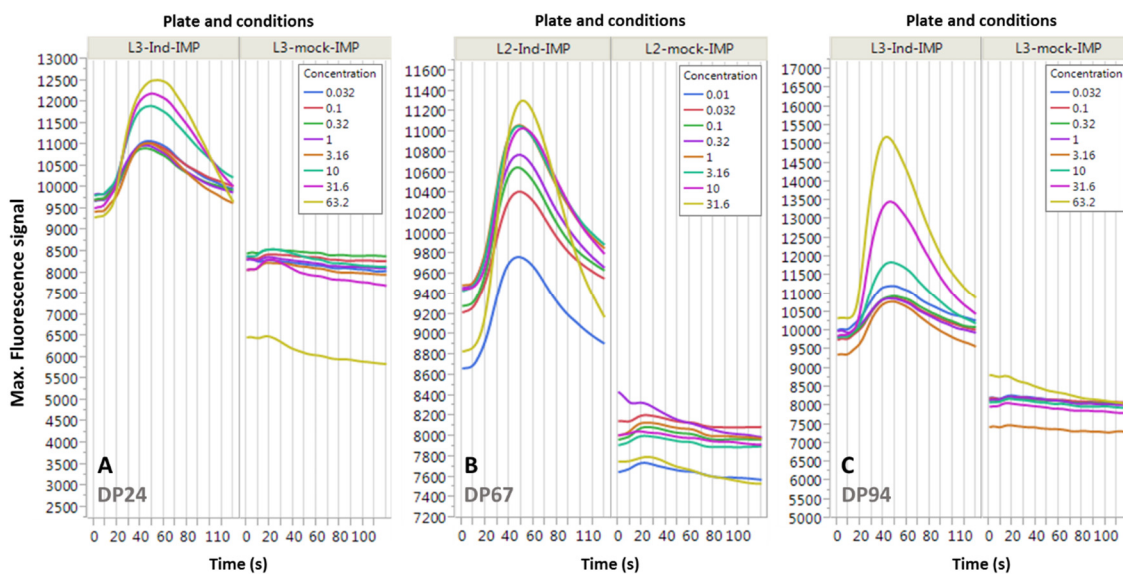


Figure 27. Raw fluorescence results of DP24 (Gly-Cys), DP67 (Phe-Leu) and DP94 (Tyr-Gly) using the FLIPR. Left (A) dose responses for DP24 (Gly-Cys). Centre (B) dose responses for DP67 (Phe-Leu). Right (C) dose responses for DP94 (Tyr-Gly). The three graphs show comparison between induced cells and mock cells, in the presence of IMP in all cases.

From the dose responses, it was determined that the EC_{50} values for the dipeptides were:

- DP24 (Gly-Cys): $EC_{50} > 60$ mM. Max. Resp.: 0.29 ($\Delta F/F$) or 38.4% (of max. L-Ala + IMP signal).
- DP67 (Phe-Leu): $EC_{50} > 30$ mM. Max. Resp.: 0.25 ($\Delta F/F$) or 33.7% (of max. L-Ala + IMP signal).
- DP94 (Tyr-Gly): $EC_{50} > 30$ mM. Max. Resp.: 0.41 ($\Delta F/F$) or 54.5% (of max. L-Ala + IMP signal).

None of the dose responses produced a plateau, so it was not possible to determine an actual EC_{50} value, but rather an estimate of the minimum concentration. The EC_{50} values suggested weaker or at best similar activity to the active amino acids shown in Table 6 in the preliminary experiments for fluorescence.

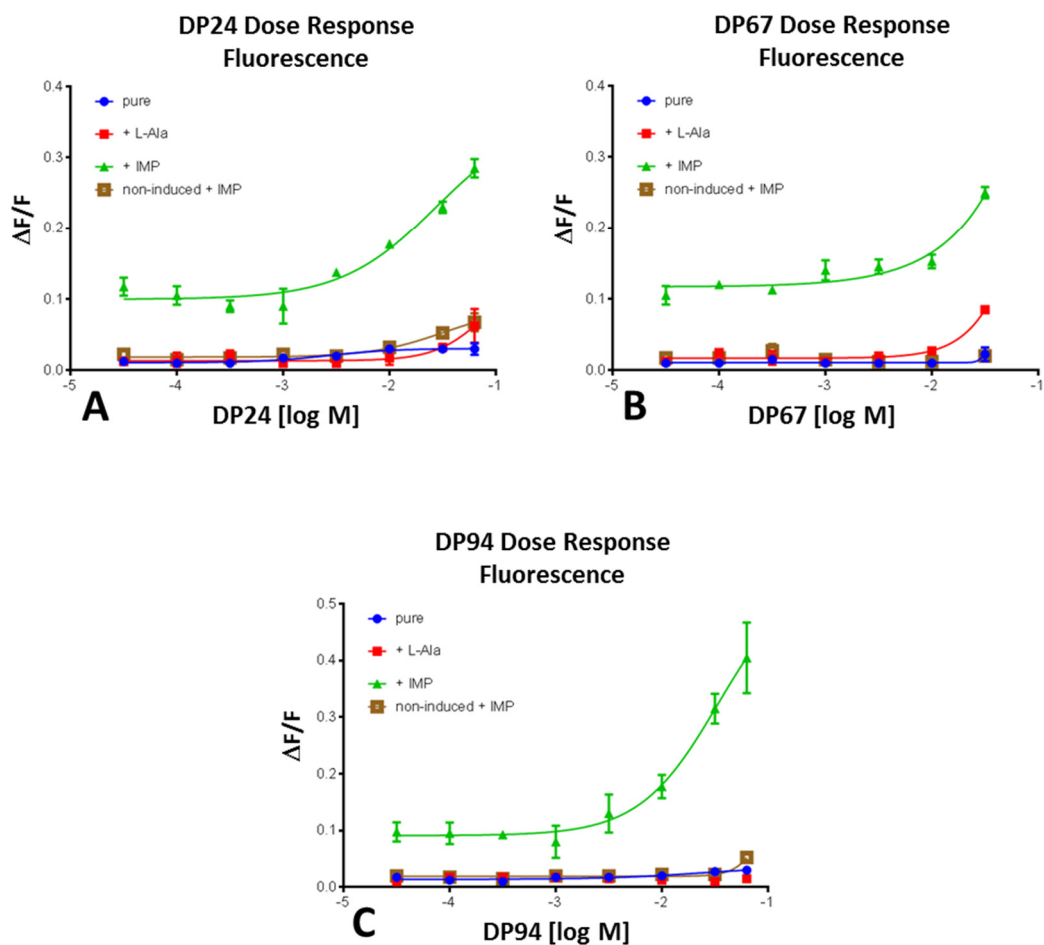


Figure 28. Dose responses of DP24 – Gly-Cys, DP67 – Phe-Leu and DP94 – Tyr-Gly (Fluorescence). (A) Dose response of DP24 – Gly-Cys, (B) Dose response of DP67 – Phe-Leu and (C) Dose response of DP94 – Tyr-Gly. Concentrations are expressed as log [M]. Signal is expressed as $\Delta F/F$. The fluorescence DR did not reach a plateau so it was not possible to determine an accurate EC_{50} . The dipeptides were not tested at higher concentrations due to shortage of compound and/or solubility issues. “Pure” meant in just buffer.

3.4.2 Luminescence experiments

The experiments conducted using luminescence detection were expected to have less interference due to auto-fluorescence and non-specific responses compared to the experiments conducted using fluorescence detection. The readings were plotted standardised (as a %) using the maximum luminescence response of the umami mixture 100 mM Ala + 1 mM IMP as the 100% benchmark. EC₅₀ calculations were attempted for each of the dipeptides but most were inactive using luminescence detection. The raw luminescence data was first analysed and visualised using ScreenWorks®. From the whole plate readings, it was evident that most wells had no activity [see an example, compound set up 3 for luminescence (L3) with induced cells in the presence of 1 mM IMP plus buffer, in Figure 29].

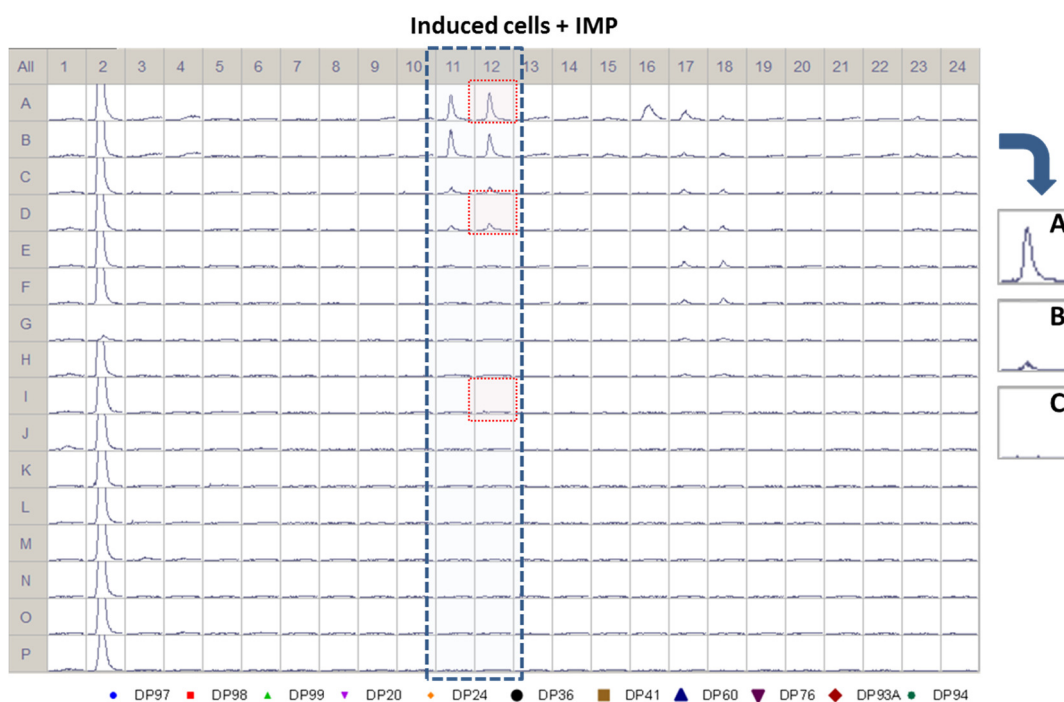


Figure 29. Example of raw luminescence activation data in the presence of IMP. Most of the dipeptides had no response or a very small response. One compound (DP24 – Gly-Cys) had a clear but small response. Different activation levels in the dose response of this dipeptide can be seen in panels A, B and C.

Even when the majority of the raw data did not show any activation in the luminescence assay, one compound (DP24 – Gly-Cys) had a clear but small response (Figure 29). Furthermore, only one of the compounds showing fluorescent activation in the previous experiment had clear luminescence signals, and suggested that most of the signals found in the fluorescence assay were in fact non-specific responses. In terms of raw data, it was found that the range of maximal signals for the dipeptides was between 800 and 4000 RLU, whilst the range of maximum signals for the umami mixture 100 mM Ala + 1 mM IMP was between 16000 and 24000 (Figure 30). An illustration of the maximum luminescence results for the different plates, using standardised data (% of maximum umami luminescence signal expected), can be seen in Figures 31, 32 and 33. The relative response (%) of most of the dipeptides when compared to the expected maximum umami response (Figure 30) was very low, in the region of 2% activation, which corresponds to around 250 RLU.

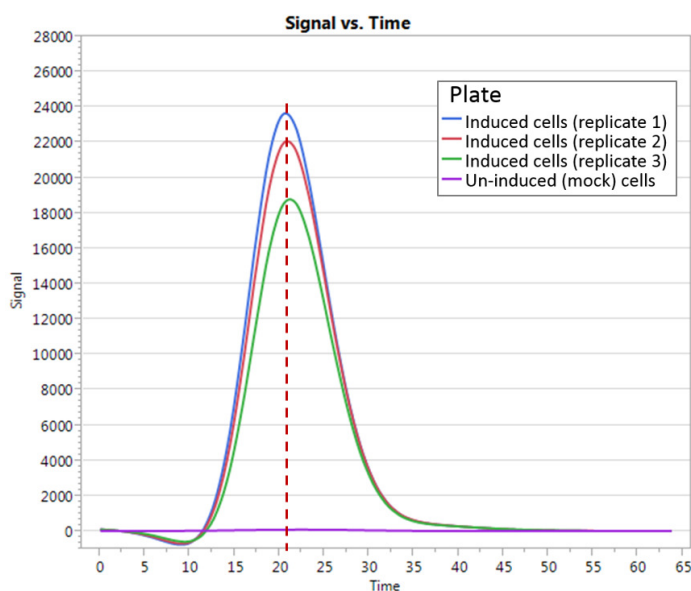


Figure 30. Reference umami luminescence response. The graph shows the luminescence response to a mixture of 100 mM Ala + 1 mM IMP. Induced cells respond in the range of 18000-24000 RLU whilst mock cells do not respond. Typical umami luminescence response is a sharp peak after around 20 seconds.

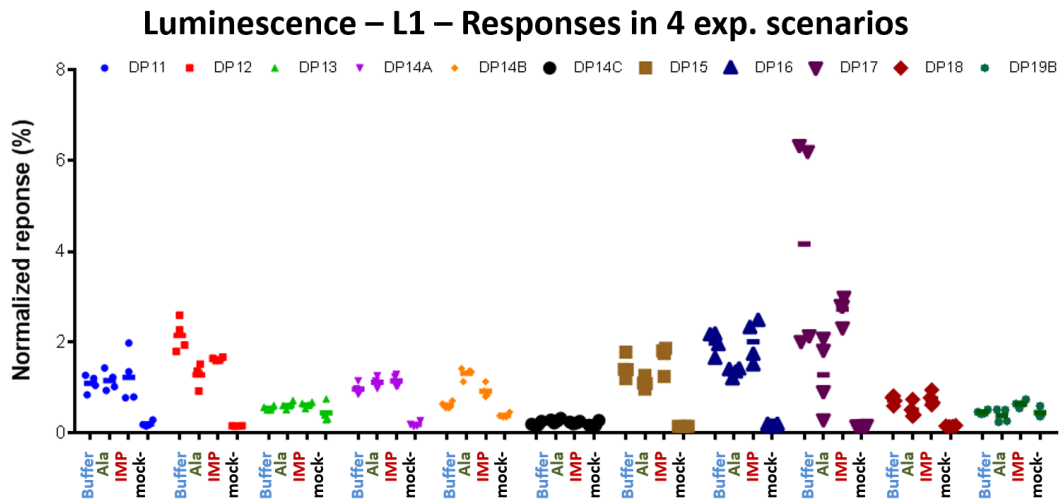


Figure 31. Maximum luminescence responses summary for dipeptide samples 1-11 (L1). The values are provided for the three experimental conditions with the induced cells (buffer, Ala, IMP) and the mock cells with IMP. All the responses were normalised versus the maximum umami response.

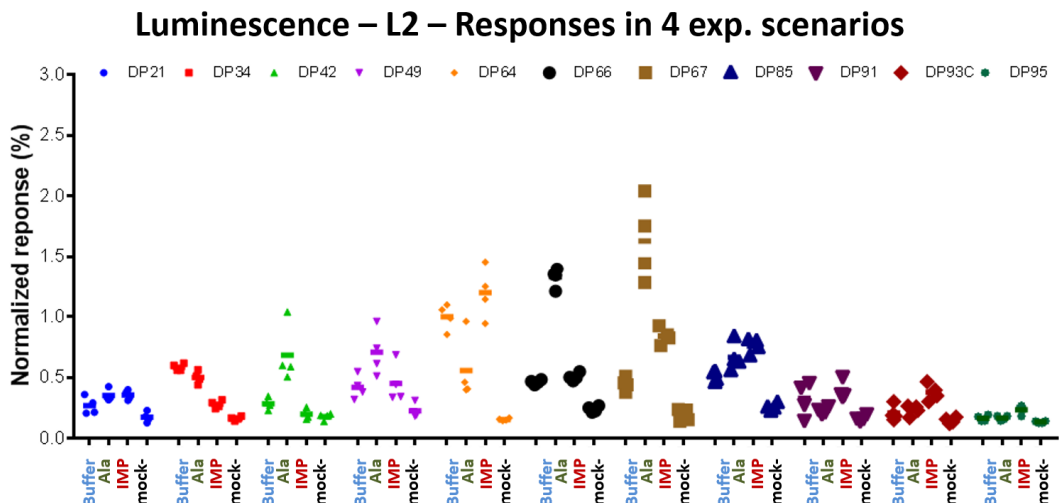


Figure 32. Maximum luminescence responses summary for dipeptide samples 12-22 (L2). The values are provided for the three experimental conditions with the induced cells (buffer, Ala, IMP) and the mock cells with IMP. All the responses were normalised versus the maximum umami response.

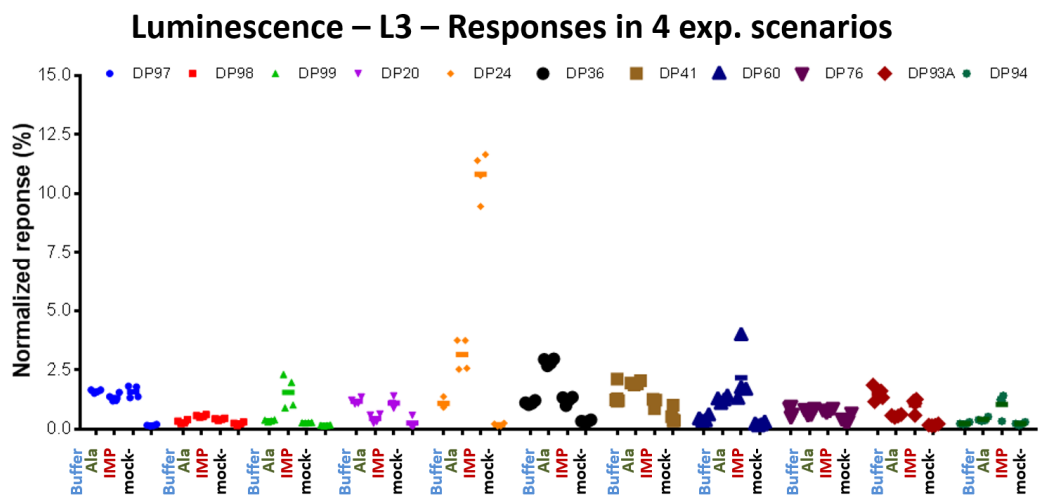


Figure 33. Maximum luminescence responses summary for dipeptide samples 23-33 (L3). The values are provided for the three experimental conditions with the induced cells (buffer, Ala, IMP) and the mock cells with IMP. All the responses were normalised versus the maximum umami response.

Two of the three dipeptides identified as active in fluorescence, DP67 – Phe-Leu and DP94 – Tyr-Gly had very low responses, however, DP24 – Gly-Cys with IMP, had a clear response close to 2300 RLU (11% relative to reference umami response). This activation for DP24 was also concentration-dependent (Figure 34).

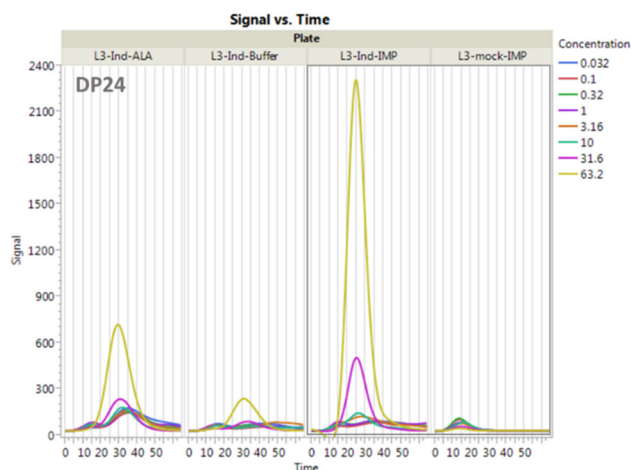


Figure 34. Luminescence response of DP24 – Gly-Cys (raw data). The luminescence at the maximum concentration with 1 mM is close to 2300 RLU, which corresponds to 11.3% of the reference response (mixture of 100 mM Ala + 1 mM IMP).

Finally, the doses response obtained with the FLIPR for DP24 – Gly-Cys, DP67 – Phe-Leu and DP94 – Tyr-Gly using luminescence are shown in Figure 35.

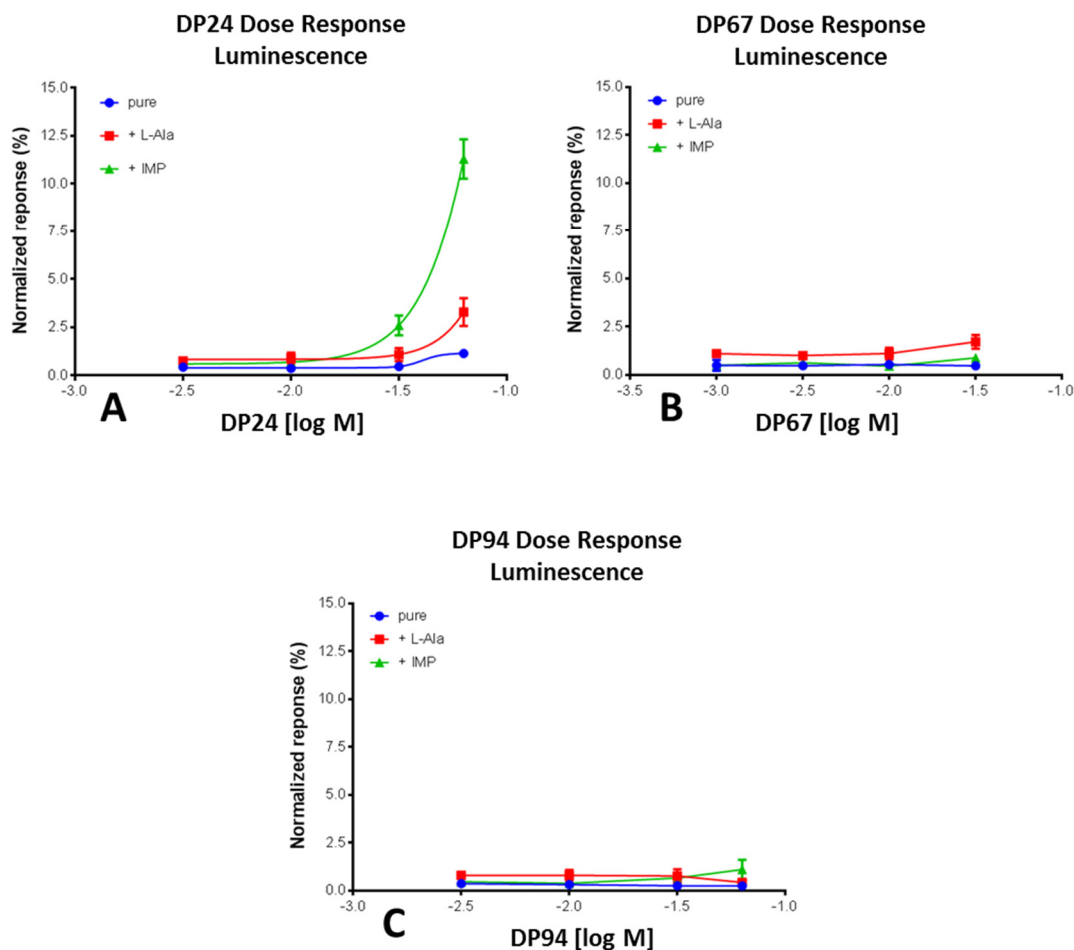


Figure 35. Dose responses of DP24 – Gly-Cys, DP67 – Phe-Leu and DP94 – Tyr-Gly (Luminescence). (A) Dose response of DP24 – Gly-Cys, (B) Dose response of DP67 – Phe-Leu and (C) Dose response of DP94 – Tyr-Gly. Concentrations are expressed as log [M]. Signal is expressed as $\Delta F/F$. The luminescence DR did not reach a plateau so it was not possible to determine a specific EC_{50} . The dipeptide was not tested at higher concentrations due to shortage of compound. “Pure” meant in just buffer.

From the dose responses, it was determined that the EC₅₀ values for the dipeptides were:

- DP24 (Gly-Cys): EC₅₀ > 60 mM. Max. Resp.: 2950 RLU or 11.3% (of max. L-Ala + IMP signal).
- DP67 (Phe-Leu): EC₅₀ = N/D (not active). Max. Resp.: < 2% (of max. L-Ala + IMP signal).
- DP94 (Tyr-Gly): EC₅₀ = N/D (not active). Max. Resp.: < 2% (of max. L-Ala + IMP signal).

3.4.3 Summary of the Fluorescence and Luminescence experiments

After the experiments with the FLIPR, including testing in dose response mode for both fluorescence and luminescence of 33 dipeptide samples, a more complete picture on the umami taste activity of dipeptides was obtained. The results from the FLIPR experiments for the 33 samples tested can be seen in Table 12.

Table 12. Summary of the results from the 33 dipeptide samples tested in the FLIPR in fluorescence and luminescence mode. The results table is divided in three compound set-ups with 11 compounds each. FlexStation fluorescence results are included for comparison. Abbreviations: AF – Auto-fluorescent; NS – Not specific; NA – Not active. IMP int. – Response due to interference of IMP; NgAct. – Negligible activity; Out. – Outlier.

Plate	Code	Dipeptide	Solub.	Supplier	Fluorescence						Luminescence		
					FlexStation			FLIPR			FLIPR		
					Activity	AF	Comments	Activity	AF	Comments	Activity	AF	Comments
PLATE 1/3	DP11	Asn-Ala	Part	PE Bio	Yes	No	NS	No	No	NS / IMP int.	No	N/A	NgAct.
	DP12	Asn-Asn	Yes	PE Bio	Yes	Yes	Prob. NS	No	No	NS / IMP int.	No	N/A	NgAct.
	DP13	Asn-Gly	Yes	PE Bio	Yes	No	NS	No	No	NS / IMP int.	No	N/A	NA
	DP14A	Asn-His	Yes	PE Bio	Yes	No	NS	No	No	NS / IMP int.	No	N/A	NA
	DP14B	Asn-His	Yes	PE Bio	Yes	No	NS	No	No	NS / IMP int.	No	N/A	NA
	DP14C	Asn-His	Yes	AnaS	Yes	No	NS	No	No	NS / IMP int.	No	N/A	NA
	DP15	Asn-Leu	Yes	PE Bio	Yes	No	NS	No	No	NS / IMP int.	No	N/A	NgAct.
	DP16	Asn-Met	Yes	PE Bio	Yes	No	NS	No	No	NS / IMP int.	No	N/A	NgAct.
	DP17	Asn-Phe	Yes	PE Bio	Yes	No	NS	No	No	NS / IMP int.	No	N/A	NgAct./Out.
	DP18	Asn-Ser	Yes	PE Bio	Yes	No	Prob. NS	No	No	NS / IMP int.	No	N/A	NA
	DP19B	Asn-Trp	Yes	PE Bio	Yes	Yes	Prob. NS	No	No	NS / IMP int.	No	N/A	NA

(Continues in next page)

Plate	Code	Dipeptide	Solub.	Supplier	Fluorescence						Luminescence		
					FlexStation			FLIPR			FLIPR		
					Activity	AF	Comments	Activity	AF	Comments	Activity	AF	Comments
PLATE 2/3	DP21	Cys-Gly	Yes	Bach	Yes	Yes	Prob. NS	No	No	IMP int.	No	N/A	NgAct.
	DP34	His-Asn	Yes	PE Bio	Yes	No	Prob. NS	No	No	NS / IMP int.	No	N/A	NgAct.
	DP42	His-Tyr	Yes	Bach	Yes	Yes	Prob. NS	No	No	NA / NS	No	N/A	NgAct./Out.
	DP49	Leu-Phe	Part	Bach	Yes	Yes	Prob. NS	No	No	IMP int.	No	N/A	NgAct.
	DP64	Phe-Asn	Yes	PE Bio	Yes	No	Prob. NS	No	No	NS / IMP int.	No	N/A	NA / NS
	DP66	Phe-His	Yes	PE Bio	No	No	Confident	No	No	NS / IMP int.	No	N/A	NgAct.
	DP67	Phe-Leu	Part	Bach	Yes	No	Confident	Yes	No	Active	No	N/A	NgAct.
	DP85	Trp-His	Yes	PE Bio	Yes	No	Prob. NS	No	No	NS / IMP int.	No	N/A	NgAct.
	DP91	Trp-Tyr	Yes	Bach	Yes	No	Prob. NS	No	No	NS / IMP int.	No	N/A	NA
	DP93C	Tyr-Asn	Yes	AnaS	Yes	No	Prob. NS	No	No	NS / Active	No	N/A	NgAct.
DP95	Tyr-His	Yes	Bach	Yes	No	Prob. NS	No	No	NS / IMP int.	No	N/A	NA	
PLATE 3/3	DP20	Asn-Tyr	Yes	PE Bio	Yes	Yes	Prob. NS	No	No	NS / IMP int.	No	N/A	NA / NS
	DP24	Gly-Cys	Yes	Bach	Yes	No	Confident	Yes	No	Active	Yes	N/A	Med. Act.
	DP36	His-His	Yes	Bach	Yes	Yes	Prob. NS	No	No	NS / IMP int.	No	N/A	NgAct. /NS
	DP41	His-Trp	Yes	Bach	Yes	Yes	Prob. NS	No	No	NS	No	N/A	NgAct./Out.
	DP60	Met-Ser	Yes	Bach	Yes	No	Prob. NS	No	No	NS / Active	No	N/A	NgAct.
	DP76	Ser-His	Yes	Bach	Yes	Yes	Prob. NS	No	Yes	NA / AF	No	N/A	NA / NS
	DP93A	Tyr-Asn	Yes	PE Bio	Yes	No	Prob. NS	No	No	NS / IMP int.	No	N/A	NA / NS
	DP94	Tyr-Gly	Part	Bach	Yes	No	Confident	Yes	No	Active	No	N/A	NgAct.
	DP97	Tyr-Met	Yes	PE Bio	Yes	No	Prob. NS	No	No	NS / IMP int.	No	N/A	NgAct. /NS
	DP98	Tyr-Phe	Part	Bach	Yes	No	Prob. NS	No	No	NS / Active	No	N/A	NgAct.
DP99	Tyr-Ser	Yes	PE Bio	Yes	No	Prob. NS	No	No	NS / IMP int.	No	N/A	NgAct. /NS	

It is important to highlight that especially in fluorescence, the analysis of raw data for a dipeptide and colour visualization of the different concentrations allowed to assess concentration-dependant patterns to differentiate real from non-specific responses. A real agonist activity showed an increase of the response when the concentration of the dipeptide increased, whereas an interference with the IMP signal showed a decrease of the response as the concentration of dipeptide increased. As mentioned before, this was possibly due to the IMP being able to better access the nucleotide binding site in the receptor when less dipeptide molecules were binding to an overlapping binding site region in the receptor. Also at the higher concentrations (normally 10 mM or more) an unusual response pattern (called before “lag time and belly” shape) was also seen with the FLIPR instrument, which supported the data obtained previously with the FlexStation and suggested an interaction of the dipeptide with the receptor

or the cells with a different mechanism to the canonical binding of amino acids to the cat umami receptor FT1R1-FT1R3.

Eventually, only three dipeptides (DP24 – Gly-Cys, DP67 – Phe-Leu and DP94 – Tyr-Gly) were identified from the fluorescence experiments as having a weak but significant umami activity. The fluorescence results for DP24, DP67 and DP94 were previously shown in Figures 27 and 28.

In terms of the luminescence experiments, only one dipeptide, DP24 – Gly-Cys, had any significant activity (11.3% of the response provided by a 100 mM Ala + 1 mM IMP mixture), which was also identified as being active in the fluorescence experiments. None of the other dipeptides (including the two other dipeptides identified as active in fluorescence) had higher response than 2% in luminescence. This was a bit surprising as the results of luminescence and fluorescence normally correlate, although given the low responses we obtained with luminescence this result could be due to several factors such as the level of expression of the photoprotein in the cells used, or the different interactions with the different dipeptides.

Auto-fluorescent compounds:

The investigation with the FLIPR of the possible auto-fluorescent dipeptides found with the FlexStation showed only one possible auto-fluorescent compound, DP76 – Ser-His (soluble dipeptide), as it is shown in Figure 36A, with a very characteristic response pattern in the fluorescence reading (comparison with the FlexStation results are shown in Figures 36B and 36C), which disappeared in the luminescence reading. Auto-fluorescence can be identified from the typical shape of the response curve (sharp increase after injection, followed by a plateau), however, other interactions provided similar patterns before in fluorescence with the FlexStation (see previous Figure 19). With luminescence, none of the previously suspected

auto-fluorescent compounds kept the unusual response pattern, which indicated that they might be auto-fluorescent, however, only the unusual response pattern was reproducible in fluorescence for DP76, so only this compound was marked as genuinely auto-fluorescent.

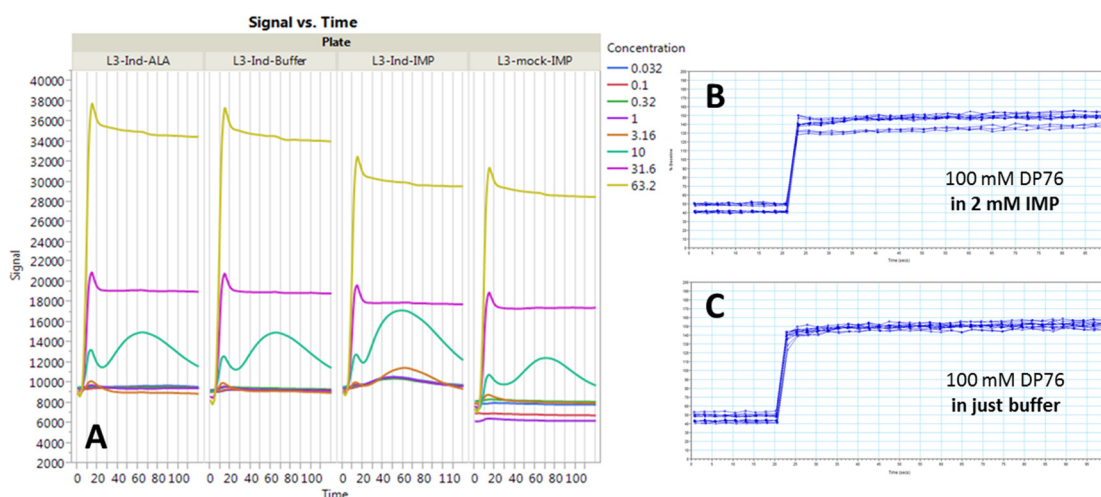


Figure 36. Fluorescence results for the auto-fluorescent dipeptide DP76 – Ser-His. Left (A) dose responses for DP76 (Ser-His) using the FLIPR (in luminescence the response of DP76 was flat). Right top (B) Raw data corresponding to the primary screening of 100 mM DP76 (Ser-His) with IMP using the FlexStation. Right bottom (C) Raw data corresponding to the primary screening of 100 mM DP76 (Ser-His) with just buffer using the FlexStation.

Moreover, only one of the compounds showed auto-fluorescence in the FLIPR experiment in the fluorescence readings (from a list of 30 different chemical species), whereas up to 12 were suspected of giving an auto-fluorescent response with the FlexStation. The results in the FLIPR and the FlexStation for DP76 (Ser-His) correlated well, however the rest did not. After reviewing the initial assessment of the 12 compounds with the fluorescence data in the FlexStation, and after the learnings and experience gathered with the rest of the experiments, it was now clear that only DP76 was actually auto-fluorescent, and the response patterns of the others could be clearly explained via other phenomena (see Table 13), for example, peak after injection, solid particles in solution and other non-specific interactions.

Table 13. Final conclusions on the 12 possible auto-fluorescent compounds. The fluorescence FlexStation data was reviewed after the FLIPR experiment. The second assessment was of much higher accuracy after the learnings from the FLIPR experiment on the differences between genuine and non-specific responses.

Code	Dipeptide	Solubility	Conclusion
DP12	Asn-Asn	Soluble	Peak after injection
DP19	Asn-Trp	Soluble	Peak after injection
DP21	Cys-Gly	Soluble	Peak after injection
DP36	His-His	Soluble	Peak after injection
DP41	His-Trp	Soluble	Peak after injection
DP42	His-Tyr	Soluble	Peak after injection
DP20	Asn-Tyr	Soluble	Non-Specific
DP49	Leu-Phe	Part. Sol.	Solids
DP51	Leu-Trp	Part. Sol.	Solids
DP59	Met-Phe	Part. Sol.	Solids
DP61	Met-Trp	Part. Sol.	Solids
DP76	Ser-His	Soluble	Auto-fluorescent

Quality control experiments: batch and supplier comparisons:

In relation to the quality control experiments to determine effect of batch or supplier on the results, it must be mentioned that after the initial unusual response patterns obtained (e.g. “lag time and belly”) the purity of the dipeptides was questioned, so, in order to clarify this, and for quality control purposes, the chemical structure of the dipeptides from one supplier (PE Biosciences) with the same dipeptides from another supplier (AnaSpec) was compared. After analysis using HPLC-MS performed at WALTHAM® (see Appendix 5), it was proven that chemically the two samples chosen (for DP14 – Asn-His and DP15 – Asn-Leu) were the same.

After doing these chemical quality checks, the next step was to determine if the behaviour *in vitro* was the same or not. Due to the amount of material available, only a small set of *in vitro* experiments were designed (see Table 14).

After analysing the *in vitro* results, the conclusion was that there was a good agreement (qualitatively) between the *in vitro* results from different batches of the same supplier or batches from different suppliers (PE Biosciences and AnaSpec). Samples from Bachem were not tested.

Table 14. Differences in the results between batches and between suppliers for some dipeptides. Dipeptide code labels: **A** – First batch PE Biosciences, **B** –second batch PE Biosciences and **C** –alternative supplier AnaSpec. The three activation patterns [from fluorescence data (FlexStation and FLIPR) and luminescence data (FLIPR)] are compared for the different batches / suppliers (Left vs. Right). Green background: Match between the responses (total overlap); Blue background: Very small differences. Yellow background: Moderate differences (e.g. In the FLIPR, 93C showed some small activity in fluorescence, but not 93A). White background: Not comparable due to no data available for one of the samples in the pair being compared. “PAI” means Peak after injection. “NS” means non-specific. “NA” means not active.

Left			<i>In vitro</i> data			Right			Summary
Code	Suppl.	Batch	Fluor.	Fluor.	Lumi.	Batch	Suppl.	Code	Conclusion
DP19A	PE Bio	1	Match	Not comparable	Not comparable	2	PE Bio	DP19B	Asn-Trp PAI / NA
DP14A	PE Bio	1	Match	Moderate differences	Match	2	PE Bio	DP14B	Asn-His NS / NA
DP14C	AnaS	1	Not comparable	Very small differences	Very small differences	2	PE Bio	DP14B	
DP93A	PE Bio	1	Moderate differences	Moderate differences	Very small differences	1	AnaS	DP93C	Tyr-Asn NS / NA

3.5 Consolidation of *in vitro* experimental results

3.5.1 Answers to the questions formulated prior to the *in vitro* experiments

As mentioned in a previous section, the questions that needed to be answered after finishing all the *in vitro* experiments were:

1. Which of the dipeptides are really active?
2. Can the non-specific responses observed be assigned to a particular cause such as the experimental conditions or the compounds?
3. Is it possible to differentiate between auto-fluorescence and non-specific responses?
4. Do compounds with different batches from the same supplier or from a different supplier perform equally?
5. Do the experiments suggest a different activation mechanism for the dipeptides?

Answer to question 1 – Were the dipeptides initially selected really active?

The majority of the compounds marked as “possibly active” (although weak) after the fluorescence experiment in the FlexStation were confirmed to be non-specific responses instead of real responses in the luminescence experiment.

Even so, the dipeptides identified as being active were only weakly active, which explains why it was so difficult to extract conclusions with the primary screening experiments in the FlexStation.

The fluorescence experiment with the FLIPR in dose response mode was invaluable, because instead of seeing several “snapshots” at different times and concentrations, it was possible to see the evolution of activation with time for all the different concentrations simultaneously. This allowed to see if there was a real concentration dependency of the activation (a ligand should produce an increase of the response as the concentration increased, whereas the compounds with the opposite pattern were deemed as interfering with the baseline response induced by the IMP).

Answer to question 2 – Where the unusual response patterns due to the dipeptides?

Yes they were, although some were due to the instrument as well. The information about the non-specific responses found with the FlexStation fluorescence experiment was clarified after the FLIPR fluorescence and luminescence experiments:

(a) The unusual response pattern (“lag time and belly”) obtained in the FlexStation fluorescence experiment was also found in the FLIPR fluorescence experiment. This effect was seen only at the higher concentrations and it was related to the dipeptides.

(b) The peak just straight after injection (probably to a change in refraction properties in the well) was seen both in the FlexStation and in the FLIPR fluorescence experiments. However the FLIPR allowed analysing the results from different reading time brackets, which enabled the elimination of this effect.

(c) The possible auto-fluorescent compounds in the FlexStation experiment did not provide repeatable results with the FLIPR. Only one of the 12 compounds was actually auto-fluorescent (and completely inactive in the luminescence assay).

(d) The interference from solids found in the FlexStation was not seen at all in the experiments with the FLIPR. This could be due to the lower maximum concentrations attempted with the FLIPR.

Answer to question 3 – Which dipeptides were really auto-fluorescent?

Only one of the compounds (DP76 - Ser-His) showed auto-fluorescence in the FLIPR experiment, whereas up to 12 were suspected of auto-fluorescent response with the FlexStation. The results in the FLIPR and the FlexStation for the auto-fluorescent dipeptide correlated well, however, for the rest they did not. Their unusual responses could be explained

by other phenomena, such as changes in optical properties in the solution after compound injection, presence of particles in solution creating light scattering, and non-specific responses.

Answer to question 4 – Are batch and supplier variation influencing the results?

As mentioned before, there was a good agreement (qualitatively) between the *in vitro* results from different batches of the same supplier or batches from different suppliers (PE Biosciences and AnaSpec), so these variables did not influence the outcome of the experiments.

Answer to question 5 – Are the dipeptides active through a different mechanism?

If the dipeptides followed a nucleotide-like mechanism to activate the cat umami receptor fT1R1-fT1R3, this would have been seen in the experiments with L-alanine in buffer. There was some small activation in some cases, but this was infrequent and normally smaller than the activation with IMP (related to the amino acid mechanism). The size of the activation provided by the dipeptide in the presence of L-alanine was negligible most of the time, and often similar to the response in buffer only. After the *in vitro* experiments, the mechanism of interaction of the dipeptides with the receptor was different to that of nucleotides, although still was unclear if it was indeed the same as the amino acids. Additional binding mechanisms could not be dismissed.

3.5.2 Summary of *in vitro* experiment results

As mentioned before, the interpretation of the results was more enlightening after the FLIPR results (fluorescence and luminescence dose responses), so these were used to re-interpret the results obtained with the FlexStation experiments (fluorescence primary screening).

Three dipeptides were found to be active:

From the 101 dipeptides tested, three dipeptides were active, DP24 (Cys-Gly), DP67 (Phe-Leu) and DP94 (Tyr-Gly), with activities similar or lower than those of their corresponding L-amino acids. The rest of the dipeptides had either insignificant / no activity, or elicited non-specific responses.

The estimation of some of the activation parameters for the three active dipeptides can be seen in Table 15. The percentage activation for the three dipeptides in the fluorescence experiments was expressed firstly in relation to the expected maximum fluorescence or umami activity provided by the mixture of 100 mM L-alanine plus 1 mM IMP, and secondly in relation to the “signal to noise” ratio (as $\Delta F/F$), expressed as a decimal or as a percentage over the fluorescence activation of the baseline (i.e. an activation of 1 or 100% would mean double the fluorescence activation than the baseline). The percentage activation for the dipeptides in the luminescence experiments was expressed in relation to the expected maximum luminescence or umami activity provided by the mixture of 100 mM L-alanine plus 1 mM IMP.

Most of the 11 L-amino acids stimulating the cat umami receptor fT1R1-fT1R3 would reach an $\Delta F/F$ between 1-1.5 at 100 mM in the presence of IMP (including the reference umami signal of the 100 mM L-alanine plus 1 mM IMP mixture). As the values from the FLIPR fluorescence experiment were obtained for lower maximum concentrations (63.2 mM or 31.6 mM), it is possible that the activation of these dipeptides could be lower but in the same region than those of the individual amino acids. However, in the FLIPR luminescence experiment, the results did not fully correlate and only one of the dipeptides displayed any activation (11% of

the reference umami), whilst the rest of dipeptides did not reach a luminescence activity higher than 2%.

Table 15. Activation profiles on the three umami-active dipeptides. The EC₅₀ values were estimated from the FLIPR dose response curves [Figure 28 (fluorescence) in section 3.4.1 and Figure 35 (luminescence) in section 3.4.2].

Active Dipeptides	DP24 - Gly-Cys	DP67 - Phe-Leu	DP94 - Tyr-Gly
Dipeptide info. and qualitative data			
	Active Soluble	Active Partially soluble	Active Partially soluble
Max. Conc.	63.2 mM	31.6 mM	63.2 mM
Fluorescence	<p>$\Delta F/F = 0.29$ 38.4% of max Ala + IMP EC₅₀ > 60 mM</p>	<p>$\Delta F/F = 0.25$ 33.7% of max Ala + IMP EC₅₀ > 30 mM</p>	<p>$\Delta F/F = 0.41$ 54.5% of max Ala + IMP EC₅₀ > 30 mM</p>
Luminescence	<p>2950 RLU 11.3% of max Ala + IMP EC₅₀ > 60 mM</p>	<p>N/D (no activity) <2% of max Ala + IMP EC₅₀ N/D</p>	<p>N/D (no activity) <2% of max Ala + IMP EC₅₀ N/D</p>

Note: The maximum 100 mM Ala + 1 mM IMP signal is the reference umami response (100%). N/D means not determined.

3.6 *In silico* experiments

3.6.1 Molecular modelling

The objective of the *in silico* modelling was to identify a possible binding mechanism for the three dipeptides that were found to be active *in vitro*.

3.6.1.1 Preliminary models with L-amino acids

As mentioned in the Materials and Methods Chapter, all *in silico* modelling work was performed by BioPredict, Inc. Three-dimensional homology models of the cat T1R1 flytrap (active site) were produced based on known crystal structures from human Metabotropic Glutamate Receptors (e.g. mGluR1). This homology model constructed with the consensus cat T1R1 receptor sequence had previously been challenged with the active L-amino acids (docking experiments) to check the correlation with the *in vitro* data, which suggested responses to a broad range of L-amino acids, different to human, as mentioned in the Introduction Chapter.

As it was hypothesised that the dipeptides would follow a binding mechanism that was the same or similar to that of L-amino acids, it was necessary to examine this first in detail. From the models of L-amino acid binding, the 11 L-amino acids able to bind to the cat umami receptor fT1R1-fT1R3 *in vitro* docked well to the agonist binding site in the homology model of the fT1R1-fT1R3 receptor, and were predicted to potentiate lobe closure of the Venus flytrap (VFT) and downstream signal propagation. L-amino acids are zwitterions (a neutral molecule with one negative and one positive charge) at intermediate pH. The interaction of the amino acids was in zwitterionic form, where the amino group gained one proton and became positively charged ($-\text{NH}_3^+$), and the carboxyl group lost one proton and became negatively charged ($-\text{COO}^-$). The binding of the L-alanine zwitterion is shown in Figure 37. L-alanine was shown to form extensive interactions close to the hinge of the flytrap of the cat umami receptor fT1R1-fT1R3 model.

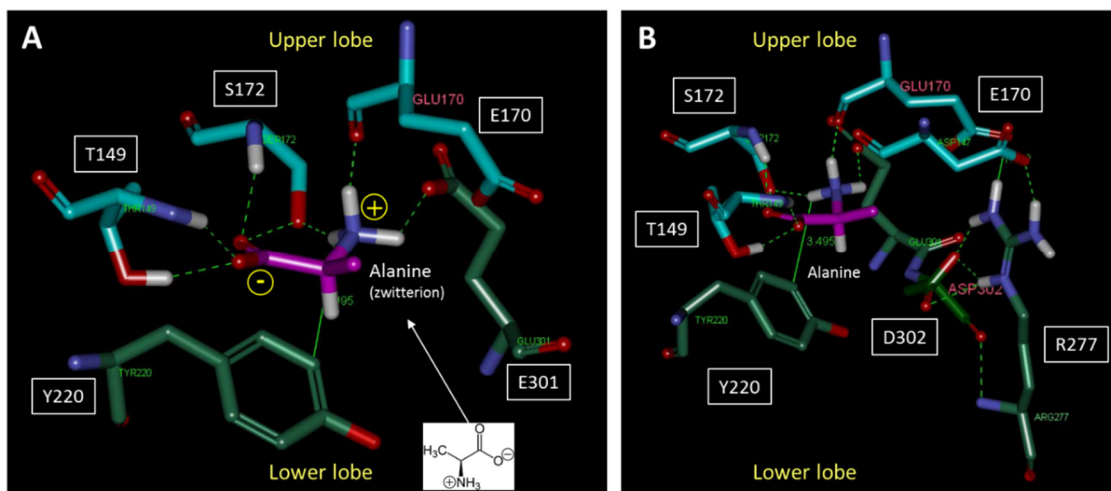


Figure 37. Example of a zwitterionic amino acid (L-alanine) binding to the Venus flytrap of the ft1R1 in the cat umami receptor ft1R1-ft1R3. Upper lobe residues are represented in blue and lower lobe residues in green. Left (A) L-alanine (as a zwitterion) binding to Thr and Ser, interacting with two Glu in the upper and lower lobes and with Tyr in the lower lobe (B) Different view showing the neighbouring positive Arg coordinating to negative residues thus balancing electrostatic charge in the binding site.

The agonist activity of L-alanine was proposed to occur in two stages, first the L-alanine binds to the upper lobe of the open conformation, then the upper lobe closes tightly onto the lower lobe, producing a conformational change and enabling signal propagation to the transmembrane domain and into the cell. The interactions in Figure 37A showed a hydrogen bond formed between Thr (T149) and Ser (S172) to both oxygens of the carboxylate of the L-alanine, and a coordination of the zwitterionic -NH_3^+ by the side chain of Ser (S172), the backbone of Glu (E170) and the side chain of another Glu (E301). The -NH_3^+ was close to the ring of the Tyr (Y220) where it could form additional anion- π interactions. The Tyr (Y220), with its planar phenolic group, formed the “floor” of pocket in the binding site. A very similar mechanism was found for the all other active L-amino acids.

As mentioned in the introduction, the main difference between the human and the cat or mouse active binding site in the T1R1 umami receptor was the substitution of neutral amino acids in the receptor sequence of human (A170 and A302) by charged amino acids in cat and mouse (E170 and D302). This created a possible electrostatic repulsion with the potential agonists docking and in the strength of the closure of the flytrap (which explains why Glu and Asp are not umami-active for cats in the *in vitro* experiments, but are the primary umami taste agonists in human). However, in Figure 37B it is shown that on binding and lobe closure, Arg (R207, which is positively charged) could effectively coordinate interactions with upper lobe residues Asp (D147) and/or Glu (E170) (which are negatively charged), further stabilising the closed form of the flytrap. Arg (R227) was also fixed through potential interaction with Asp (D302) on the lower lobe.

In the work of Zhang et al. (2008), the interacting residues on the upper and lower lobes that helped to stabilise the closed form of the flytrap were called “pincer residues”. These pincer residues are much closer to the VFT hinge (active site) in cat and mouse than in human (the pincer residues provide more stabilisation the closer they are to the hinge). This could mean that the cat T1R1 is tuned to potentiate signals for smaller L-amino acids such as L-alanine, whilst the human T1R1 lacks the stabilisation due to pincer residues in this area and is tuned instead to longer zwitterionic agonists like L-glutamic acid.

3.6.1.2 Potential molecular mechanism for dipeptide binding

From an *in silico* modelling point of view, linear L-dipeptides (H-AA1-AA2-OH) may bind *a priori* with a different canonical mechanism to that of L-amino acids due to their zwitterionic conformation being different/ longer: Their NH_3^+ (N-terminus) and COO^- (C-terminus) charges are too far apart, with five bond-lengths between the charges instead of two, to follow exactly the same mechanism as L-amino acids (see Figure 7 in the Introduction Chapter). However,

they could still bind to the same active site, as other residues in the proximity of the orthosteric binding site can stabilise the closure of the Venus flytrap in fT1R1. Toda et al. (2013) stated that the differences in residues outside the orthosteric site could confer the broadly-tuned properties to the mouse umami receptor mT1R1-mT1R3, similar to the cat, and explained some of the differences in perception between species.

In theory, it is possible to dock dipeptides to the cat T1R1 active site, and form interactions close to the hinge to stimulate closure of the flytrap. However, these interactions would not be ideal and could not be enough to stimulate a closed conformation of the Venus flytrap and generate the conformational change needed for signal transduction. As the dipeptides are also zwitterions, in many cases the negative carboxylate group in the dipeptide could still form hydrogen bonds in the upper lobe of the VFT, however the positive amino residue could not bind in the same way as the L-amino acids and had to form alternative bonds. This may mean that even if the dipeptide could bind, it would not stimulate the same agonist activity as the L-amino acids due to not having enough interactions that stabilise the closed conformation of the VFT. In any case, the binding strength of the dipeptides could be as strong but not be stronger than the binding of free L-amino acids.

3.6.1.3 In silico modelling of the three active dipeptides

Computer models of the three active dipeptides (DP24 – Gly-Cys, DP67 – Phe-Leu and DP94 – Tyr-Gly) were generated using the same homology model of the cat umami receptor fT1R1-fT1R3 in order to ascertain possible molecular mechanisms of interaction with the receptor. Other dipeptides were also modelled (e.g. DP33 – Ala-His, DP28 – Gly-Met) in order to identify why these dipeptides specifically were active and others not. The dipeptide binding was also

modelled with and without the presence of a nucleotide, in order to confirm the rationale made previously of the dipeptide and the IMP interfering with each other.

DP24 – Gly-Cys:

The *in silico* model of the binding of DP24 - Gly-Cys is shown in Figures 38A and 38B. In this binding mode the sulphur of the Cys residue was pointed into a tight pocket. Gly-Cys exhibited a binding mode that mimicked the classic binding mode of amino acids as they bind to the hinge, but with a notable difference. For amino acids, a key conserved interaction is a salt bridge between the zwitterionic N of the amino acid and Glu170 on the upper lobe of the flytrap (Figure 38C). This is seen in all crystal structures of amino acids bound to the hinge of flytraps, for example in all mGluR crystal structures. Because the $-NH_3^+$ is part into the peptide bond in the dipeptide (Gly-Cys), the interaction to Glu170 from this nitrogen can only be a weaker hydrogen bond. For Gly-Cys this is compensated by the ability of the amino-terminal group to wrap around to form a salt bridge to the same GLU170, which suggests Gly-Cys is a very good candidate for agonizing ft1R1/ft1R3.

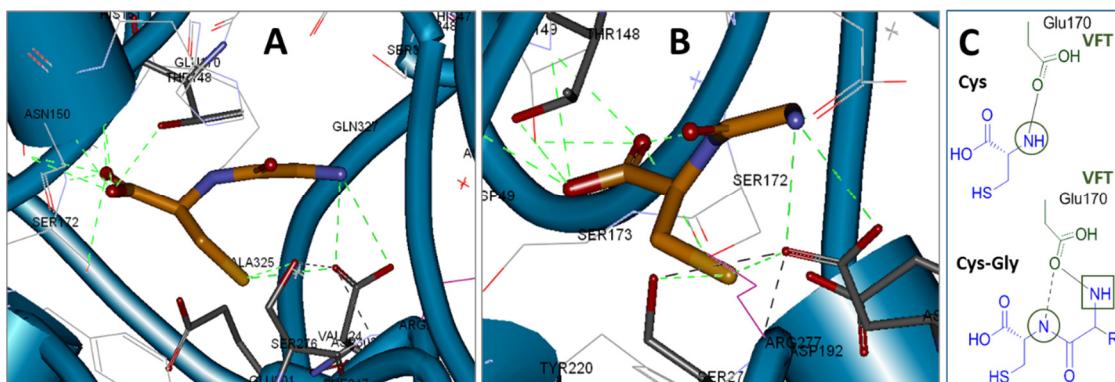


Figure 38. Docking of Gly-Cys (DP24) in the umami active site in the VFT of ft1R1. (A/B) Gly-Cys dipeptide is represented in gold. Multiple possible hydrogen bonds (HB) and salt bridges (SB) are highlighted in green. **(C)** Different salt bridge interactions for Cys and Gly-Cys.

Other dipeptides cannot form this salt bridge to Glu170. Larger N-terminal amino acid side chains would generate potential “clashes” with the receptor that drive the N-terminal nitrogen away from Glu170. In the case of Gly-Cys, the terminal nitrogen also forms a salt bridge to Asp302 on the lower lobe of the flytrap. This is seen for other dipeptides with larger side chains (for example, Tyr-Gly). While this is highly desirable to stabilise the closed form of the flytrap, it may not provide sufficient binding energy initially to the upper lobe in the resting, open form of the flytrap. Variations of Gly-Cys, such as the longer DP28 - Gly-Met would not fit well, with the expectation that there would be a loss of activity.

DP67 – Phe-Leu:

The *in silico* model of the binding of DP67 – Phe-Leu is shown in Figure 39. In this binding mode, the dipeptide was bound by forming a salt bridge to Glu (E170) and Asp (D302) (arrows). The Phe side chain (phenyl-) extended into a region of the active site normally occupied by the head-group of nucleotides, which would hinder the binding of the dipeptide. To accommodate both the dipeptide and the nucleotide would mean either a movement of the dipeptide away from this “preferred” binding mode that mimics L-amino acid binding modes, or a movement of the nucleotide away from its “preferred” binding position. Some amino acids in the Phe position could accommodate this adjustment differently depending on the side chain, resulting in a sensitive structure-activity relationship (SAR). In any case, the *in silico* modelling predicts weaker binding for this dipeptide.

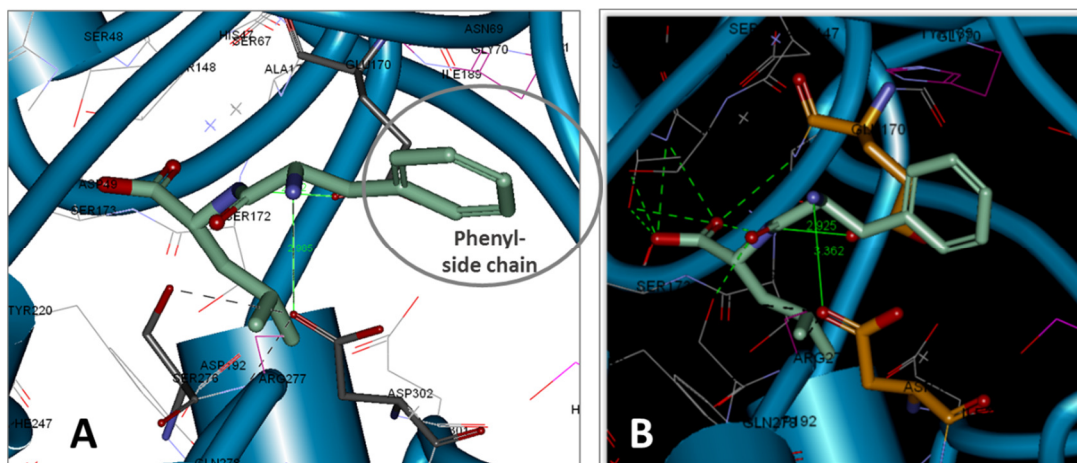


Figure 39. Docking of Phe-Leu (DP67) in the umami active site in the VFT of ft1R1. Phe-Leu molecule is represented in light green. **A** – Frontal view. **B** – Lateral view. Multiple possible hydrogen bonds (HB) and salt bridges (SB) are highlighted in green.

DP94 – Tyr-Gly:

The *in silico* model of the binding of DP94 – Tyr-Gly is shown in Figure 40. In this binding mode, there was a salt bridge to Asp (D302) (in gold) of the lower lobe. One point worth noting is that a Gly in the second position gave the ligand significant flexibility to fit to the hinge of the flytrap; e.g. H-Tyr-Ala-OH was more rigid (which is inactive). This suggested a structural reason why a glycine in the second position would be preferred.

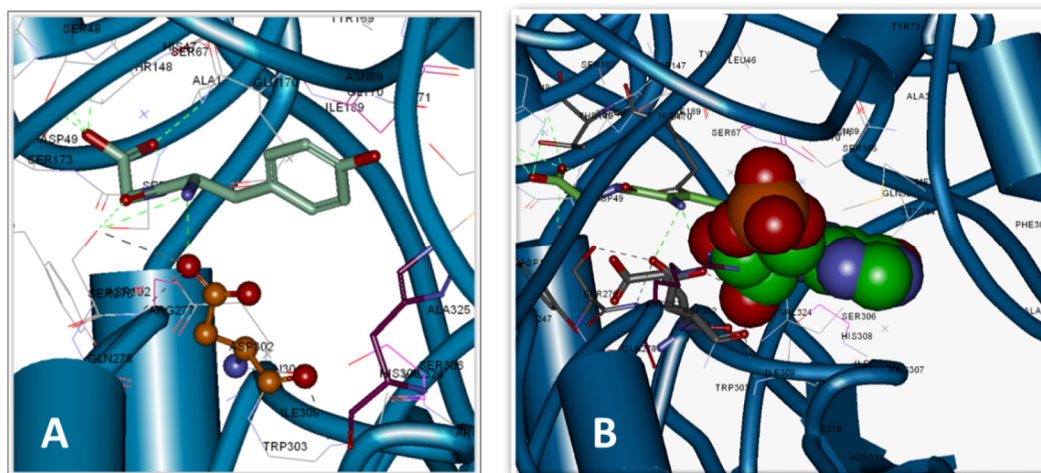


Figure 40. Docking of Tyr-Gly (DP94) in the umami active site in the VFT of ft1R1. (A) Tyr-Gly molecule is represented in light green. Asp (D302) receptor residue is represented in gold. Multiple possible hydrogen bonds (HB) and salt bridges (SB) are highlighted in green. (B) With nucleotide (IMP, bigger molecule on the right) – there is significant overlap.

3.6.1.4 *In silico models of inactive dipeptides*

Some inactive dipeptides were also modelled (e.g. DP28 – Gly-Met, DP92 – Tyr-Ala) in order to identify why the previous three dipeptides specifically were active and others not. While Gly-Cys fitted the active site (Figure 38), Gly-Met with its extended side chain did not (see Figure 41A). The clashes shown as red dashed lines in the purple circle (arrow) would prevent binding to the active closed form of the flytrap.

Tyr-Ala could fit the active site, but poorly (see Figure 41B). There were clashes (red dash line in the purple circle, arrow) to Glu170 which would force Glu170 to rotate away, losing critical canonical interactions to the ligand as discussed previously. In the case of Tyr-Ala, the N-terminal amino group could form a salt bridge to Asp302 on the lower lobe; but this might not compensate for loss of the canonical salt bridge to Glu170 on the upper lobe (as for Gly-Met).

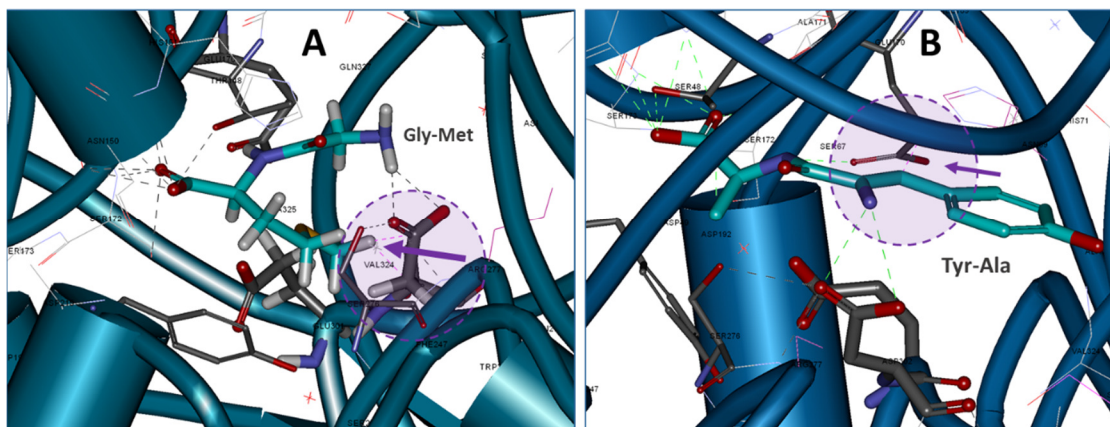


Figure 41. Docking of Gly-Met (DP28) and Tyr-Ala (DP92) in the umami active site in the VFT of ft1R1. (A) Gly-Met and (B) Tyr-Ala molecules are represented in light blue. Purple circles and arrows denote the region where the dipeptides clash with the receptor.

3.6.1.5 Possible explanations of unusual response patterns

IMP and dipeptides interacting with each other and competing for space in the binding site could be one of the explanations for the unusual response pattern (belly and lag time) observed in the *in vitro* experiments.

The dipeptides are longer than amino acids, and will (in favoured binding modes) extend into the nucleotide binding region. The nucleotide (e.g. IMP, GMP) normally occupies a binding position that would overlap with the phenol of the tyrosine in the H-Tyr-Gly-OH example shown (Figure 42). To accommodate the dipeptide, a rearrangement of the nucleotide is required if it is already bound. An initial dip in response would result as the two ligands compete for this overlap area, with the dipeptide moving the nucleotide from its binding position, and then a recovery when the two settle into new positions. Binding assays were not conducted as part of this project, only functional assays, so it was not possible to see, for example, the nucleotide bound and not agonizing the flytrap. It was only possible to see competition in a form like the observed belly and lag, which suggested a displacement of agonists by higher affinity ligands.

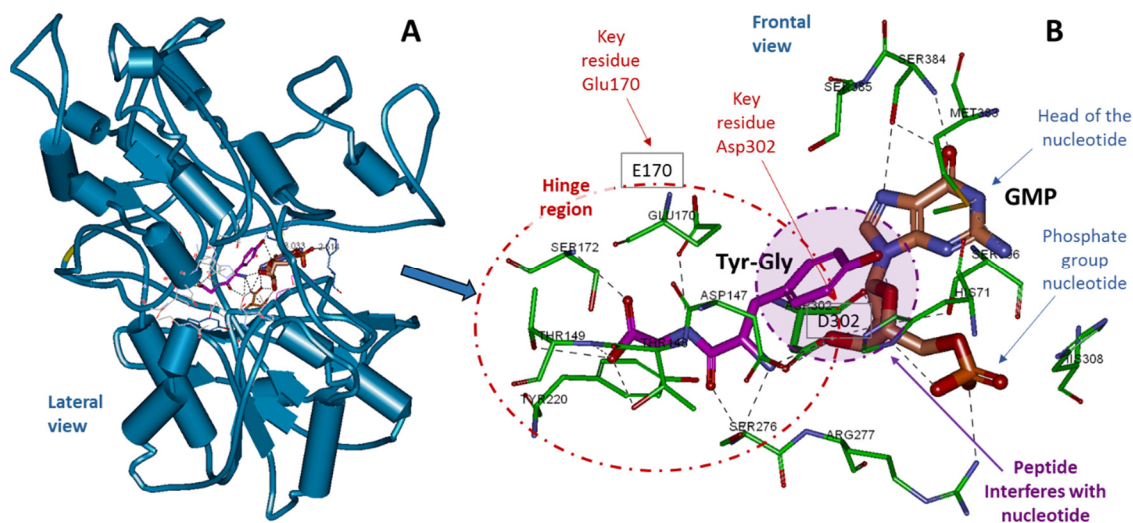


Figure 42. Overlap of Tyr-Gly (DP94) with GMP binding in the umami active site in the VFT of ft1R1. Multiple possible hydrogen bonds (HB) and salt bridges (SB) are highlighted in green. (A) Lateral view of the pocket in the VFT of ft1R1 containing the dipeptide and the nucleotide. (B) Frontal view with overlap of GMP (gold) with Tyr-Gly (purple). GMP was chosen in this model as it is bulkier than IMP, and would represent a worst case scenario. The area of interference is highlighted in a purple circle.

3.6.2 Summary of the *in silico* modelling

The binding of amino acids to the hinge region (amino acid binding site) is carefully constructed to arrange a zwitterionic carboxylate and nitrogen in such a way as to be well-coordinated by amino acid residues at the hinge, forming interactions both to the hinge and to the upper and lower lobes of the flytrap. The zwitterionic N is critical; in SAR experiments, modifying the nature or position of this charge relative to that of the carboxylate results in an inactive amino acid (e.g. beta amino acids, see Figure 43). In a dipeptide there is still a charged N, but it is further away from the carboxylate (though flexible, there is hindrance in getting as close as in an L-amino acid, see Figure 43).

As a result, salt bridge interactions can form to the residues responsible for coordinating the zwitterionic N of an L-amino acid, but the geometries are less ideal.

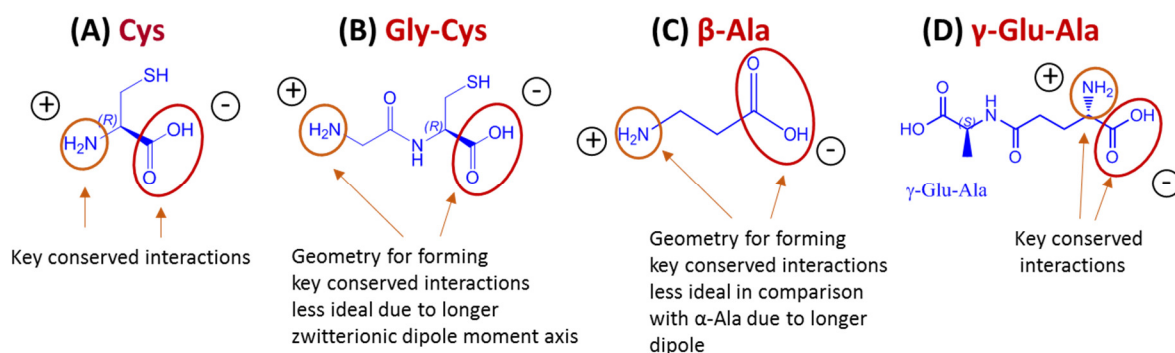


Figure 43. Representation of the different zwitterionic configurations in amino acids and dipeptides. (A) L-cysteine. (B) H-Gly-Cys-OH. (C) H- β -Ala-OH. (D) H-Glu-(Ala-OH)-OH.

In human umami taste, L-amino acids (Glu, Asp) are agonists, while the nucleotides GMP, IMP are positive allosteric modulators (PAMs). On the other hand, it is possible that in cat, with relatively higher *in vitro* activation for nucleotides, GMP and IMP are agonists, while amino acids act as PAMs to these. If the same happened for dipeptides, it would be expected to need a nucleotide present to see activity for dipeptides in general.

In summary, the *in silico* modelling predicts that some dipeptides could bind to the active site in the VFT of the cat T1R1, however, if they do, (a) their binding will be less energetic than that of L-amino acids, (b) they will be either weak agonists (themselves) or modulators (of nucleotide binding), since they are less effective at closing the VFT (active conformation) and (c) as L-amino acids have weaker activity than nucleotides for cat T1R1, further reduction in stabilisation of the closed conformation by dipeptides could result in inability to see any activity in the *in vitro* assays.

As mentioned before, it is critical for the cat umami receptor ft1R1-ft1R3 activation by L-amino acids that a zwitterionic arrangement between the carboxylate and amino groups at the right distances take place, and this is somewhat reduced when two free amino acids join to form a dipeptide. The only chance of keeping the zwitterionic arrangement in place in a dipeptide would be the case of γ -glutamyl dipeptides (see Figure 43 for an example). Gamma-glutamyl dipeptides are natural dipeptides (see Introduction Chapter) and could use their second carboxylate in the side chain of the glutamate for the peptidic bond but keep the first carboxylate in the alpha-carbon free to bind to the receptor (preserving the necessary zwitterionic arrangement with the right distances between charges). This would be possible as there is in general room in the VFT for these compounds, and that they could form canonical interactions with the hinge.

3.7 Overall summary of the results

In summary, from the 101 dipeptides tested, only three were finally identified as being active (DP24 – Gly-Cys, DP67 – Phe-Leu and DP-94 – Tyr-Gly), with activities similar or lower than those of their corresponding L-amino acids. The IMP conditions generated the maximum activation, which suggested a mechanism of activation for the dipeptides similar to that of L-amino acids. Furthermore, the experiments testing a nucleotide-like mechanism of activation showed that dipeptides do not interact with the ft1R1-ft1R3 receptor in this manner. However, the dipeptides displayed an unusual pattern response which was investigated and attributed to non-specific responses. It is possible that overlap between the binding site of the dipeptide and the nucleotide was the cause of this unusual response pattern. Using a range of experimental conditions, receptor activation measurements and different data visualisation techniques, it was possible to differentiate between specific and non-specific activities. The

quality control checks showed no differences between dipeptides coming from different batches or between different suppliers.

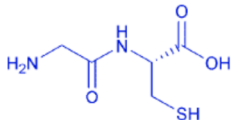
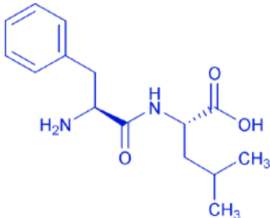
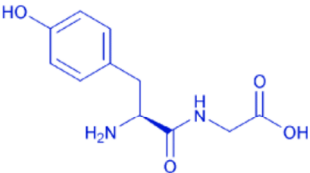
The *in silico* modelling of the dipeptides showed that the active dipeptides (and other dipeptides tested for comparison) could bind to the active site in the VFT of the FT1R1 and achieve some stabilisation with the pincer residues in a region close to the active site. However, the zwitterionic configuration of the dipeptides was not ideal (longer dipole than the L-amino acids) to achieve full stabilisation of the closed conformation of the VFT (active conformation), which resulted in the dipeptides having lower activity.

4 Conclusions and suggested further work

4.1 General conclusions

The aim of this project was to determine if linear α -L-dipeptides containing active amino acids were active *in vitro* when screened with the cat umami receptor ft1R1-ft1R3, using a range of different experimental conditions. In relation to the results, it has been determined that the library of linear α -L-dipeptides tested had either no or weak activity when binding to the cat umami receptor (ft1R1-ft1R3) *in vitro*. In terms of the project hypothesis: "There will be some linear α -L-dipeptides active *in vitro*. Dipeptides containing L-amino acids, known to be umami taste active in cats, will stimulate the cat umami receptor", it was identified that only a few of the dipeptides tested were active, with the binding probably occurring at least partially at the same active site as amino acids, but the resulting activation was weaker. Only three out of the 101 dipeptides tested showed some activity with the fluorescence and luminescence reporting cell-based assays used, which were Gly-Cys (DP24), Phe-Leu (DP67) and Tyr-Gly (DP94), as shown in Table 16.

Table 16. Three dipeptides activating the cat umami receptor ft1R1-ft1R3 *in vitro*.

DP24	DP67	DP94
H-Gly-Cys-OH	H-Phe-Leu-OH	H-Tyr-Gly-OH
		
Active Soluble	Active Partially soluble	Active Partially soluble
CAS [57281-78-4]	CAS [3303-55-7]	CAS [673-08-5]
Mw = 178.21 g/mol	Mw = 278.35 g/mol	Mw = 238.24 g/mol

The three dipeptides had lower activity *in vitro* than their constituent single amino acids. This reduction in activity could be explained at a molecular level due to the increase in the distance between the positive and the negative charge centres in the molecule (zwitterion), and the overlapping of the dipeptide and the nucleotide when bound to their respective binding sites. This overlap could be responsible for some of the unusual response patterns found in the screening. The molecular mechanism proposed after *in silico* modelling suggested that the dipeptides, even with a different zwitterionic conformation than L-amino acids, could still bind to the cat umami receptor fT1R1-fT1R3 and depending on their chemical structures, could find additional stabilisation due to molecular interactions with amino acid residues relatively far away from the hinge of the Venus flytrap (VFT). However, the stabilisation would not be as strong as in the case of the constituent L-amino acids, and in most cases would not be strong enough to stabilise the closed conformation of the Venus flytrap in the cat fT1R1 subunit of the receptor.

As mentioned before, it is critical for the cat umami receptor fT1R1-fT1R3 activation by L-amino acids that a zwitterionic arrangement between the carboxylate and amino groups at the right distances take place, and this is somewhat reduced when two free amino acids join to form a dipeptide. The only chance of keeping the zwitterionic arrangement in place would be by exploring γ -glutamyl dipeptides. Gamma-glutamyl dipeptides are natural dipeptides (see Introduction Chapter) and could use their second carboxylate in the side chain of the glutamate for the peptidic bond but keep the first carboxylate in the alpha-carbon free to bind to the receptor (preserving the necessary zwitterionic arrangement with the right distances between charges). This would be possible as there is in general room in the VFT for these compounds, and that they could form canonical interactions with the hinge.

Some unusual response patterns were obtained with the α -L-dipeptides, which were produced by the interaction of the dipeptide with the cell or the umami taste receptor in the cell in a different way than known umami agonists like L-amino acids and could be further investigated. There was also an interaction between the dipeptide and IMP, potentially due to overlap in the binding site for the two molecules.

In order to investigate the suggested interference of dipeptides to nucleotides, it would be necessary to separate binding from agonism. To achieve this, a binding assay would need to be performed, but these assays are complex (often involve radiolabelling) and are not in scope for this project. An experiment that could be done *in vitro* with the current resources would be an antagonist assay (the screening could be further expanded to screenings in agonist, and antagonist modes, but also PAM/NAM). This could reveal whether the dipeptides are binding and interfering with the binding of nucleotides.

All the objectives of the project were successfully met: Candidate dipeptides were selected and sourced, a suitable *in vitro* model to test cat umami taste was selected and validated with known active compounds, a library of dipeptides was tested using fluorescence and luminescence detection in different conditions, the *in vitro* results were interpreted and summarised, with the aid of *in silico* modelling, and finally the conclusions allowed to make recommendations on next steps.

4.2 Contribution of this work to the chemoreception field

In the recent years there has been an increase on publications about taste receptors of livestock and pets; however the knowledge on cat taste in the public domain is still very sparse. In humans, the early sensory data on the umami taste attributes of dipeptides has been disputed more recently, and there are only a few papers that report on human *in vitro* assay responses to dipeptides in general, mostly bitter (Sakurai et al., 2009, Kohl et al., 2013) and sweet (Shim et al., 2015), and even dipeptides decreasing bitterness using bitter receptor assays (Kim et al., 2015), but no *in vitro* data using the umami receptor T1R1-T1R3 has been found for umami dipeptides in any species. This research and the methodologies used contributes to the overall field of peptide (dipeptide) taste perception and mechanisms, and expands the knowledge specifically on umami taste by cats. The type of molecules tested, α -L-dipeptides, are an emerging field of research due to the processes to synthesise these molecules reducing in cost recently, which makes this type of research more affordable (Yagasaki and Hashimoto, 2008).

Due to the importance of delivering complete and balanced nutrition to cats around the world, it is necessary that cats find their food appetising so they eat it. As mentioned before, cats are obligate carnivores (Bradshaw et al., 1996) and as such they have evolved to taste meat and its components. This work expands the fundamental understanding on cat taste perception and will inform future fundamental research in the field.

4.3 Contribution of this work to the pet food industry

As mentioned in the Introduction Chapter, cat food manufacturing requires protein-derived ingredients to deliver the required nutrition for the growth, development and wellbeing of the animal. Many of these proteinaceous ingredients contain free peptides, indeed, peptides could be produced intentionally due to nutritional, allergenic, organoleptic or process-related reasons, thus the interest for the cat food industry in the taste of peptides. Fermented raw material extracts and protein hydrolysates (rich in small peptides) can deliver taste and are often included in pet food.

Scientists specialised in pet food sensory properties will benefit from the learnings generated in this research project as there was a gap of knowledge on umami dipeptide perception by cats.

4.4 Further work

Due to the large number of possible amino acid combinations, only a subset of α -L-dipeptides (the ones containing only active amino acids) have been tested with the cat umami receptor (FT1R1-FT1R3) in this project, so more combinations could be tested (e.g. α -L-dipeptides containing one active and one inactive amino acid). A possible way forward in potential umami perception with dipeptides would be to study other types of dipeptides, such as *gamma*-glutamyl-dipeptides (not in scope for this project), which could potentially leave the L-glutamic acid zwitterion dipole in the α -carbon unchanged, if they formed the peptidic bond with their carboxylic group in the γ -position. Moreover, as mentioned in the Introduction Chapter, other types of peptides were outside of the scope of this project that could be investigated in the future, such as pyro-glutamyl dipeptides, β -alanyl dipeptides and others.

Another interesting stream of research could be the investigation of the influence of dipeptides on other taste modalities. It is known that α -L-dipeptides can be very bitter for human (Kim and Li-Chan, 2006, Maehashi et al., 2008), and γ -glutamyl dipeptides have been found to display kokumi taste properties (Toelstede et al., 2009, Toelstede and Hofmann, 2009, Dunkel and Hofmann, 2009, Dunkel et al., 2007, Feng et al., 2016). Hence, it would be interesting to test if these dipeptides could bind to other cat taste receptors, for example, be bitter-active or kokumi-active *in vitro* (if the assays were available).

In terms of learnings, it is recommended in the future to run the *in vitro* screenings in dose response mode and in both fluorescence and luminescence, in a high-throughput fully automated instrument (e.g. FLIPR), if available and if time and resources allow it. This recommendation is made as working with the FLIPR was the stage of the project that more valuable information provided in the least amount of time and allowed differentiation between genuine responses and non-specific responses of the dipeptides.

Fluorescence detection was a sensitive method but produced numerous cases of non-specific responses in comparison with luminescence, so, if it is necessary to prioritise, luminescence seems as the cleaner and clearer reporting system to detect active compounds with the receptor in the future. It must be mentioned that it might be less sensitive than fluorescence (e.g. two of the active dipeptides did not provide activation in luminescence), but this could not be a problem if screening for compounds with strong taste activity.

As mentioned previously, in order to further investigate the suggested interference of dipeptides to nucleotides, it would be necessary to separate binding from agonism. To achieve this, a binding assay would have to be performed, but these assays are more complex (often

involving radiolabelling). Experiments that could be run *in vitro* would be an antagonist assay and allosteric modulation assays, both positive (PAM) and negative (NAM). This could reveal whether the dipeptides were binding and interfering with the binding of nucleotides.

In terms of the investigation of the other unusual response patterns produced by the dipeptides and to test if they might be interacting with the cells in a non-specific manner, several experiments with the controls (ATP, Isoproterenol, L-alanine) could be conducted, in a dose response design. The controls could confirm the interaction of the dipeptide with the cell, however, to determine by which mechanism would be very difficult, as there are numerous cell membrane receptors and transporters.

Finally, a phenomenon that has not been mentioned before and could help explaining the drop below the baseline (in the “belly”) after dipeptide injection in the fluorescence experiments, could be inverse agonism (see schematic in Figure 44) (Kenakin, 2004, Khilnani and Khilnani, 2011).

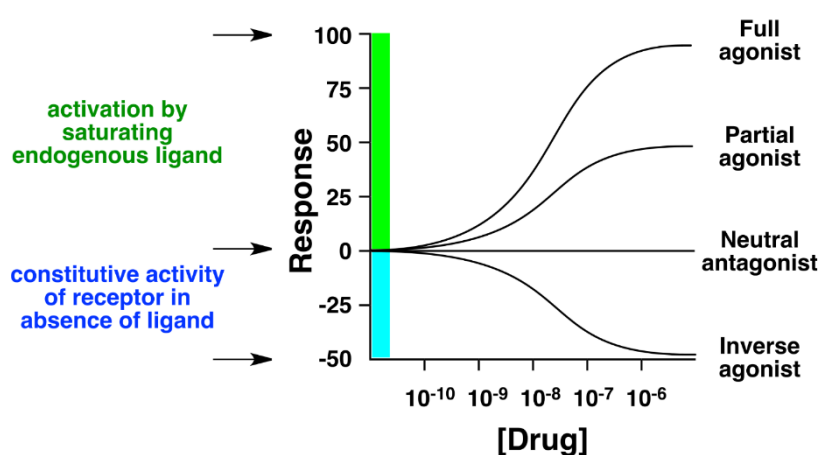


Figure 44. Schematic of the response produced by an inverse agonist (Boghog, 2014). An inverse agonist produces a reduction of the baseline activity of the receptor in the absence of any ligand.

An inverse agonist would bind to the receptor, but produce an effect contrary to the natural agonist/s of the receptor. For example, this has been found in some psychoactive drugs in pharmacology (Sieghart, 1994, Aloyo et al., 2010). It is known that different receptors produced different levels of intrinsic or baseline activity in the absence or agonists. This is very specific of the receptor, and it is mainly seen in fluorescence. If some of the dipeptides were at least partial inverse agonists, they could be inducing the cell to sequester calcium or pump it out of the cell after binding, which could be translated into a decrease of baseline fluorescence. These decrease could be compensated with time by other effects, driving the fluorescence response up. This phenomenon could be also studied in the future in order to further investigate the non-specific responses found during this project.

Bibliography

- ADACHI, A., FUNAKOSHI, M. & KAWAMURA, Y. 1967. Neurophysiological studies on taste effectiveness of chemical taste enhancers. *Olfaction and taste*, 2, 411-413.
- AHN, S. R., AN, J. H., SONG, H. S., PARK, J. W., LEE, S. H., KIM, J. H., JANG, J. & PARK, T. H. 2016. Duplex Bioelectronic Tongue for Sensing Umami and Sweet Tastes Based on Human Taste Receptor Nanovesicles. *ACS Nano*, 10, 7287-7296.
- ALOYO, V. J., BERG, K. A., CLARKE, W. P., SPAMPINATO, U. & HARVEY, J. A. 2010. Inverse agonism at serotonin and cannabinoid receptors. *Prog Mol Biol Transl Sci*, 91, 1-40.
- ANDERSEN, L. T., SCHLICHTERLE-CERNY, H. & ARDÖ, Y. 2008. Hydrophilic di- and tripeptides are not a precondition for savoury flavour in mature Cheddar cheese. *Dairy Science & Technology*, 88, 467-475.
- ANDERSEN, M. E. & KREWSKI, D. 2009. Toxicity Testing in the 21st Century: Bringing the Vision to Life. *Toxicological Sciences*, 107, 324-330.
- APRIYANTONO, A., SETYANINGSIH, D., HARIYADI, P. & NURAIDA, L. 2004. Sensory and Peptides Characteristics of Soy Sauce Fractions Obtained by Ultrafiltration. In: SHAHIDI, F., SPANIER, A. M., HO, C.-T. & BRAGGINS, T. (eds.) *Quality of Fresh and Processed Foods*. Boston, MA: Springer US.
- ARAI, S., YAMASHITA, M. & FUJIMAKI, M. 1972. Glutamyl Oligopeptides as Factors Responsible for Tastes of a Proteinase-modified Soybean Protein. *Agricultural and Biological Chemistry*, 36, 1253-1256.
- ARAI, S., YAMASHITA, M., NOGUCHI, M. & FUJIMAKI, M. 1973. Tastes of L-Glutamyl Oligopeptides in Relation to Their Chromatographic Properties. *Bioscience, Biotechnology, and Biochemistry*, 37, 151-156.
- BAGNASCO, L., PAPPALARDO, V. M., MEREGAGLIA, A., KAEWMANEE, T., UBIALI, D., SPERANZA, G. & COSULICH, M. E. 2013. Use of food-grade proteases to recover umami protein-peptide mixtures from rice middlings. *Food Research International*, 50, 420-427.
- BARTOSHUK, L. M. & BEAUCHAMP, G. K. 1994. Chemical senses. *Annu Rev Psychol*, 45, 419-49.
- BASSOLI, A., BORGONOVO, G., CAREMOLI, F. & MANCUSO, G. 2014. The taste of D- and L-amino acids: *In vitro* binding assays with cloned human bitter (TAS2Rs) and sweet (TAS1R2/TAS1R3) receptors. *Food Chem*, 150, 27-33.

- BEAUCHAMP, G. K., MALLER, O. & ROGERS, J. G. 1977. FLAVOR PREFERENCES IN CATS (FELIS-CATUS AND PANTHERA SP). *Journal of Comparative and Physiological Psychology*, 91, 1118-1127.
- BEHRENS, M., BROCKHOFF, A., KUHN, C., BUFE, B., WINNIG, M. & MEYERHOF, W. 2004. The human taste receptor hTAS2R14 responds to a variety of different bitter compounds. *Biochemical and Biophysical Research Communications*, 319, 479-485.
- BEHRENS, M., MEYERHOF, W., HELLFRITSCH, C. & HOFMANN, T. 2011. Sweet and umami taste: natural products, their chemosensory targets, and beyond. *Angew Chem Int Ed Engl*, 50, 2220-42.
- BEKSAN, E., SCHIEBERLE, P., ROBERT, F., BLANK, I., FAY, L. B., SCHLICHTERLE-CERNY, H. & HOFMANN, T. 2003. Synthesis and sensory characterization of novel umami-tasting glutamate glycoconjugates. *Journal of Agricultural and Food Chemistry*, 51, 5428-5436.
- BELITZ, H. D. & WIESER, H. 1985. Bitter compounds: Occurrence and structure-activity relationships. *Food Reviews International*, 1, 271-354.
- BOGHOG. 2014. *Dose response curves of a full agonist, partial agonist, neutral antagonist, and inverse agonist* [Online]. Available: https://commons.wikimedia.org/wiki/File%3AInverse_agonist_3.svg [Accessed].
- BOOTMAN, M. D., RIETDORF, K., COLLINS, T., WALKER, S. & SANDERSON, M. 2013a. Ca²⁺-Sensitive Fluorescent Dyes and Intracellular Ca²⁺ Imaging. *Cold Spring Harbor Protocols*, 2013, pdb.top066050.
- BOOTMAN, M. D., RIETDORF, K., COLLINS, T., WALKER, S. & SANDERSON, M. 2013b. Loading Fluorescent Ca²⁺ Indicators into Living Cells. *Cold Spring Harbor Protocols*, 2013, pdb.prot072801.
- BOUDREAU, J. 1987. Mammalian neural taste responses to amino acids and nucleotides. *Umami, a basic taste*. New York: Marcel Dekker, 201-217.
- BOUDREAU, J. C., SIVAKUMAR, L., DO, L. T., WHITE, T. D., ORAVEC, J. & HOANG, N. K. 1985. Neurophysiology of geniculate ganglion (facial nerve) taste systems: species comparisons. *Chemical Senses*, 10, 89-127.
- BRADSHAW, J. W. 1991. Sensory and experiential factors in the design of foods for domestic dogs and cats. *Proc Nutr Soc*, 50, 99-106.
- BRADSHAW, J. W. 2006. The evolutionary basis for the feeding behavior of domestic dogs (Canis familiaris) and cats (Felis catus). *J Nutr*, 136, 1927s-1931s.

- BRADSHAW, J. W., GOODWIN, D., LEGRAND-DEFRETIN, V. & NOTT, H. M. 1996. Food selection by the domestic cat, an obligate carnivore. *Comp Biochem Physiol A Physiol*, 114, 205-9.
- BUFE, B., HOFMANN, T., KRAUTWURST, D., RAGUSE, J. D. & MEYERHOF, W. 2002. The human TAS2R16 receptor mediates bitter taste in response to beta-glucopyranosides. *Nat Genet*, 32, 397-401.
- CARPENTER, J. A. 1956. Species differences in taste preferences. *J Comp Physiol Psychol*, 49.
- CHALBERG, T. W., PHILLIPS, J. E. & CALOS, M. P. 2001. Transfection of DNA into Mammalian Cells in Culture. *eLS*. John Wiley & Sons, Ltd.
- CHANDRASHEKAR, J., MUELLER, K. L., HOON, M. A., ADLER, E., FENG, L., GUO, W., ZUKER, C. S. & RYBA, N. J. P. 2000. T2Rs Function as Bitter Taste Receptors. *Cell*, 100, 703-711.
- CHAUDHARI, N., LANDIN, A. M. & ROPER, S. D. 2000. A metabotropic glutamate receptor variant functions as a taste receptor. *Nat Neurosci*, 3, 113-9.
- CHAUDHARI, N., PEREIRA, E. & ROPER, S. D. 2009. Taste receptors for umami: the case for multiple receptors. *American Journal of Clinical Nutrition*, 90, 738S-742S.
- CHAUDHARI, N. & ROPER, S. D. 2010. The cell biology of taste. *J Cell Biol*, 190, 285-96.
- CHEN, C. A. & MANNING, D. R. 2001. Regulation of G proteins by covalent modification. *Oncogene*, 20, 1643-52.
- CLARKSON, C. W. 2016. *Basic Principles of Pharmacology* [Online]. TUSOM - Pharmwiki. Available: <http://tmedweb.tulane.edu/pharmwiki/> [Accessed 24/10/2016 2016].
- CONIGRAVE, A. D., MUN, H.-C. & LOK, H.-C. 2007. Aromatic l-Amino Acids Activate the Calcium-Sensing Receptor. *The Journal of Nutrition*, 137, 1524S-1527S.
- DAMAK, S., RONG, M., YASUMATSU, K., KOKRASHVILI, Z., PEREZ, C. A., SHIGEMURA, N., YOSHIDA, R., MOSINGER, B., JR., GLENDINNING, J. I., NINOMIYA, Y. & MARGOLSKEE, R. F. 2006. Trpm5 null mice respond to bitter, sweet, and umami compounds. *Chem Senses*, 31, 253-64.
- DAMAK, S., RONG, M., YASUMATSU, K., KOKRASHVILI, Z., VARADARAJAN, V., ZOU, S., JIANG, P., NINOMIYA, Y. & MARGOLSKEE, R. F. 2003. Detection of sweet and umami taste in the absence of taste receptor T1r3. *Science*, 301, 850-3.
- DANG, Y., GAO, X., MA, F. & WU, X. 2015. Comparison of umami taste peptides in water-soluble extractions of Jinhua and Parma hams. *LWT - Food Science and Technology*, 60, 1179-1186.
- DI PIZIO, A. & NIV, M. Y. 2014. Computational Studies of Smell and Taste Receptors. *Israel Journal of Chemistry*, 54, 1205-1218.

- DUNKEL, A. & HOFMANN, T. 2009. Sensory-directed identification of beta-alanyl dipeptides as contributors to the thick-sour and white-meaty orosensation induced by chicken broth. *J Agric Food Chem*, 57, 9867-77.
- DUNKEL, A., KOSTER, J. & HOFMANN, T. 2007. Molecular and sensory characterization of gamma-glutamyl peptides as key contributors to the kokumi taste of edible beans (*Phaseolus vulgaris* L.). *J Agric Food Chem*, 55, 6712-9.
- ENGEL, E., SEPTIER, C., LECONTE, N., SALLES, C. & LE QUERE, J. L. 2001. Determination of taste-active compounds of a bitter Camembert cheese by omission tests. *J Dairy Res*, 68, 675-88.
- FEDIAF, T. E. P. F. I. F. 2014. Facts & Figures 2014. FEDIAF - The European Pet Food Industry Federation.
- FENG, T., ZHANG, Z., ZHUANG, H., ZHOU, J. & XU, Z. 2016. Effect of Peptides on New Taste Sensation: Kokumi-Review. *Mini-Reviews in Organic Chemistry*, 13, 255-261.
- FERREIRA, L., DOS SANTOS, R., OLIVA, G. & ANDRICOPULO, A. 2015. Molecular Docking and Structure-Based Drug Design Strategies. *Molecules*, 20, 13384.
- FESTRING, D. & HOFMANN, T. 2011. Systematic Studies on the Chemical Structure and Umami Enhancing Activity of Maillard-Modified Guanosine 5'-Monophosphates. *Journal of Agricultural and Food Chemistry*, 59, 665-676.
- FINGER, T. E., DANILOVA, V., BARROWS, J., BARTEL, D. L., VIGERS, A. J., STONE, L., HELLEKANT, G. & KINNAMON, S. C. 2005. ATP Signaling Is Crucial for Communication from Taste Buds to Gustatory Nerves. *Science*, 310, 1495-1499.
- FUJIMAKI, M., ARAI, S., YAMASHITA, M., KATO, H. & NOGUCHI, M. 1973. Taste peptide fractionation from a fish protein hydrolysate. *Agricultural and Biological Chemistry*, 37, 2891-2898.
- GÓMEZ-RUIZ, J. Á., TABORDA, G., AMIGO, L., RAMOS, M. & MOLINA, E. 2007. Sensory and Mass Spectrometric Analysis of the Peptidic Fraction Lower Than One Thousand Daltons in Manchego Cheese. *Journal of Dairy Science*, 90, 4966-4973.
- GRIGOROV, M. G., SCHLICHTERLE-CERNY, H., AFFOLTER, M. & KOCHHAR, S. 2003. Design of virtual libraries of umami-tasting molecules. *Journal of Chemical Information and Computer Sciences*, 43, 1248-1258.
- Haid, D., WIDMAYER, P., VOIGT, A., CHAUDHARI, N., BOEHM, U. & BREER, H. 2013. Gustatory sensory cells express a receptor responsive to protein breakdown products (GPR92). *Histochemistry and cell biology*, 140, 137-145.

- HAMADA, J. S., SPANIER, A. M., BLAND, J. M. & DIACK, M. 1998. Preparative separation of value-added peptides from rice bran proteins by high-performance liquid chromatography. *Journal of Chromatography A*, 827, 319-327.
- HAU, J., CAZES, D. & FAY, L. B. 1997. Comprehensive Study of the "Beefy Meaty Peptide". *Journal of Agricultural and Food Chemistry*, 45, 1351-1355.
- HELLEKANT, G., SCHMOLLING, J., MARAMBAUD, P. & ROSE-HELLEKANT, T. A. 2015. CALHM1 Deletion in Mice Affects Glossopharyngeal Taste Responses, Food Intake, Body Weight, and Life Span. *Chemical Senses*, 40, 373-379.
- HILLMANN, H., BEHR, J., EHRMANN, M. A., VOGEL, R. F. & HOFMANN, T. 2016. Formation of Kokumi-Enhancing γ -Glutamyl Dipeptides in Parmesan Cheese by Means of γ -Glutamyltransferase Activity and Stable Isotope Double-Labeling Studies. *Journal of Agricultural and Food Chemistry*, 64, 1784-1793.
- HOLLINGER, S. & HEPLER, J. R. 2002. Cellular regulation of RGS proteins: modulators and integrators of G protein signaling. *Pharmacol Rev*, 54, 527-59.
- HORVAT, S. & JAKAS, A. 2004. Peptide and amino acid glycation: new insights into the Maillard reaction. *J Pept Sci*, 10, 119-37.
- HOU, H., LI, B. & ZHAO, X. 2011. Enzymatic hydrolysis of defatted mackerel protein with low bitter taste. *Journal of Ocean University of China*, 10, 85-92.
- IKEDA, K. 1909. New seasonings. *Journal of the Chemical Society of Tokyo*, 30, 820-836.
- IKEDA, K. 2002. New seasonings. *Chem Senses*, 27, 847-9.
- INOUE, S. & SAHARA, Y. 2007. Expression, purification and characterization of a photoprotein, clytin, from *Clytia gregarium*. *Protein Expression and Purification*, 53, 384-389.
- ISHIBASHI, N., ONO, I., KATO, K., SHIGENAGA, T., SHINODA, I., OKAI, H. & FUKUI, S. 1988. Role of the Hydrophobia Amino Acid Residue in the Bitterness of Peptides. *Agricultural and Biological Chemistry*, 52, 91-94.
- JIANG, P., JOSUE, J., LI, X., GLASER, D., LI, W., BRAND, J. G., MARGOLSKEE, R. F., REED, D. R. & BEAUCHAMP, G. K. 2012. Major taste loss in carnivorous mammals. *Proceedings of the National Academy of Sciences of the United States of America*, 109, 4956-4961.
- KAWAI, M., SEKINE-HAYAKAWA, Y., OKIYAMA, A. & NINOMIYA, Y. 2012. Gustatory sensation of l- and d-amino acids in humans. *Amino Acids*, 43, 2349-2358.
- KENAKIN, T. 2004. Principles: Receptor theory in pharmacology. *Trends in Pharmacological Sciences*, 25, 186-192.
- KEW, J. N. C. & KEMP, J. A. 2005. Ionotropic and metabotropic glutamate receptor structure and pharmacology. *Psychopharmacology*, 179, 4-29.

- KHILNANI, G. & KHILNANI, A. K. 2011. Inverse agonism and its therapeutic significance. *Indian J Pharmacol*, 43, 492-501.
- KIM, H.-O. & LI-CHAN, E. C. Y. 2006. Quantitative Structure–Activity Relationship Study of Bitter Peptides. *Journal of Agricultural and Food Chemistry*, 54, 10102-10111.
- KIM, M. J., SON, H. J., KIM, Y., MISAKA, T. & RHYU, M.-R. 2015. Umami–bitter interactions: The suppression of bitterness by umami peptides via human bitter taste receptor. *Biochemical and Biophysical Research Communications*, 456, 586-590.
- KIM, T. K. & EBERWINE, J. H. 2010. Mammalian cell transfection: the present and the future. *Analytical and Bioanalytical Chemistry*, 397, 3173-3178.
- KINNAMON, S. C. 2009. Umami taste transduction mechanisms. *Am J Clin Nutr*, 90, 753s-755s.
- KINNAMON, S. C. 2016. Chapter 15 - G Protein–Coupled Taste Transduction A2 - Zufall, Frank. *In: MUNGER, S. D. (ed.) Chemosensory Transduction*. Academic Press.
- KIRIMURA, J., SHIMIZU, A., KIMIZUKA, A., NINOMIYA, T. & KATSUYA, N. 1969. Contribution of peptides and amino acids to the taste of foods. *Journal of Agricultural and Food Chemistry*, 17, 689-695.
- KOHL, S., BEHRENS, M., DUNKEL, A., HOFMANN, T. & MEYERHOF, W. 2013. Amino Acids and Peptides Activate at Least Five Members of the Human Bitter Taste Receptor Family. *Journal of Agricultural and Food Chemistry*, 61, 53-60.
- KRISTIANSEN, K. 2004. Molecular mechanisms of ligand binding, signaling, and regulation within the superfamily of G-protein-coupled receptors: molecular modeling and mutagenesis approaches to receptor structure and function. *Pharmacol Ther*, 103, 21-80.
- KRUGER, S. & BOUDREAU, J. C. 1972. Responses of cat geniculate ganglion tongue units to some salts and physiological buffer solutions. *Brain Res*, 47, 127-45.
- KUMAZAWA, T., NAKAMURA, M. & KURIHARA, K. 1991. Canine taste nerve responses to umami substances. *Physiology & Behavior*, 49, 875-881.
- KURAMITSU, R., TAKAHASHI, M., TAHARA, K., NAKAMURA, K. & OKAI, H. 1996. Tastes produced by peptides containing ionic groups and by related compounds. *Biosci Biotechnol Biochem*, 60, 1637-42.
- LEE, K.-P. D. & WARTHESEN, J. J. 1996. Preparative Methods of Isolating Bitter Peptides from Cheddar Cheese. *Journal of Agricultural and Food Chemistry*, 44, 1058-1063.
- LI, X., LI, W., WANG, H., BAYLEY, D. L., CAO, J., REED, D. R., BACHMANOV, A. A., HUANG, L., LEGRAND-DEFRETIN, V., BEAUCHAMP, G. K. & BRAND, J. G. 2006. Cats lack a sweet taste receptor. *J Nutr*, 136, 1932s-1934s.

- LI, X., LI, W., WANG, H., CAO, J., MAEHASHI, K., HUANG, L., BACHMANOV, A. A., REED, D. R., LEGRAND-DEFRETIN, V., BEAUCHAMP, G. K. & BRAND, J. G. 2005. Pseudogenization of a sweet-receptor gene accounts for cats' indifference toward sugar. *PLoS Genet*, 1, 27-35.
- LI, X. & SERVANT, G. 2008. Functional Characterization of the Human Sweet Taste Receptor: High-Throughput Screening Assay Development and Structural Function Relation. *Sweetness and Sweeteners*. American Chemical Society.
- LI, X., STASZEWSKI, L., XU, H., DURICK, K., ZOLLER, M. & ADLER, E. 2002. Human receptors for sweet and umami taste. *Proc Natl Acad Sci U S A*, 99, 4692-6.
- LINDEMANN, B. 2001. Receptors and transduction in taste. *Nature*, 413, 219-25.
- LIOE, H. N., APRIYANTONO, A., TAKARA, K., WADA, K., NAOKI, H. & YASUDA, M. 2004. Low Molecular Weight Compounds Responsible for Savory Taste of Indonesian Soy Sauce. *Journal of Agricultural and Food Chemistry*, 52, 5950-5956.
- LIOE, H. N., SELAMAT, J. & YASUDA, M. 2010. Soy sauce and its umami taste: a link from the past to current situation. *J Food Sci*, 75, R71-6.
- LIOE, H. N., TAKARA, K. & YASUDA, M. 2006. Evaluation of Peptide Contribution to the Intense Umami Taste of Japanese Soy Sauces. *Journal of Food Science*, 71, S277-S283.
- LIU, J., SONG, H., LIU, Y., LI, P., YAO, J. & XIONG, J. 2015. Discovery of kokumi peptide from yeast extract by LC-Q-TOF-MS/MS and sensomics approach. *J Sci Food Agric*, 95, 3183-94.
- MACDONALD, M. L., ROGERS, Q. R. & MORRIS, J. G. 1985. Aversion of the cat to dietary medium-chain triglycerides and caprylic acid. *Physiology & Behavior*, 35, 371-375.
- MAEHASHI, K., MATANO, M., WANG, H., VO, L. A., YAMAMOTO, Y. & HUANG, L. 2008. Bitter peptides activate hTAS2Rs, the human bitter receptors. *Biochemical and Biophysical Research Communications*, 365, 851-855.
- MAEHASHI, K., MATSUZAKI, M., YAMAMOTO, Y. & UDAKA, S. 1999. Isolation of peptides from an enzymatic hydrolysate of food proteins and characterization of their taste properties. *Biosci Biotechnol Biochem*, 63, 555-9.
- MARUYAMA, Y., YASUDA, R., KURODA, M. & ETO, Y. 2012. Kokumi Substances, Enhancers of Basic Tastes, Induce Responses in Calcium-Sensing Receptor Expressing Taste Cells. *Plos One*, 7.
- MCGRANE, S. J., HERNANGOMEZ DE ALVARO CJ., GIBBS M., FINE R., KLEBANSKY B., TAYLOR AJ. 2014. Understanding Cat Umami Flavor Perception Through *In Silico* and *In Vivo*

- Studies. In: THOMAS T., K. D., SCHIEBERLE P., ed. 10th Wartburg Symposium, 2013 Eisenach, Germany. DFA, 35-40.
- MCGRANE, S. J. & TAYLOR, A. J. 2014. Physiological relevance of the Taste 1 Receptor (T1R) family in the domestic cat and dog. *24th International Conference of the European Chemoreception Research Organization (ECRO), Dijon, France*, 68.
- MCGRANE, S. J., TAYLOR, ANDY J 2015. Abstracts from the 24th Annual Meeting of the European Chemoreception Research Organization (ECRO 2014), Dijon, France, September 10-13th, 2014. *Chemical Senses*, 40, 211-297.
- METHVEN, L. 2012. 4 - Natural food and beverage flavour enhancer. *Natural Food Additives, Ingredients and Flavourings*. Woodhead Publishing.
- MEYERHOF, W., BATRAM, C., KUHN, C., BROCKHOFF, A., CHUDOBA, E., BUFE, B., APPENDINO, G. & BEHRENS, M. 2010. The molecular receptive ranges of human TAS2R bitter taste receptors. *Chem Senses*, 35, 157-70.
- MONASTYRSKAIA, K., LUNDSTROM, K., PLAHL, D., ACUNA, G., SCHWEITZER, C., MALHERBE, P. & MUTEL, V. 1999. Effect of the umami peptides on the ligand binding and function of rat mGlu4a receptor might implicate this receptor in the monosodium glutamate taste transduction. *British Journal of Pharmacology*, 128, 1027-1034.
- MORINI, G., BASSOLI, A. & BORGONOVO, G. 2011. Molecular modelling and models in the study of sweet and umami taste receptors. A review. *Flavour and Fragrance Journal*, 26, 254-259.
- MOURITSEN, O. G. & KHANDELIA, H. 2012. Molecular mechanism of the allosteric enhancement of the umami taste sensation. *FEBS Journal*, 279, 3112-3120.
- NAKATA, T., TAKAHASHI, M., NAKATANI, M., KURAMITSU, R., TAMURA, M. & OKAI, H. 1995. Role of basic and acidic fragments in delicious peptides (Lys-Gly-Asp-Glu-Glu-Ser-Leu-Ala) and the taste behavior of sodium and potassium salts in acidic oligopeptides. *Biosci Biotechnol Biochem*, 59, 689-93.
- NELSON, G., CHANDRASHEKAR, J., HOON, M. A., FENG, L., ZHAO, G., RYBA, N. J. & ZUKER, C. S. 2002. An amino-acid taste receptor. *Nature*, 416, 199-202.
- NEY, K. H. 1971. Prediction of bitterness of peptides from their amino acid composition. *Zeitschrift für Lebensmittel-Untersuchung und Forschung*, 147, 64-68.
- NOGUCHI, M., ARAI, S., YAMASHITA, M., KATO, H. & FUJIMAKI, M. 1975. Isolation and identification of acidic oligopeptides occurring in a flavor potentiating fraction from a fish protein hydrolysate. *J Agric Food Chem*, 23, 49-53.

- OHSU, T., AMINO, Y., NAGASAKI, H., YAMANAKA, T., TAKESHITA, S., HATANAKA, T., MARUYAMA, Y., MIYAMURA, N. & ETO, Y. 2010. Involvement of the Calcium-sensing Receptor in Human Taste Perception. *Journal of Biological Chemistry*, 285, 1016-1022.
- OHYAMA, S., ISHIBASHI, N., TAMURA, M., NISHIZAKI, H. & OKAI, H. 1988. STUDIES ON FLAVORED PEPTIDES .6. SYNTHESIS OF BITTER PEPTIDES COMPOSED OF ASPARTIC-ACID AND GLUTAMIC-ACID. *Agricultural and Biological Chemistry*, 52, 871-872.
- PAL CHOUDHURI, S., DELAY, R. J. & DELAY, E. R. 2015. L-Amino Acids Elicit Diverse Response Patterns in Taste Sensory Cells: A Role for Multiple Receptors. *PLoS ONE*, 10, e0130088.
- PAREDES, R. M., ETZLER, J. C., WATTS, L. T., ZHENG, W. & LECHLEITER, J. D. 2008. Chemical calcium indicators. *Methods*, 46, 143-151.
- PARK, J.-N., ISHIDA, K., WATANABE, T., ENDOH, K.-I., WATANABE, K., MURAKAMI, M. & ABE, H. 2002. Taste effects of oligopeptides in a Vietnamese fish sauce. *Fisheries Science*, 68, 921-928.
- PARK, Y. W. & NAM, M. S. 2015. Bioactive Peptides in Milk and Dairy Products: A Review. *Korean J Food Sci Anim Resour*, 35, 831-40.
- PIN, J. P., KNIAZEFF, J., GOUDET, C., BESSIS, A. S., LIU, J., GALVEZ, T., ACHER, F., RONDARD, P. & PRÉZEAU, L. 2004. The activation mechanism of class-C G-protein coupled receptors. *Biology of the Cell*, 96, 335-342.
- PONTIUS, J. U., MULLIKIN, J. C., SMITH, D. R., LINDBLAD-TOH, K., GNERRE, S., CLAMP, M., CHANG, J., STEPHENS, R., NEELAM, B. & VOLFOVSKY, N. 2007. Initial sequence and comparative analysis of the cat genome. *Genome Res*, 17.
- ROURA, E., HUMPHREY, B., KLASING, K. & SWART, M. 2011. Is the pig a good umami sensing model for humans? A comparative taste receptor study. *Flavour and Fragrance Journal*, 26, 282-285.
- RUNNING, C. A. 2015. High false positive rates in common sensory threshold tests. *Attention, Perception, & Psychophysics*, 77, 692-700.
- SAKURAI, T., MISAKA, T., NAGAI, T., ISHIMARU, Y., MATSUO, S., ASAKURA, T. & ABE, K. 2009. pH-Dependent Inhibition of the Human Bitter Taste Receptor hTAS2R16 by a Variety of Acidic Substances. *Journal of Agricultural and Food Chemistry*, 57, 2508-2514.
- SALLES, C., HERVÉ, C., SEPTIER, C., DEMAIZIÈRES, D., LESSCHAEVE, I., ISSANCHOU, S. & LE QUÉRÉ, J. L. 2000. Evaluation of taste compounds in water-soluble extract of goat cheeses. *Food Chemistry*, 68, 429-435.

- SALLES, C., SEPTIER, C., ROUDOT-ALGARON, F., GUILLOT, A. & ETIEVANT, P. X. 1995. Sensory and Chemical Analysis of Fractions Obtained by Gel Permeation of Water-Soluble Comte Cheese Extracts. *Journal of Agricultural and Food Chemistry*, 43, 1659-1668.
- SAN GABRIEL, A., MAEKAWA, T., UNEYAMA, H. & TORII, K. 2009. Metabotropic glutamate receptor type 1 in taste tissue. *Am J Clin Nutr*, 90, 743s-746s.
- SANDAU, M. M. & RAWSON, N. E. 2014. *Feline bitter taste receptors and methods*. USA patent application US 14/198,795.
- SATOH-KURIWADA, S., KAWAI, M., IIKUBO, M., SEKINE-HAYAKAWA, Y., SHOJI, N., UNEYAMA, H. & SASANO, T. 2014. Development of an Umami Taste Sensitivity Test and Its Clinical Use. *PLoS ONE*, 9, e95177.
- SCHLICHTERLE-CERNY, H. & AMADO, R. 2002. Analysis of taste-active compounds in an enzymatic hydrolysate of deamidated wheat gluten. *J Agric Food Chem*, 50, 1515-22.
- SENTANDREU, M. A., STOEVA, S., ARISTOY, M. C., LAIB, K., VOELTER, W. & TOLDRÁ, E. 2003. Identification of Small Peptides Generated in Spanish Dry-cured Ham. *Journal of Food Science*, 68, 64-69.
- SERVANT, G., TACHDJIAN, C., TANG, X.-Q., WERNER, S., ZHANG, F., LI, X., KAMDAR, P., PETROVIC, G., DITSCHUN, T., JAVA, A., BRUST, P., BRUNE, N., DUBOIS, G. E., ZOLLER, M. & KARANEWSKY, D. S. 2010. Positive allosteric modulators of the human sweet taste receptor enhance sweet taste. *Proceedings of the National Academy of Sciences of the United States of America*, 107, 4746-4751.
- SHIM, J., SON, H. J., KIM, Y., KIM, K. H., KIM, J. T., MOON, H., KIM, M. J., MISAKA, T. & RHYU, M.-R. 2015. Modulation of Sweet Taste by Umami Compounds via Sweet Taste Receptor Subunit hT1R2. *PLoS ONE*, 10, e0124030.
- SHIMOMURA, O. & JOHNSON, F. H. 1975. Regeneration of the photoprotein aequorin. *Nature*, 256, 236-8.
- SIEGHART, W. 1994. Pharmacology of benzodiazepine receptors: an update. *Journal of Psychiatry and Neuroscience*, 19, 24-29.
- SOLMS, J. 1969. Taste of amino acids, peptides, and proteins. *Journal of Agricultural and Food Chemistry*, 17, 686-688.
- SPANIER, A. M., BLAND, J. M., MILLER, J. A., GLINKA, J., WASZ, W. & DUGGINS, T. 1995. BMP: a flavor enhancing peptide found naturally in beef. Its chemical synthesis, descriptive sensory analysis, and some factors affecting its usefulness. In: GEORGE, C. (ed.) *Developments in Food Science*. Elsevier.

- SU, G. W., CUI, C., ZHENG, L., YAN, B., REN, J. Y. & ZHAO, M. M. 2012. Isolation and identification of two novel umami and umami-enhancing peptides from peanut hydrolysate by consecutive chromatography and MALDI-TOF/TOF MS. *Food Chemistry*, 135, 479-485.
- SUESS, B., FESTRING, D. & HOFMANN, T. 2015. 15 - Umami compounds and taste enhancers. *Flavour Development, Analysis and Perception in Food and Beverages*. Woodhead Publishing.
- SVOBODA, P., TEISINGER, J., NOVOTNY, J., BOUROVA, L., DRMOTA, T., HEJNOVA, L., MORAVCOVA, Z., LISY, V., RUDAJEV, V., STOHR, J., VOKURKOVA, A., SVANDOVA, I. & DURCHANKOVA, D. 2004. Biochemistry of transmembrane signaling mediated by trimeric G proteins. *Physiol Res*, 53 Suppl 1, S141-52.
- TAMURA, M., NAKATSUKA, T., TADA, M., KAWASAKI, Y., KIKUCHI, E. & OKAI, H. 1989. The Relationship between Taste and Primary Structure of "Delicious Peptide" (Lys-Gly-Asp-Glu-Glu-Ser-Leu-Ala) from Beef Soup. *Agricultural and Biological Chemistry*, 53, 319-325.
- TARUNO, A., VINGTDEUX, V., OHMOTO, M., MA, Z., DVORYANCHIKOV, G., LI, A., ADRIEN, L., ZHAO, H., LEUNG, S., ABERNETHY, M., KOPPEL, J., DAVIES, P., CIVAN, M. M., CHAUDHARI, N., MATSUMOTO, I., HELLEKANT, G., TORDOFF, M. G., MARAMBAUD, P. & FOSKETT, J. K. 2013. CALHM1 ion channel mediates purinergic neurotransmission of sweet, bitter and umami tastes. *Nature*, 495, 223-226.
- TEMUSSI, P. A. 2012. The good taste of peptides. *J Pept Sci*, 18, 73-82.
- TODA, Y., NAKAGITA, T., HAYAKAWA, T., OKADA, S., NARUKAWA, M., IMAI, H., ISHIMARU, Y. & MISAKA, T. 2013. Two distinct determinants of ligand specificity in T1R1/T1R3 (the umami taste receptor). *J Biol Chem*, 288, 36863-77.
- TODA, Y., OKADA, S. & MISAKA, T. 2011. Establishment of a new cell-based assay to measure the activity of sweeteners in fluorescent food extracts. *J Agric Food Chem*, 59, 12131-8.
- TOELSTEDE, S., DUNKEL, A. & HOFMANN, T. 2009. A Series of Kokumi Peptides Impart the Long-Lasting Mouthfulness of Matured Gouda Cheese. *Journal of Agricultural and Food Chemistry*, 57, 1440-1448.
- TOELSTEDE, S. & HOFMANN, T. 2009. Kokumi-Active Glutamyl Peptides in Cheeses and Their Biogenesis by *Penicillium roquefortii*. *Journal of Agricultural and Food Chemistry*, 57, 3738-3748.

- UEDA, Y., YONEMITSU, M., TSUBUKU, T., SAKAGUCHI, M. & MIYAJIMA, R. 1997. Flavor characteristics of glutathione in raw and cooked foodstuffs. *Biosci Biotechnol Biochem*, 61, 1977-80.
- VALERIO, L. G. 2010. Computational science in drug metabolism and toxicology. *Expert Opinion on Drug Metabolism & Toxicology*, 6, 781-784.
- VAN DEN OORD, A. H. A. & VAN WASSENAAR, P. D. 1997. Umami peptides: assessment of their alleged taste properties. *Zeitschrift Lebensmittel Untersuchung und Forschung A*, 205, 125-130.
- VAN LANCKER, F., ADAMS, A. & DE KIMPE, N. 2011. Chemical modifications of peptides and their impact on food properties. *Chem Rev*, 111, 7876-903.
- VAN LANCKER, F., ADAMS, A. & DE KIMPE, N. 2012. Impact of the N-terminal amino acid on the formation of pyrazines from peptides in Maillard model systems. *J Agric Food Chem*, 60, 4697-708.
- VAN WASSENAAR, P. D., VAN DEN OORD, A. H. A. & SCHAAPER, W. M. M. 1995. Taste of "Delicious" Beefy Meaty Peptide. Revised. *Journal of Agricultural and Food Chemistry*, 43, 2828-2832.
- VYSOTSKI, E. S. & LEE, J. 2004. Ca²⁺-Regulated Photoproteins: Structural Insight into the Bioluminescence Mechanism. *Accounts of Chemical Research*, 37, 405-415.
- WANG, K., MAGA, J. A. & BECHTEL, P. J. 1996. Taste Properties and Synergisms of Beefy Meaty Peptide. *Journal of Food Science*, 61, 837-839.
- WELLENDORPH, P. & BRAUNER-OSBORNE, H. 2009. Molecular basis for amino acid sensing by family C G-protein-coupled receptors. *Br J Pharmacol*, 156, 869-84.
- WHITE, T. D. & BOUDREAU, J. C. 1975. Taste preferences of the cat for neurophysiologically active compounds. *Physiological Psychology*, 3, 405-410.
- YAGASAKI, M. & HASHIMOTO, S. 2008. Synthesis and application of dipeptides; current status and perspectives. *Appl Microbiol Biotechnol*, 81, 13-22.
- YAMAMOTO, S., SHIGA, K., KODAMA, Y., IMAMURA, M., UCHIDA, R., OBATA, A., BAMBIA, T. & FUKUSAKI, E. 2014. Analysis of the correlation between dipeptides and taste differences among soy sauces by using metabolomics-based component profiling. *J Biosci Bioeng*, 118, 56-63.
- YAMASAKI, Y. & MAEKAWA, K. 1978. A Peptide with Delicious Taste. *Agricultural and Biological Chemistry*, 42, 1761-1765.
- YAMASAKI, Y. & MAEKAWA, K. 1980. Synthesis of a Peptide with Delicious Taste. *Agricultural and Biological Chemistry*, 44, 93-97.

- YARMOLINSKY, D. A., ZUKER, C. S. & RYBA, N. J. P. 2009. Common Sense about Taste: From Mammals to Insects. *Cell*, 139, 234-244.
- YOSHII, K., YOKOUCHI, C. & KURIHARA, K. 1986. Synergistic effects of 5'-nucleotides on rat taste responses to various amino acids. *Brain Research*, 367, 45-51.
- ZHANG, F., KLEBANSKY, B., FINE, R. M., LIU, H., XU, H., SERVANT, G., ZOLLER, M., TACHDJIAN, C. & LI, X. 2010. Molecular mechanism of the sweet taste enhancers. *Proceedings of the National Academy of Sciences*, 107, 4752-4757.
- ZHANG, F., KLEBANSKY, B., FINE, R. M., XU, H., PRONIN, A., LIU, H., TACHDJIAN, C. & LI, X. 2008. Molecular mechanism for the umami taste synergism. *Proceedings of the National Academy of Sciences of the United States of America*, 105, 20930-20934.
- ZHANG, M. X., WANG, X. C., LIU, Y., XU, X. L. & ZHOU, G. H. 2012. Isolation and identification of flavour peptides from Puffer fish (*Takifugu obscurus*) muscle using an electronic tongue and MALDI-TOF/TOF MS/MS. *Food Chem*, 135, 1463-70.
- ZHAO, C. J., SCHIEBER, A. & GÄNZLE, M. G. 2016. Formation of taste-active amino acids, amino acid derivatives and peptides in food fermentations – A review. *Food Research International*, 89, Part 1, 39-47.
- ZHAO, G. Q., ZHANG, Y., HOON, M. A., CHANDRASHEKAR, J., ERLBACH, I., RYBA, N. J. & ZUKER, C. S. 2003. The receptors for mammalian sweet and umami taste. *Cell*, 115, 255-66.
- ZHOU, Y., FREY, T. K. & YANG, J. J. 2009. Viral calciomics: Interplays between Ca²⁺ and virus. *Cell Calcium*, 46, 1-17.
- ZHUANG, M., LIN, L., ZHAO, M., DONG, Y., SUN-WATERHOUSE, D., CHEN, H., QIU, C. & SU, G. 2016. Sequence, taste and umami-enhancing effect of the peptides separated from soy sauce. *Food Chem*, 206, 174-81.

Appendices

Appendix 1 - Preliminary experiments with DMSO (Fluorescence)

Given that several of the amino acids which form the dipeptides in the library were hydrophobic, solubility was identified *a priori* as one of the challenges to address. It was believed that the dipeptides would need to be solubilised first in DMSO (Dimethyl sulfoxide, a water miscible solvent and has wide applications in cell biology). Some experiments to determine the effect of DMSO in the *in vitro* experiments were conducted to determine the level of interference of this solvent in the assay if it was used to solubilise the dipeptides.

It is known that in general 0.1% DMSO is generally not toxic to the cells and does not interfere with *in vitro* assays, however some assays could use higher concentrations of DMSO. As the toxicity of DMSO depends on the type of cells, several levels of DMSO were tested (0.1%, 0.5%, 1%, 2%, 3%, 5% and 10%) to determine the effect in the assay response, using 20 mM Alanine + 2 mM IMP as umami agonists (Figure 1). It was found that 0.1% DMSO in the experiment did not interfere with the cell response. Levels of 0.5% and 1% minimally interfered by increasing slightly the baseline and the magnitude of the response. At 2% DMSO the response started to noticeably change (e.g. the raw data curve, not shown, did not reach a plateau) and at 3%, 5% and 10% DMSO there was a very large increase of response, probably due to Ca^{2+} leaching due to the DMSO interfering with the cell membrane, and no differences between induced and un-induced cells (control) in maximum response.

Hence, it was determined that levels of DMSO up to 1% could be used to solubilise the dipeptides without changing the response significantly.

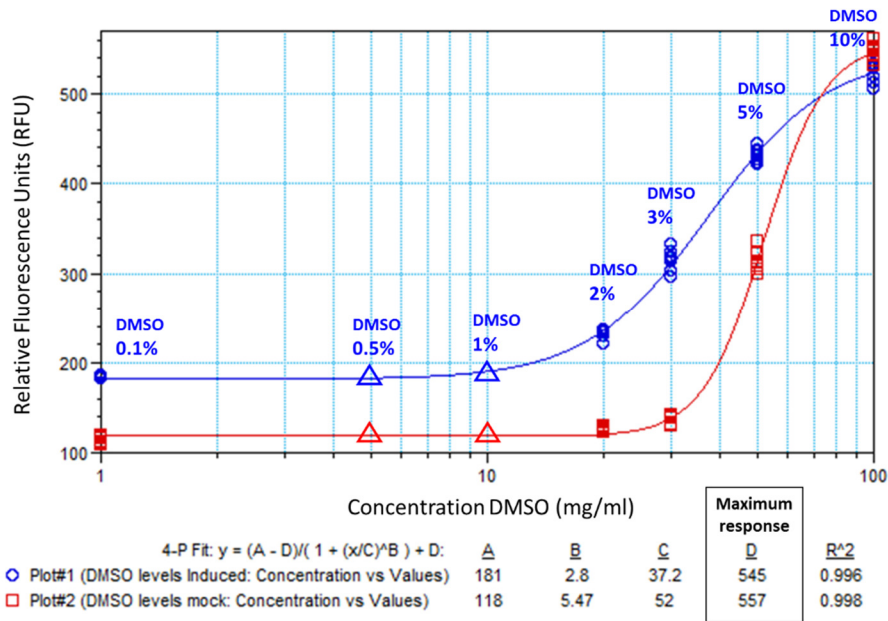


Figure AP-1. Illustration of the effect of the solvent DMSO in the cat umami ft1R1-ft1R3 assay. A mixture of 20 mM L-Alanine and 2 mM IMP dissolved in Tyrode's buffer was tested with different levels of DMSO using induced (blue) and un-induced cells (red). There was no difference in the response up to DMSO 10 mg/ml (1%) [Horizontal parallel lines, indicating no effect of DMSO]. After this point the response started increasing due to the DMSO. At the higher levels, the response of the un-induced cells (control) was the same as the induced cells (receptor).

Appendix 2 – Plate layouts

Primary screening 384-plate compound layout example (Fluorescence - FlexStation):

Each concentration in the primary screening had six replicates for the induced cells and another six for the un-induced cells for comparison.

		Conc. 1 mM			10 mM			100 mM			Conc. 1 mM			10 mM			100 mM			Controls					
		1	2	3	4	5	6	7	8	9	10	11	12	13	14	15	16	17	18	19	20	21	22	23	24
DP1-2	A	1 mM Trp-Tyr DP91			10 mM Trp-Tyr DP91			100 mM Trp-Tyr DP91			1 mM Tyr-Phe DP98			10 mM Tyr-Phe DP98			100 mM Tyr-Phe DP98			0 mM					
	B	1 mM Trp-Tyr DP91			10 mM Trp-Tyr DP91			100 mM Trp-Tyr DP91			1 mM Tyr-Phe DP98			10 mM Tyr-Phe DP98			100 mM Tyr-Phe DP98			100 mM					
	C	1 mM Trp-Tyr DP91			10 mM Trp-Tyr DP91			100 mM Trp-Tyr DP91			1 mM Tyr-Phe DP98			10 mM Tyr-Phe DP98			100 mM Tyr-Phe DP98			60 mM					
DP3-4	D	1 mM Trp-Tyr DP91			10 mM Trp-Tyr DP91			100 mM Trp-Tyr DP91			1 mM Tyr-Phe DP98			10 mM Tyr-Phe DP98			100 mM Tyr-Phe DP98			30 mM					
	E	1 mM Tyr-Gly DP94			10 mM Tyr-Gly DP94			100 mM Tyr-Gly DP94			1 mM Tyr-Ser DP99			10 mM Tyr-Ser DP99			100 mM Tyr-Ser DP99			Dose response Alanine + 2 mM IMP					
	F	1 mM Tyr-Gly DP94			10 mM Tyr-Gly DP94			100 mM Tyr-Gly DP94			1 mM Tyr-Ser DP99			10 mM Tyr-Ser DP99			100 mM Tyr-Ser DP99			ATP 10 uM					
DP5-6	G	1 mM Tyr-Gly DP94			10 mM Tyr-Gly DP94			100 mM Tyr-Gly DP94			1 mM Tyr-Ser DP99			10 mM Tyr-Ser DP99			100 mM Tyr-Ser DP99			Isoproterenol 10 uM					
	H	1 mM Tyr-Gly DP94			10 mM Tyr-Gly DP94			100 mM Tyr-Gly DP94			1 mM Tyr-Ser DP99			10 mM Tyr-Ser DP99			100 mM Tyr-Ser DP99			Tyrode's buffer only (blank)					
	I	1 mM Tyr-Gly DP94			10 mM Tyr-Gly DP94			100 mM Tyr-Gly DP94			1 mM Tyr-Ser DP99			10 mM Tyr-Ser DP99			100 mM Tyr-Ser DP99								
DP7-8	J	1 mM Tyr-His DP95			10 mM Tyr-His DP95			100 mM Tyr-His DP95			1 mM Tyr-Trp DP100			10 mM Tyr-Trp DP100			100 mM Tyr-Trp DP100			10 mM					
	K	1 mM Tyr-His DP95			10 mM Tyr-His DP95			100 mM Tyr-His DP95			1 mM Tyr-Trp DP100			10 mM Tyr-Trp DP100			100 mM Tyr-Trp DP100			3 mM					
	L	1 mM Tyr-His DP95			10 mM Tyr-His DP95			100 mM Tyr-His DP95			1 mM Tyr-Trp DP100			10 mM Tyr-Trp DP100			100 mM Tyr-Trp DP100			1 mM					
DP7-8	M	1 mM Tyr-Met DP97			10 mM Tyr-Met DP97			100 mM Tyr-Met DP97			1 mM Tyr-Tyr DP101			10 mM Tyr-Tyr DP101			100 mM Tyr-Tyr DP101			0.3 mM					
	N	1 mM Tyr-Met DP97			10 mM Tyr-Met DP97			100 mM Tyr-Met DP97			1 mM Tyr-Tyr DP101			10 mM Tyr-Tyr DP101			100 mM Tyr-Tyr DP101								
	O	1 mM Tyr-Met DP97			10 mM Tyr-Met DP97			100 mM Tyr-Met DP97			1 mM Tyr-Tyr DP101			10 mM Tyr-Tyr DP101			100 mM Tyr-Tyr DP101								
P	1 mM Tyr-Met DP97			10 mM Tyr-Met DP97			100 mM Tyr-Met DP97			1 mM Tyr-Tyr DP101			10 mM Tyr-Tyr DP101			100 mM Tyr-Tyr DP101									

Figure AP-2A. Primary screening compound plate layout. The controls used were: Full dose response curve for L-alanine + 2 mM IMP as reference of adequate umami activation, ATP for cell downstream signalling working properly, Isoproterenol for induction of expression checks, and Tyrode's buffer for background response checks.

Dose response screening 384-plate compound layout example (Fluorescence / Luminescence - FLIPR):

Each concentration in the dose response had four replicates for the induced cells. The un-induced cell plate was run separately also with four replicates. In this case four instead of six replicates were conducted due to the need of maximising the output from the experiment (as the FLIPR was not available at WALTHAM®).

		Controls		DP1	DP2	DP3	DP4	DP5	DP6	DP7	DP8	DP9	DP10	DP11											
		1	2	3	4	5	6	7	8	9	10	11	12	13	14	15	16	17	18	19	20	21	22	23	24
A	20 mM L-Ala 100 mM L-Ala + 1 IMP			31.6 mM	31.6 mM	10 mM	20 mM	63.2 mM	63.2 mM	31.6 mM	63.2 mM	31.6 mM	20 mM	63.2 mM											
B				10 mM	10 mM	3.16 mM	10 mM	31.6 mM	31.6 mM	10 mM	31.6 mM	10 mM	10 mM	31.6 mM											
C				3.16 mM	3.16 mM	1 mM	3.16 mM	10 mM	10 mM	3.16 mM	10 mM	3.16 mM	3.16 mM	10 mM											
D				1 mM	1 mM	0.32 mM	1 mM	3.16 mM	3.16 mM	1 mM	3.16 mM	1 mM	1 mM	3.16 mM											
E		1 mM IMP 33 uM Isoproterenol			0.32 mM	0.32 mM	0.1 mM	0.32 mM	1 mM	1 mM	0.32 mM	1 mM	0.32 mM	0.32 mM	1 mM										
F					0.1 mM	0.1 mM	0.032 mM	0.1 mM	0.32 mM	0.32 mM	0.1 mM	0.32 mM	0.1 mM	0.1 mM	0.32 mM										
G					0.032 mM	0.032 mM	0.01 mM	0.032 mM	0.1 mM	0.1 mM	0.032 mM	0.1 mM	0.032 mM	0.032 mM	0.1 mM										
H					0.01 mM	0.01 mM	0.0032 mM	0.01 mM	0.032 mM	0.032 mM	0.01 mM	0.032 mM	0.01 mM	0.01 mM	0.032 mM										
I																									
J																									
K																									
L																									
M																									
N																									
O																									
P																									

Figure AP-2B. Example of compound layout for FLIPR experiments (both for Fluorescence and Luminescence assays. 384-well plate). The dipeptide and concentrations given are for example only and do not correspond to any particular compound plates prepared. Four different starting concentrations were used for the dilutions (63.2, 31.6, 20 or 10 mM) depending on the amount of compound available and its solubility. The dilutions were made using a semi-logarithmic dilution series, with 1 in 3.16 dilutions (half a logarithm) each time.

Appendix 3 - Controls used in primary screening (Fluorescence-FlexStation)

ATP control:

ATP causes release of intracellular Ca^{2+} via the phospholipase C and IP_3 pathway. These molecules are necessary for the signal transduction cascade. The test with ATP ensures the necessary machinery for the cell to be able to transmit a signal from the receptor is present. In Figure AP-3A the response to ATP from the induced cells (expressing the receptor) and the mock cells (not expressing it) is shown. It is usual for the mock cells to have a higher response than the induced cells as the expression of the alien receptor slightly disturbs the normal functioning of the cell (in this case HEK293T).

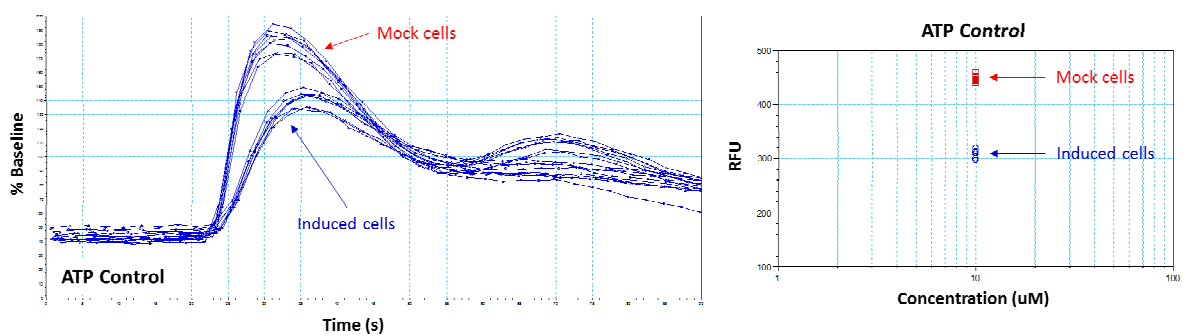


Figure AP-3A. Response to 10 μM ATP control by induced and un-induced (mock) cells.

(Left) Raw data with activation as % baseline. (Right) Average fluorescence response as RFU.

Induced cells are represented in blue and mock cells in red.

Isoproterenol control:

Isoproterenol was used to check for adequate induction of expression of the cat umami taste receptor ft1R1-ft1R3 . Cells expressing the receptor should provide a higher fluorescent response than un-induced (mock) cells.

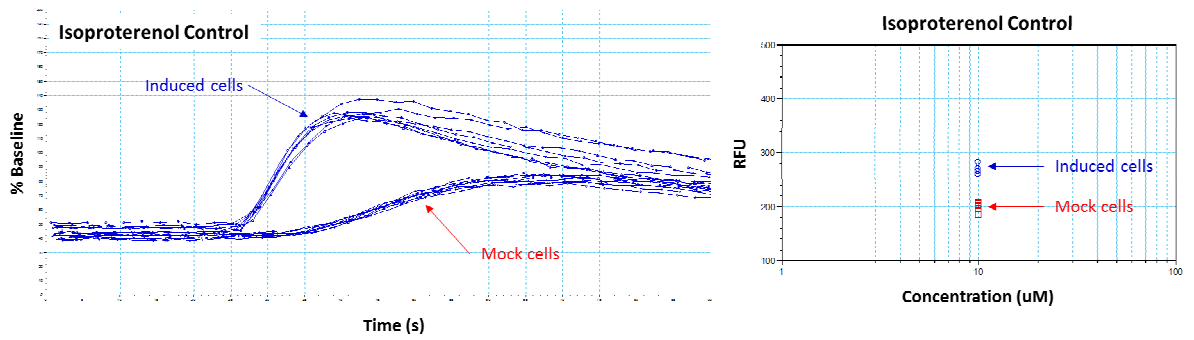


Figure AP-3B. Response to 10 μM isoproterenol control by induced and un-induced (mock) cells. (Left) Raw data with activation as % baseline. (Right) Average fluorescence response as RFU. Induced cells are represented in blue and mock cells in red.

Tyrode's buffer control:

Cells with Tyrode's only should not produce any fluorescence response as there are no molecules able to produce any intracellular release of calcium.

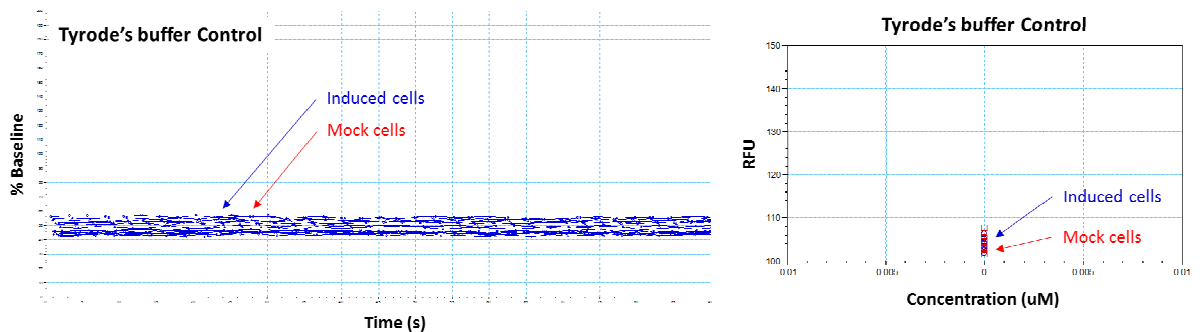


Figure AP-3C. Response to Tyrode's buffer control by induced and un-induced (mock) cells. (Left) Raw data with activation as % baseline. (Right) Average fluorescence response as RFU. Induced cells are represented in blue and mock cells in red.

Appendix 4 - Primary screening results for the 101 dipeptides

Table AP-4. Primary screening results in 2 mM IMP and in Tyrode's buffer of the 101 dipeptides tested (FlexStation – Fluorescence assay). Dipeptides marked with a “DR” were also tested using a dose response curve. “AF” means suspected of having auto-fluorescence. “NS” means non-specific response.

Code	Dipeptide	Solubility	In 2 mM IMP plus buffer			In Tyrode's buffer		
			Activity	AF	Comments	Activity	AF	Comments
DP1	Ala-Ala	Soluble	Inactive	No	Confident	Inactive	No	Confident
DP2	Ala-Asn	Soluble	Inactive	No	Confident	Inactive	No	Confident
DP3	Ala-Gly	Soluble	Inactive	No	Confident	Inactive	No	Confident
DP4	Ala-His	Soluble	Inactive	No	Confident	Inactive	No	Confident
DP5	Ala-Leu	Soluble	Inactive	No	Confident	Inactive	No	Confident
DP6	Ala-Met	Soluble	Inactive	No	Confident	Inactive	No	Confident
DP7	Ala-Phe	Soluble	Inactive	No	Confident	Inactive	No	Confident
DP8	Ala-Ser	Soluble	Inactive	No	Confident	Inactive	No	Confident
DP9	Ala-Trp	Soluble	Inactive	No	Confident	Inactive	No	Confident
DP10	Ala-Tyr	Part. Sol.	Inactive	No	Confident	Inactive	No	Confident
DP11	Asn-Ala	Part. Sol.	Active	No	Not specific	Active	No	Not specific
DP12	Asn-Asn	Soluble	Active	Yes	Prob. NS	Active	Yes	Not specific
DP13	Asn-Gly	Soluble	Active	No	Not specific	Active	No	Prob. NS
DP14A	DR Asn-His	Soluble	Active	No	Not specific	Active	No	Not specific
DP15	Asn-Leu	Soluble	Active	No	Not specific	Active	No	Not specific
DP16	DR Asn-Met	Soluble	Active	No	Not specific	Active	No	Not specific
DP17	Asn-Phe	Soluble	Active	No	Not specific	Active	No	Not specific
DP18	Asn-Ser	Soluble	Active	No	Prob. NS	Active	No	Not specific
DP19	Asn-Trp	Soluble	Active	Yes	Prob. NS	Active	Yes	Prob. NS
DP20	Asn-Tyr	Soluble	Active	Yes	Prob. NS	Active	Yes	Not specific
DP21	Cys-Gly	Soluble	Active	Yes	Prob. NS	Inactive	No	Confident
DP22	Gly-Ala	Soluble	Inactive	No	Confident	Inactive	No	Confident
DP23	Gly-Asn	Soluble	Active	No	Prob. NS	Inactive	No	Confident
DP24	DR Gly-Cys	Soluble	Active	No	Prob. NS	Inactive	No	Confident
DP25	Gly-Gly	Soluble	Inactive	No	Confident	Inactive	No	Confident
DP26	Gly-His	Soluble	Inactive	No	Confident	Inactive	No	Confident
DP27	Gly-Leu	Soluble	Inactive	No	Confident	Inactive	No	Confident
DP28	Gly-Met	Soluble	Inactive	No	Confident	Inactive	No	Confident
DP29	Gly-Phe	Soluble	Inactive	No	Confident	Active	No	Prob. NS
DP30	Gly-Ser	Soluble	Inactive	No	Confident	Inactive	No	Confident
DP31	Gly-Trp	Part. Sol.	Inactive	No	Confident	Inactive	No	Confident
DP32	Gly-Tyr	Soluble	Inactive	No	Confident	Inactive	No	Confident
DP33	His-Ala	Soluble	Inactive	No	Confident	Inactive	No	Confident
DP34	His-Asn	Soluble	Active	No	Prob. NS	Inactive	No	Confident
DP35	His-Gly	Soluble	Inactive	No	Confident	Inactive	No	Confident
DP36	His-His	Soluble	Active	Yes	Prob. NS	Active	Yes	Prob. NS
DP37	His-Leu	Part. Sol.	Inactive	No	Confident	Inactive	No	Confident
DP38	His-Met	Soluble	Inactive	No	Confident	Inactive	No	Confident
DP39	His-Phe	Part. Sol.	Inactive	No	Confident	Inactive	No	Confident
DP40	His-Ser	Soluble	Inactive	No	Confident	Inactive	No	Confident

(continues in next page)

Table AP-4 (cont.). Primary screening results in 2 mM IMP and in Tyrode's buffer of the 101 dipeptides tested (FlexStation – Fluorescence assay).

Code	Dipeptide	Solubility	In 2 mM IMP plus buffer			In Tyrode's buffer		
			Activity	AF	Comments	Activity	AF	Comments
DP41	His-Trp	Soluble	Active	Yes	Prob. NS	Inactive	Yes	Prob. NS
DP42	His-Tyr	Soluble	Active	Yes	Prob. NS	Inactive	Yes	Prob. NS
DP43	Leu-Ala	Soluble	Inactive	No	Confident	Inactive	No	Confident
DP44	Leu-Asn	Soluble	Inactive	No	Confident	Inactive	No	Confident
DP45	Leu-Gly	Soluble	Inactive	No	Confident	Inactive	No	Confident
DP46	Leu-His	Part. Sol.	Inactive	No	Confident	Inactive	No	Confident
DP47	Leu-Leu	Part. Sol.	Inactive	No	Confident	Inactive	No	Confident
DP48	Leu-Met	Soluble	Active	No	Prob. NS	Inactive	No	Confident
DP49	Leu-Phe	Part. Sol.	Active	Yes	Prob. NS	Inactive	No	Confident
DP50	Leu-Ser	Soluble	Inactive	No	Confident	Inactive	No	Confident
DP51	Leu-Trp	Part. Sol.	Inactive	Yes	Prob. NS	Inactive	No	Confident
DP52	Leu-Tyr	Part. Sol.	Inactive	No	Not specific	Inactive	No	Confident
DP53	Met-Ala	Soluble	Inactive	No	Confident	Inactive	No	Confident
DP54	Met-Asn	Soluble	Active	No	Prob. NS	Inactive	No	Confident
DP55	Met-Gly	Soluble	Inactive	No	Confident	Inactive	No	Confident
DP56	Met-His	Soluble	Active	No	Prob. NS	Inactive	No	Confident
DP57	Met-Leu	Soluble	Inactive	No	Confident	Inactive	No	Confident
DP58	Met-Met	Part. Sol.	Inactive	No	Confident	Inactive	No	Confident
DP59	Met-Phe	Part. Sol.	Inactive	Yes	Prob. NS	Inactive	No	Confident
DP60	Met-Ser	Soluble	Active	No	Prob. NS	Inactive	No	Confident
DP61	Met-Trp	Part. Sol.	Inactive	Yes	Prob. NS	Inactive	No	Confident
DP62	Met-Tyr	Part. Sol.	Inactive	No	Prob. NS	Inactive	No	Confident
DP63	Phe-Ala	Soluble	Inactive	No	Confident	Inactive	No	Confident
DP64	Phe-Asn	Soluble	Active	No	Prob. NS	Active	No	Prob. NS
DP65	Phe-Gly	Soluble	Inactive	No	Confident	Inactive	No	Confident
DP66	Phe-His	Soluble	Inactive	No	Confident	Inactive	Yes	Prob. NS
DP67	Phe-Leu	Part. Sol.	Active	No	Prob. NS	Inactive	No	Confident
DP68	Phe-Met	Part. Sol.	Active	No	Prob. NS	Inactive	No	Confident
DP69	Phe-Phe	Part. Sol.	Inactive	No	Confident	Inactive	No	Confident
DP70	Phe-Ser	Soluble	Inactive	No	Confident	Inactive	No	Confident
DP71	Phe-Trp	Part. Sol.	Inactive	No	Confident	Inactive	No	Confident
DP72	Phe-Tyr	Part. Sol.	Inactive	No	Confident	Inactive	No	Confident
DP73	Ser-Ala	Part. Sol.	Inactive	No	Confident	Inactive	No	Confident
DP74	Ser-Asn	Soluble	Inactive	No	Confident	Inactive	No	Confident
DP75	Ser-Gly	Soluble	Inactive	No	Confident	Inactive	No	Confident
DP76	Ser-His	Soluble	Active	Yes	Prob. NS	Inactive	No	Confident
DP77	Ser-Leu	Part. Sol.	Inactive	No	Confident	Inactive	No	Confident
DP78	Ser-Met	Soluble	Inactive	No	Confident	Inactive	No	Confident
DP79	Ser-Phe	Part. Sol.	Inactive	No	Confident	Inactive	No	Confident
DP80	Ser-Ser	Part. Sol.	Inactive	No	Confident	Inactive	No	Confident

(continues in next page)

Table AP-4 (cont.). Primary screening results in 2 mM IMP and in Tyrode's buffer of the 101 dipeptides tested (FlexStation – Fluorescence assay).

Code	Dipeptide	Solubility	In 2 mM IMP plus buffer			In Tyrode's buffer		
			Activity	AF	Comments	Activity	AF	Comments
DP81	Ser-Tyr	Soluble	Inactive	No	Confident	Inactive	No	Confident
DP82	Trp-Ala	Soluble	Inactive	No	Confident	Inactive	No	Confident
DP83	Trp-Asn	Soluble	Inactive	No	Confident	Inactive	No	Confident
DP84	Trp-Gly	Soluble	Inactive	No	Confident	Inactive	No	Confident
DP85	^{DR} Trp-His	Soluble	Active	No	Dubious	Active	No	Prob. NS
DP86	Trp-Leu	Part. Sol.	Inactive	No	Confident	Inactive	No	Confident
DP87	Trp-Met	Part. Sol.	Inactive	No	Confident	Inactive	No	Confident
DP88	Trp-Phe	Part. Sol.	Inactive	No	Confident	Inactive	No	Confident
DP89	Trp-Ser	Part. Sol.	Inactive	No	Confident	Inactive	No	Confident
DP90	Trp-Trp	Part. Sol.	Inactive	No	Confident	Inactive	No	Confident
DP91	Trp-Tyr	Soluble	Active	No	Dubious	Inactive	No	Confident
DP92	Tyr-Ala	Soluble	Inactive	No	Confident	Inactive	No	Confident
DP93	^{DR} Tyr-Asn	Soluble	Active	No	Dubious	Active	No	Prob. NS
DP94	^{DR} Tyr-Gly	Part. Sol.	Active	No	Confident	Inactive	No	Confident
DP95	Tyr-His	Soluble	Active	No	Dubious	Inactive	No	Prob. NS
DP96	Tyr-Leu	Part. Sol.	Inactive	No	Confident	Inactive	No	Confident
DP97	Tyr-Met	Soluble	Active	No	Dubious	Active	No	Prob. NS
DP98	Tyr-Phe	Part. Sol.	Active	No	Dubious	Active	No	Prob. NS
DP99	Tyr-Ser	Soluble	Active	No	Dubious	Active	No	Prob. NS
DP100	Tyr-Trp	Part. Sol.	Active	No	Dubious	Inactive	No	Confident
DP101	Tyr-Tyr	Part. Sol.	Active	No	Dubious	Inactive	No	Confident

Appendix 5 - Quality control checks – Chemical analysis

Chemical analysis of the same two dipeptides from two different suppliers:

Two dipeptides sourced from two different suppliers (PE Biosciences and AnaSpec) were analysed by High Performing Liquid Chromatography – Mass Spectrometry (HPLC-MS) by the Analytical Chemistry Team at WALTHAM®: DP14 (Asn-His) and DP15 (Asn-Leu). In this section, the LC chromatograms and the MS spectra are shown for comparison of the two dipeptides.

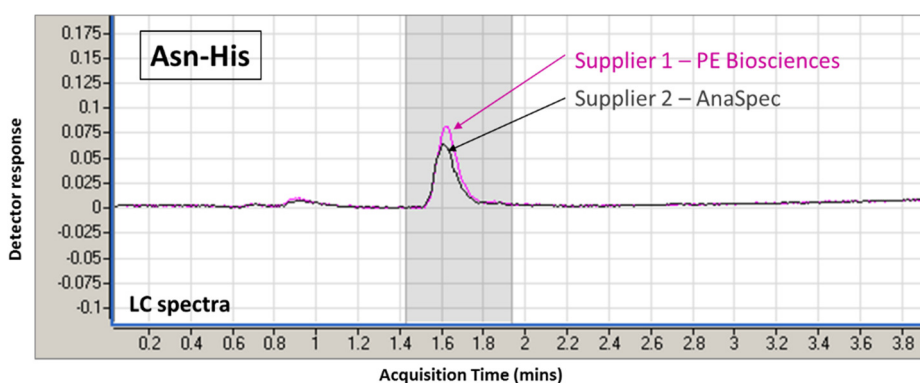


Figure AP-5A. LC chromatogram comparing the signals of Asn-His from the two suppliers. The peaks overlap (same compound DP14 – Asn-His). The peaks have similar but a slightly different height/area probably due to a weighing discrepancy when preparing the samples (very small difference, $\ll 1$ mg).

Chemically the two samples chosen (DP14 – Asn-His and DP15 – Asn-Leu) were proven to be the dipeptides, with comparable purity ($\geq 95\%$) from both suppliers (all chromatograms overlapped well with each other). The same LC peaks and MS ion abundances were found. Also the qualitative analysis revealed a strong signal in the MS for the parent dipeptide in both cases (which suggests highly pure compounds).

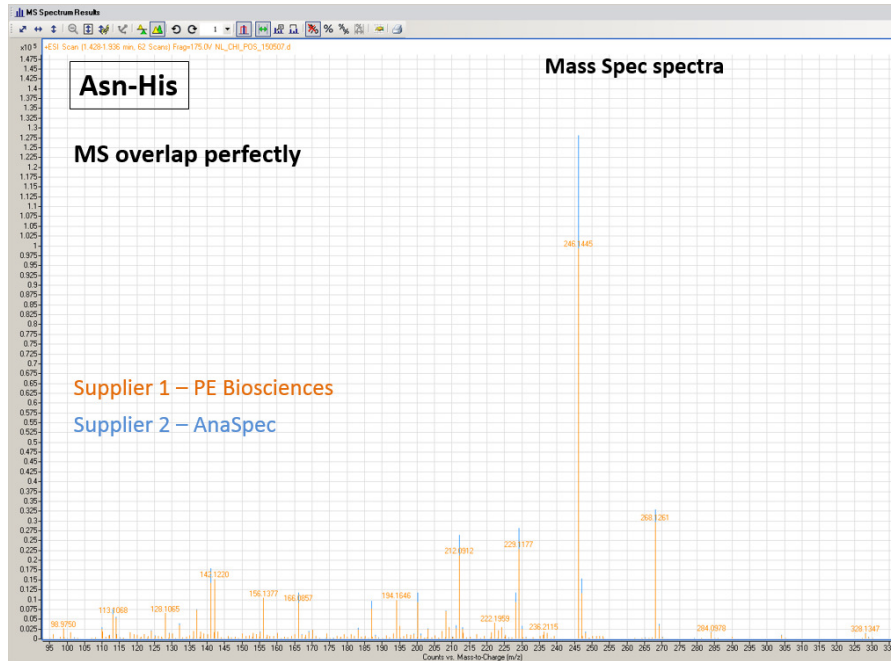


Figure AP-5B. MS spectra comparing the signals of Asn-His from the two suppliers. The molecular ions and fragments (m/z) overlap completely (same compound DP14 – Asn-His).

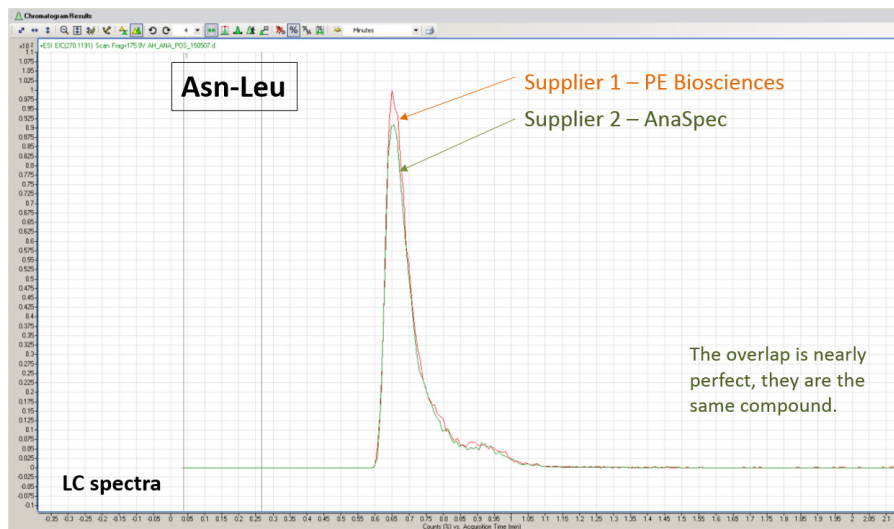


Figure AP-5C. LC chromatogram comparing the signals of Asn-Leu from the two suppliers. The peaks overlap completely (same compound DP15 – Asn-Leu). The peaks have similar but a slightly different height/area probably due to a weighing discrepancy when preparing the samples (very small difference, <<1 mg).

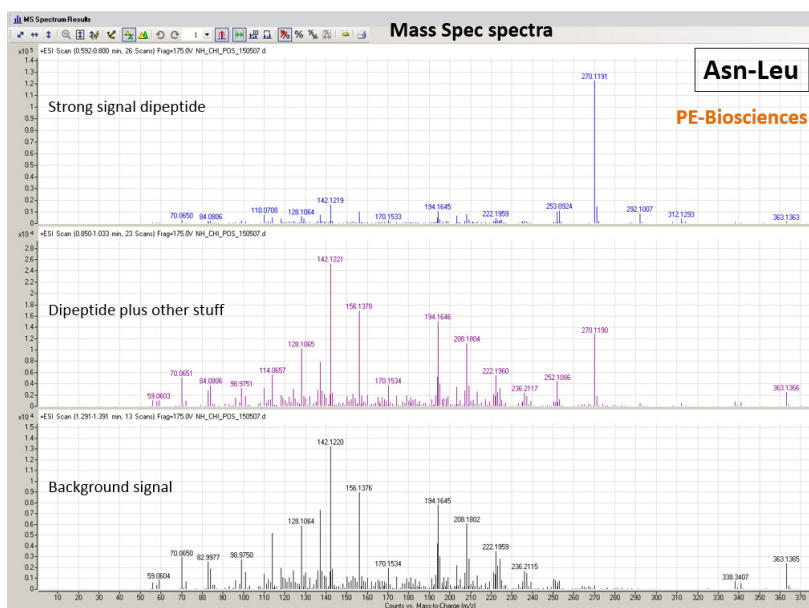


Figure AP-5D. MS spectra of Asn-Leu from supplier 1 (PE Biosciences). The molecular ions and fragments (m/z) correspond to compound DP15 – Asn-Leu). The m/z scans showed in the graph include the dipeptide (top), the additional chemical species (centre) and the background signal (bottom). They overlap fully with the spectra from the other supplier shown in Table AP-5E.

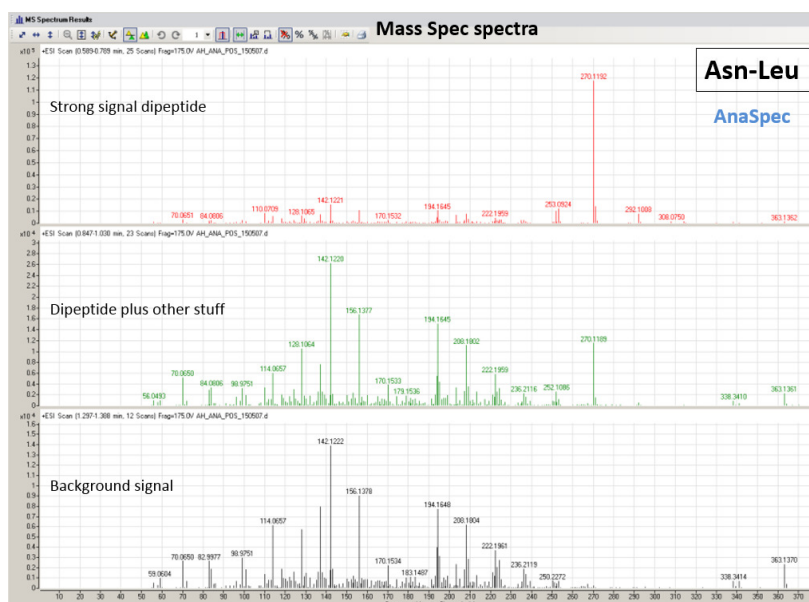


Figure AP-5E. MS spectra of Asn-Leu from supplier 2 (AnaSpec). The molecular ions and fragments (m/z) correspond to compound DP15 – Asn-Leu). The m/z scans showed in the graph include the dipeptide (top), the additional chemical species (centre) and the background signal (bottom). They overlap fully with the spectra from the other supplier shown in Table AP-5D.

